



Universiteit
Leiden
The Netherlands

Chromatin dynamics resolved with force spectroscopy

Chien, F.T.

Citation

Chien, F. T. (2011, June 28). *Chromatin dynamics resolved with force spectroscopy*. *Casimir PhD Series*. Retrieved from <https://hdl.handle.net/1887/17738>

Version: Not Applicable (or Unknown)

License: [Leiden University Non-exclusive license](#)

Downloaded from: <https://hdl.handle.net/1887/17738>

Note: To cite this publication please use the final published version (if applicable).

Chromatin Dynamics resolved with Force Spectroscopy

Fan-Tso Chien

Chromatin Dynamics resolved with Force Spectroscopy

Proefschrift

ter verkrijging van

de graad van Doctor aan de Universiteit Leiden,

op gezag van de Rector Magnificus prof. mr. P.F. van der Heijden,

volgens besluit van het College voor Promoties

te verdedigen op dinsdag 28 juni 2011

klokke 11:15 uur

door

Fan-Tso Chien

geboren te Changhua, Taiwan

in 1976

Promotiecommissie

Promotor: Prof. Dr. T. Schmidt
Co-promotor: Dr. Ir. S.J.T. van Noort
Overige leden: Prof. Dr. J. Brouwer
Prof. Dr. N.H. Dekker (Delft University of Technology)
Prof. Dr. E.R. Eliel
Dr. C. Logie (Radboud University, Nijmegen)
Dr. D. Rhodes (MRC Laboratory of Molecular Biology, Cambridge)
Prof. Dr. H. Schiessel

Casimir PhD series 2011-12

ISBN 978-90-8593-102-7

an electronic version of this thesis can be found at <https://openaccess.leidenuniv.nl>

Contents

1	Chromatin: Results From Single Molecule Spectroscopy	1
1.1	Introduction	2
1.2	Higher-order folding	3
1.3	Single molecule force spectroscopy	4
1.4	DNA unwrapping in mononucleosomes	7
1.5	Chromatin assembly strategies	9
1.6	Nucleosome-nucleosome interactions in chromatin	10
1.7	DNA unwrapping in chromatin	13
1.8	Nucleosome dynamics in cell-extract assembled chromatin	15
1.9	Structural influences of histone modifications	16
1.10	Diversity in experimental conditions	16
1.11	Structural transitions in chromatin under force	18
1.12	More tension on chromatin	20
1.13	Scope of this thesis	21
	Bibliography	22
2	Chromatin: A Highly Compliant Helical Folding	27
2.1	Introduction	28
2.2	Results	29
2.2.1	Reconstitution of 601 arrays yields regular 30 nm chromatin fibers	29
2.2.2	197 bp NRL fibers stretch like a Hookean spring	31
2.2.3	Linker histones do not affect the stiffness of a chromatin fiber	34
2.2.4	The nucleosomes in a 30 nm fiber are arranged in a solenoidal structure	36
2.2.5	Quantification of the nucleosome-nucleosome interaction energy	38
2.2.6	Mg ²⁺ stabilizes nucleosome stacking under physiological conditions	39

2.2.7	167 bp NRL chromatin fibers are longer and stiffer, consistent with a two-start helix	41
2.3	Discussion	42
2.4	Methods	47
2.4.1	DNA and chromatin fibers	47
2.4.2	Flow cell	47
2.4.3	Sample preparation	47
2.4.4	Magnetic tweezers	48
2.5	Acknowledgments	48
	Bibliography	48
3	Quantification of force induced structural changes	51
3.1	Introduction	52
3.2	Theory	54
3.3	Results	55
3.3.1	Accurate contour length measurements on small tethers with magnetic tweezers	55
3.3.2	Nucleosomes do not reconstitute on DNA handles	57
3.3.3	Low force analysis of chromatin stretching recovers the composition of single chromatin fibers	58
3.3.4	The force plateau at 3-4 pN represents simultaneous unstacking and unwrapping of nucleosomes	61
3.3.5	Irreversible unfolding points to H2A-H2B dimer dissociation	62
3.3.6	Mono- and divalent salts change the nucleosome-nucleosome interaction energy in folded fibers	64
3.4	Discussion	66
3.5	Materials and Methods	69
3.5.1	Chromatin fibers	69
3.5.2	Flow cell preparation	70
3.5.3	Magnetic Tweezers	70
3.6	Acknowledgements	70
	Bibliography	70
4	Force-dependent dynamics of single nucleosomes in chromatin	73
4.1	Introduction	74
4.2	Theory	76
4.2.1	A two-state model for force induced conformational changes in nucleosomes	76
4.2.2	Conformational changes of multiple nucleosomes in a fiber	77

Contents

4.2.3	A parameterized Hidden Markov Model of nucleosome dynamics	79
4.3	Results	80
4.3.1	Force-Extension traces capture structural transitions in a stretched chromatin fiber.	80
4.3.2	Constant force measurements reveal dynamic transitions	82
4.3.3	The kinetics of conformational changes of single nucleosomes embedded in chromatin fibers	83
4.4	Discussion	86
4.4.1	HMM analysis of chromatin unfolding	86
4.4.2	A structural interpretation of force induced chromatin unfolding	87
4.4.3	Consequences for chromatin organization <i>in vivo</i>	91
4.5	Materials and Methods	92
4.5.1	Chromatin fibers	92
4.5.2	Experimental configuration	92
4.5.3	Fitting routine	92
	Bibliography	93
	Summary	97
	Samenvatting	101
	List of Publications	107
	Curriculum Vitae	109

Chapter 1

Chromatin: Results From Single Molecule Spectroscopy

The compact, yet dynamic organization of chromatin plays an essential role in regulating gene expression. Although the static structure of chromatin fibers has been studied extensively, the controversy about the higher order folding remains. In the past decade a number of studies have addressed chromatin folding with single molecule force spectroscopy. By manipulating chromatin fibers individually, the mechanical properties of the fibers were quantified with piconewton and nanometer accuracy. Here, we review the results of force induced chromatin unfolding and compare the differences between experimental conditions and single molecule manipulation techniques like force and position clamps. From these studies, five major features appeared upon forced extension of chromatin fibers: the elastic stretching of chromatin's higher order structure, the breaking of internucleosomal contacts, unwrapping of the first turn of DNA, unwrapping of the second turn of DNA, and the dissociation of histone octamers. These events occur sequentially at the increasing force. Resolving force induced structural changes of chromatin fibers will help to provide a physical understanding of processes involving chromatin that occur *in vivo* and will reveal the mechanical constraints that are relevant for processing and maintenance of DNA in eukaryotes.

This chapter is based on: F.T. Chien and J. van Noort, *10 years of tension on chromatin: results from single molecule force spectroscopy*, Current pharmaceutical biotechnology **10**, 474-485 (2009)

1.1 Introduction

In the eukaryotic genome DNA is organized in chromatin fibers. The compaction into chromatin allows for the storage of several meters of genomic DNA into a nucleus that is several micrometers in diameter. The repetitive unit of chromatin fibers is a nucleosome, which is composed of 147 base pair (bp) of DNA wrapped in 1.7 turns around a histone octamer[1]. The histone octamer consists of two copies of the histone proteins H2A, H2B, H3, and H4. A fifth type of histone, the linker histone, is located on the DNA exit site of nucleosomes[2]. Linear arrays of nucleosomes connected by 20 to 60 bp of linker DNA fold into chromatin fibers with a diameter of approximately 30 nm[3, 4]. This stage of chromatin compaction depends on the intrinsic properties of the fibers, such as DNA sequence dependent histone binding affinity, the presence of linker histones, the presence of post-translational histone modifications, the length of linker DNA, and nucleosome-nucleosome interactions. The ionic strength of buffers and the presence of divalent ions also dramatically affect chromatin folding[5, 6]. Furthermore, *in vivo* the presence and activity of many DNA binding and chromatin organizing factors like the transcription machinery[7], DNA repair machinery[8], topoisomerases[9], ATP-dependent remodellers[10], and condensins[11] will directly affect its structure. With this many parameters influencing its structure it has proved a magnificent challenge to extract a coherent image of the structure of chromatin and it is likely that different structures coexist.

Chromatin fibers are compact, yet dynamic structures. Their dynamics is critically related to biological functions, such as gene regulation. Transcriptional silent genes are typically located in chromatin dense regions in a nucleus. In more open regions chromatin is relatively depleted in linker histones, enriched in acetylation and features larger linker lengths. With the advance of Chromatin Immuno Precipitation (ChIP) techniques many correlations between the biochemical state of chromatin and its underlying DNA sequence have been exposed[12]. The accumulating data in this field of epigenetics emphasizes the role of chromatin as a key regulatory factor in gene expression. However, a structural interpretation of the mechanisms involved with epigenetic regulation is largely absent.

Although chromatin has been the subject of scrutinous investigation for three decades, many structural aspects remain unresolved. With the development of single molecule force spectroscopy techniques it is now possible to manipulate individual chromatin fibers with sub piconewton (pN) force sensitivity and nanometer (nm) resolution. Single molecule techniques have many features that complement more traditional approaches, such as the ability to discriminate sub-populations and to directly reveal molecular dynamics without time or population

averaging. Force spectroscopy in particular presents the possibility to accurately measure the mechanical properties in the terms of extension, elastic properties, and force and torque dependence. These parameters are arguably relevant *in vivo*, as chromatin is continuously subjected to the actions of DNA based molecular motors[13], such as RNA polymerases[14], DNA polymerases[15], and ATP dependent chromatin remodellers[16, 17], which typically have stalling forces in excess of several pNs. Additionally, force spectroscopy does not require staining and can be performed in conditions that closely resemble the nuclear environment. In the past 10 years a number of studies that make use of these techniques have been published. Here we review these exciting results. First we will briefly summarize the understanding of chromatin structure gained from biochemical, crystallographic and microscopy studies. For a more comprehensive overview on this we refer to other excellent reviews[18–22]. Given the wide range of parameters influencing the structure of chromatin and the different approaches to force spectroscopy that have been developed, we aim to compare these studies and relate the obtained results to the properties of chromatin as obtained from other experiments.

The emerging picture is that of an extremely flexible fiber that has many options to extend its length as a response to external applied forces. With its high elasticity, even thermal fluctuations are sufficient to significantly stretch the fiber and expose the wrapped DNA. It appears that chromatin folding is tailored to combine a high level of compaction with the ability to keep DNA accessible for transactions with other proteins. Force spectroscopy has substantiated the structural effects of a number of mechanisms with which eukaryotes fine-tune the balance between compaction and accessibility.

1.2 Higher-order folding

Early studies of chromatin organization using Electron Microscopy (EM) and low angle X-ray scattering on unfolded fibers resolved particles of approximately 10 nm diameter in size, corresponding to single nucleosomes, connected by linker DNA[23–27]. At Mg^{2+} concentrations exceeding 1 mM arrays of nucleosomes assemble into such a dense structure that it has been impossible to unequivocally reveal the path of the DNA connecting the nucleosomes. Though preparation protocols and imaging techniques have been improved since these pioneering studies, more recent Atomic Force Microscopy (AFM)[28] and EM studies[29] have not been able to discriminate between two main models of chromatin folding: a one-start solenoid in which neighboring nucleosomes stack to form a superhe-

lical structure[3, 4, 30] and a two-start zig-zag structure in which neighboring nucleosomes are stacked in two parallel twisted ribbons[31–33].

A different approach to measure chromatin compaction involves sedimentation velocity analysis[34]. The increase of compaction of chromatin fibers is proportional to the ionic strength[35], the concentration of Mg^{2+} [36], and the presence of linker histones[37]. The H4 tail was shown to be essential in a chromatin folding[38]. Disulfide crosslinking via H4-V21C/H2A-E64C mediated disulfide formation confirmed the interaction between these regions in stacked nucleosomes[32]. Importantly, acetylation of H4K16 was shown to lead to defects in folding[39]. Sedimentation analysis can be used for a direct comparison of reconstituted chromatin, as often used for force spectroscopy, with native chromatin. However, though the level of compaction can be accurately compared, sedimentation velocity analysis does not provide sufficient structural detail to resolve the higher order folding of chromatin.

The crystallization of a tetranucleosome was a major break-through in the understanding of chromatin folding[31]. In this structure straight linker DNA connects neighboring nucleosomes. Even and odd nucleosomes stacked on each other, pointing to a two-start helix when extrapolated to fibers containing more nucleosomes. The interaction between the H4 tail and an acidic patch at the surface of H2A that was present in the original structure of the mononucleosome[1] and was implicated in mediating nucleosome stacking was not observed in the tetranucleosome. Importantly, the straight linker DNA configuration observed in the tetramer is not compatible with the observation that the diameter of the folded fibers is independent of the linker DNA length between 30 and 50 bp[29]. Thus, even X-ray crystallography, elegant crosslinking experiments and detailed EM studies have not been able to settle the controversy of chromatin folding.

1.3 Single molecule force spectroscopy

The unique ability of single molecule force spectroscopy to unravel chromatin from its maximally folded to, and beyond, its fully extended structure directly addresses the connectivity puzzle that has persisted. Several force spectroscopy techniques have been developed and applied to chromatin. In this section we will summarize the different approaches and discuss the particular aspects of each technique in relation to the chromatin studies that have been published.

Optical Tweezers (OT) have been used most frequently for chromatin unfolding studies. In OT, a polystyrene bead is trapped by a focused laser beam and its lateral position is typically monitored by measuring the deflection of a second

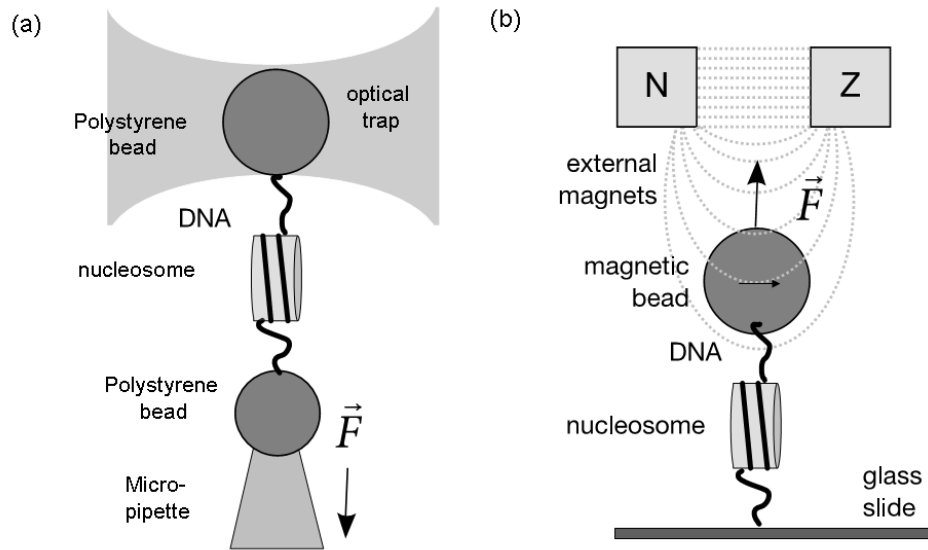


Figure 1.1: Schematic representation of optical and magnetic tweezers (a) A mononucleosome is tethered between two polystyrene beads at both ends. One bead is trapped in a focused laser beam and the other is held with a micropipette. By moving the pipette, the mononucleosome is stretched. Without further feedback optical tweezers function as a position-clamp (b) A mononucleosome is anchored on the the glass-slide and is tethered to a magnetic bead. The bead is attracted towards the highest magnetic field gradient which is generated by a pair of external magnets. Decreasing the height of the magnets increases the applied force on the mononucleosome.

laser beam. Chromatin fibers can be attached to the bead, typically using biotin modified DNA ends and streptavidin coated beads. The other end of the fiber is attached to a different surface, being a cover slide[40, 41], a second bead fixed to a micropipette[42–44] or a second bead trapped in a second optical trap. Either by moving the trapped bead, or by displacing the laser beam (Figure 1.1a) or the anchoring point on the other side of the fiber with a piezo actuator, the fiber can be stretched to forces between 1 and 100 pN. During the stretching, the extension of the fiber is recorded and the applied force is calculated from the multiplication of the trap stiffness and the displacement of the bead from the center of the optical trap. The results are presented as Force-Extension (FE) traces. In this configuration OT act as a position-clamp: any reorganization of the fiber that changes its contour length will not be observed as a change in end-to-end distance but will increase or decrease the force acting on the fiber. With a force feed-back loop, OT can be converted to a force-clamp in which the extension is adjusted

to maintain the preset force[40]. Typically, position-clamps excel in measuring (rupture) forces and force-clamps excel in measuring (rupture) distances. In OT, the bead is free to rotate preventing accumulation of twist.

In Magnetic Tweezers (MT) a molecule is anchored to the surface of a cover slip and tethered to a super-paramagnetic bead. The bead's permanent magnetic moment aligns with the field of a pair of magnets above the sample and as such the bead is torsionally constrained in the direction of the magnetic field (Figure 1.1b). The force decreases exponentially with the distance between the bead and the magnets[45]. The decay length of the magnetic field gradient is two orders of magnitude larger than the dimensions of the fibers and the bead, so MT function as a force-clamp. The position of the bead is measured in three dimensions by video microscopy and image processing, from which the force is calculated by dividing the height of the bead by its lateral fluctuations[46]. MT has the advantage of detecting the changes of the end-to-end distance of the measured molecules in the low force regime below 1 pN, and its sensitivity is inevitably decreased by the increase of Brownian fluctuations. When the fiber is attached to the bead and the surface with multiple bonds, nucleosome translocation caused by nucleosome remodelers could induce a torque on the bead. Reversibly, rotation of the external magnets will twist the fiber, making MT applicable in its ability to address the topology of chromatin fibers.

A third convenient means of single molecule force spectroscopy on chromatin fibers is flow stretching[47]. Here, chromatin fibers are also attached to a surface, in this case the bottom of a flow cell and optionally to a bead on the other end. During flow, the viscous drag of the tether and the bead will stretch the fiber and changes in contour length due to association and dissociation of proteins in the buffer are recorded as a change in the extension of the fiber. Though this approach has the potential of increasing the throughput by monitoring multiple fibers in parallel, the control and determination of the applied forces is less direct than using optical or magnetic tweezers.

Atomic Force Microscopy (AFM) can not only be used for imaging biomolecules but also to stretch them between a surface and the tip of the cantilever[48]. The relatively stiff cantilevers, compared to the stiffness of the optical trap in OT and the tether stiffness in MT, allow for application of large forces of several hundreds of pNs. Leuba *et al.* adhered a chromatin fiber on the surface of a glass slide and pulled on one end of the chromatin fiber with the AFM tip[49]. However, the relatively strong non-specific interactions between chromatin and the surface made it difficult to discriminate between detachment of the nucleosome from the surface and the unfolding of the chromatin fiber. The large rupture forces that were reported indicate that the first dominated the FE

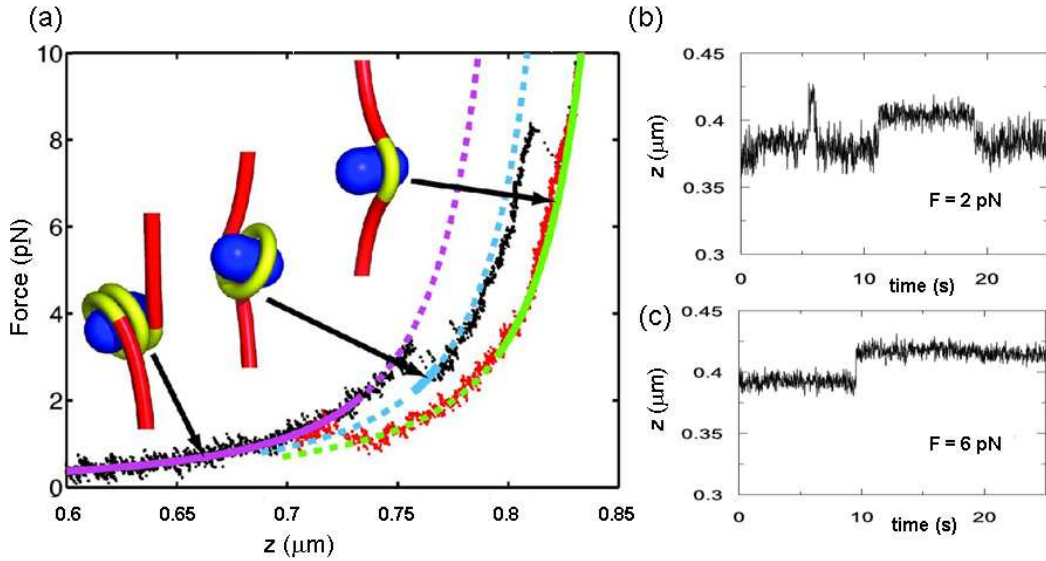


Figure 1.2: Stepwise force induced DNA unwrapping of a mononucleosome. (a) The FE trace shows two distinct steps that can be attributed to DNA unwrapping. Adapted from [52], with permission. The mononucleosome was reconstituted on a 878 nm DNA construct with one 601 nucleosome positioning element. Solid lines in each curve show the FE behavior of the thermodynamically preferred structures. At constant force MT time traces of mononucleosomes reconstituted on a 500 nm DNA with one 601 nucleosome positioning element in 10 mM NaCl and 2 mM Mg^{2+} feature (b) reversible unwrapping of the first turn of DNA at 2 pN and (c) irreversible unwrapping of the second turn of DNA at 6 pN. Reproduced from [53], with permission.

traces.

Each of these single molecule force spectroscopy techniques has its own traits. Here we restrict our discussion to studies that have used OT or MT to measure the response of chromatin in the range between a few fN and 60 pN, at which an overstretching is observed in DNA and nucleosomes dissociate from the DNA. For more information on OT we refer to other reviews [50, 51].

1.4 DNA unwrapping in mononucleosomes

Before dissecting the FE relation of chromatin fibers it is informative to evaluate the stretching behavior of a single nucleosome, avoiding the complex but important interactions between nucleosomes. Using OT, Mihardja *et al.* demonstrated that with increasing force DNA unwraps from the histone octamer in two separate stages (Figure 1.2a) [52]. In 50 mM KAc and 10 mM Mg^{2+} the first reversible transition occurred around 3 pN, which resulted from unwrapping the

first turn of DNA and induced an increase in end-to-end length of 21 nm. The force-dependent unwrapping and wrapping rates were determined from this the equilibrium constant. Using an Arrhenius type expression the rates can be extrapolated to zero force and the free energy associated with first turn unwrapping $\Delta G_{F=0}$ was found to be $12 k_B T$. At $\sim 8-9$ pN a second rupture step occurred with a size of 22 nm, consistent with the length of DNA remaining on the core particle after the first unwrapping event (Figure 1.2a). The second turn of DNA unwraps irreversibly. Therefore the $\Delta G_{F=0}$ of the second turn unwrapping cannot be deduced from the equilibrium constant

In 200 mM KAc the first turn of DNA unwrapping transformed from a well defined rupture to a gradual plateau whereas constant force measurements featured multiple intermediate states of the first turn unwrapping. Based on these observations in the high ionic buffer, Mihardja *et al.* suggested to a link between the strength of electrostatic interactions and histone-DNA interactions[52]. The increased ionic strength shields the histone's positive charges, thus weakens histone-DNA interactions. The free energy of first turn DNA wrapping was only marginally affected by the increase in ionic strength. Kruithof and van Noort reported similar results with MT at constant force and 2 mM Mg^{2+} as shown in Figure 1.2b and c[53]. The unwrapping of the first turn occurred in both studies around 3 pN. The second turn unwrapping involved multiple transition states and intermediates and was strongly dependent on the loading rate[52]. Consistent with this finding, constant force measurements exhibited a lifetime on the order of 10 s at 6 pN[53], showing that given enough time, unwrapping of the second turn can take place at forces significantly smaller than observed at loading rates of several pN/s. By accurately measuring the length fluctuations of the tether in different stages of unwrapping it was possible to retrieve the opening angle of the DNA from the nucleosome which is related to the effective persistence length of the tether[54], yielding a detailed picture of the different conformations. Overall, force spectroscopy on single nucleosomes reveals a force induced unwrapping of DNA from the nucleosome in two distinct steps at 3 and 8 pN that is moderately salt dependent.

The force spectroscopy results on DNA unwrapping in mononucleosomes at first seem at odds with other measurements based on restriction enzyme accessibility[55] or single pair Forster Resonance Energy Transfer (FRET)[56], which generally show a more open structure and $\Delta G_{F=0}$ for unwrapping of $2.5 k_B T$. These essays however are also sensitive for partial unwrapping, extending over less than a full wrap and should therefore resolve many more unwrapping events than the full turn unwrapping that is observed with tweezers. Furthermore, the bandwidth of OT and MT is limited due to the small stiffness of the

trap and the high compliance of the tether. Therefore unwrapping events with a lifetime less than several tens of ms, as measured by FRET, can generally not be resolved using force spectroscopy.

An alternative approach to pulling on a single nucleosome has been developed by the Wang's group[57]. By hooking up both DNA strands at the same end of the wrapped DNA fragment around a histone octamer and subsequently unzipping the DNA, it is possible to measure the increased resistance against strand separation provided by the nucleosome. The resulting disruption-force signatures revealed the locations of histone-DNA interactions and allowed measurement of the position of nucleosomes with 2.6 bp precision. The positioning of a nucleosome before and after remodeling by yeast SWI/SNF, an ATP-dependent chromatin remodeler, was measured by unzipping single DNA molecules [58]. Furthermore, a distinct 5 bp periodicity was revealed in the interaction map together with three broad regions of strong interactions, occurring at the dyad and at 40 bp from the dyad. Thus, in contrast to pulling on both ends of the nucleosome, unzipping experiments reveal gradual unwrapping of DNA from the nucleosome.

1.5 Chromatin assembly strategies

Whereas the assembly, analysis and comparison of mononucleosomes is relatively straightforward, chromatin fibers are intrinsically more complex. Four different strategies for chromatin preparation have been used. Natively assembled chromatin was isolated from chicken erythrocyte nuclei and was biotinylated at both ends prior to insertion to the OT flow cell[43, 44]. Natively assembled chromatin arguably forms the most relevant material for understanding chromatin organization *in vivo* but provides more challenges for interpreting the FE traces. In particular one will find heterogeneity in terms of the number of nucleosomes, the DNA length and sequence, the presence of histone modifications and the possible presence of linker histones and other DNA associated proteins. Though this heterogeneity may be characteristic for the situation in the nucleus, it complicates comparison and reproduction of the experiments. On top of this the purification protocol is not trivial and purification may affect the integrity of the fiber.

An alternative approach is the reconstitution of chromatin from bare DNA, typically lambda DNA, and *Xenopus laevis* egg extract[59]. The cell extract not only provides the part of the histone proteins, but also contains other factors that induce nucleosome formation. Although the DNA substrate is well-characterized and easily obtained, reconstitution in the tweezers setup does not allow additional characterization of the chromatin material. Therefore it is not clear how many

nucleosomes assembled on the DNA, resulting in an unknown linker length, which is key to folding into higher-order structure. Like the natively assembled fibers, the cell extract based reconstitution products may also incorporate non-histone proteins which will affect its structure. Interestingly this method does allow for following chromatin assembly in real-time.

Highly regular periodic arrays of nucleosomes can be assembled on heterogeneous DNA using core histones, the histone chaperon Nuclear Assembly Protein (NAP-1), and ATP-dependent Chromatin assembly and remodeling Factor (ACF)[60]. In this way a better control over protein composition is obtained, though some ACF remains bound to the chromatin.

Nearly perfect control of the composition of the chromatin fiber can be obtained by salt-dialysis reconstitution of nucleosomes on arrays of DNA containing nucleosome positioning elements[61]. Though nucleosomes form on any DNA, some sequences, typically displaying 10 bp repeats of TA dimers, have an increased affinity for histones[62]. Such nucleosome positioning elements occur in nature, for example at the 5S rDNA gene or in MMTV viral DNA. Synthetic sequences have been shown to outperform natural sequences in terms of nucleosome positioning[63]. The 601 sequence reported by Widom for example has a $\Delta\Delta G$ of $-5.7\pm 0.3 k_B T$ relative to random DNA, whereas the 5S rDNA has a $\Delta\Delta G$ of $-0.8\pm 0.2 k_B T$. Using arrays of 601 sequences, the Rhodes group has shown that genuine 30 nm fibers can reproducibly be obtained for repeat lengths of 177 to 207 bp[61]. Though perhaps the reconstituted chromatin fibers are highly idealized compared to chromatin structure *in vivo*, salt-dialysis based reconstitution allows for designing tailored chromatin fibers with defined linker lengths and the use of recombinant histones, thereby avoiding heterogeneity in terms of post-translational modifications.

1.6 Nucleosome-nucleosome interactions in chromatin

Cui and Bustamante were the first to probe nucleosome-nucleosome interactions of purified chicken chromatin with single molecule force spectroscopy[43]. Between 3 pN and 5 pN, they observed a plateau in the FE trace that could be attributed to the transition between a folded chromatin fiber and an unfolded fiber in which all interactions between the nucleosomes were disrupted. Using a simple two-state model, an internucleosomal attractive energy of $3.4 k_B T$ was obtained in 40 mM NaCl (Figure 1.3a). In these experiments Mg^{2+} was absent. The interaction was salt-dependent and disappeared in 5 mM NaCl. At intermediate

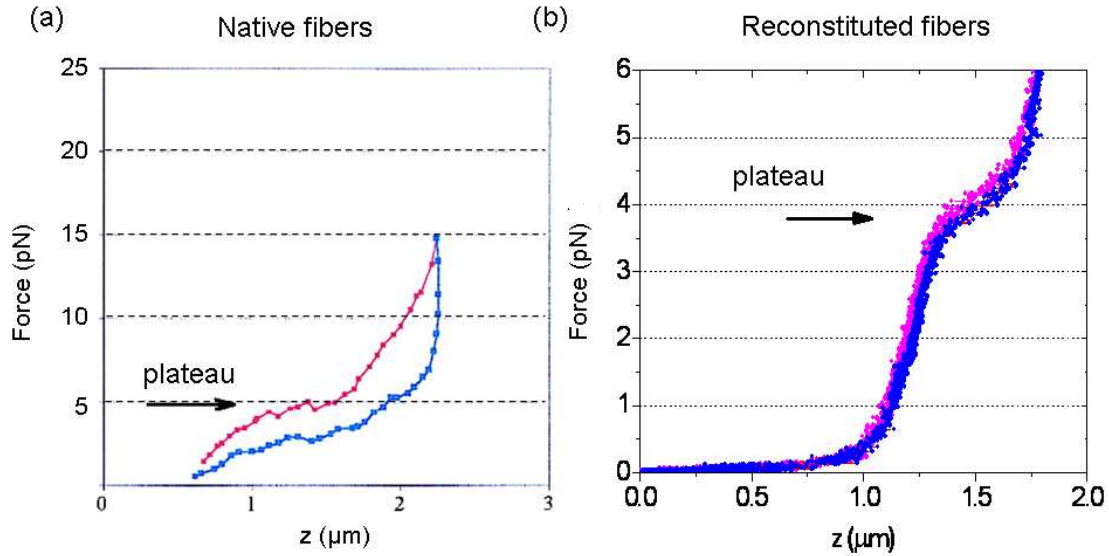


Figure 1.3: The breaking of nucleosome-nucleosome interactions in chromatin fibers was observed in FE traces. (a) A purified chicken chromatin fiber showed a plateau at 5 pN. Hysteresis was observed in 40 mM NaCl and the absence of Mg^{2+} . Adapted from [43], with permission. (b) A chromatin fiber reconstituted with chicken histones on 27 repeats of the 601 positioning element featured a plateau at comparable force. No hysteresis occurs in 100 mM KAc and 2 mM Mg^{2+} , indicating the reversibility of the unfolding and refolding of the chromatin fiber under tension. Original data, conditions as described in [64].

forces (7-20 pN), significant hysteresis occurred pointing to the non-equilibrium disruption of the fiber. The hysteresis was reproducible in successive stretching events on a single fiber. Above 20 pN, the FE traces became neither reversible nor reproducible, possibly indicating dissociation of linker histones or histone octamers.

Recently we exploited the better force resolution of MT and the control over the composition of reconstituted fibers on 601 positioning elements to advance on these findings (Figure 1.3b) [64]. The FE traces showed four major stages of extension at increasing forces: an extension of the DNA handles flanking the fiber following a Worm-Like-Chain (WLC), a linear extension of the chromatin fiber up to three times more than its rest length, a plateau corresponding to the rupture of internucleosomal interactions at 4 pN, and a WLC-like extension of the beads-on-a string fiber with a reduced persistence length relative to DNA (Figure

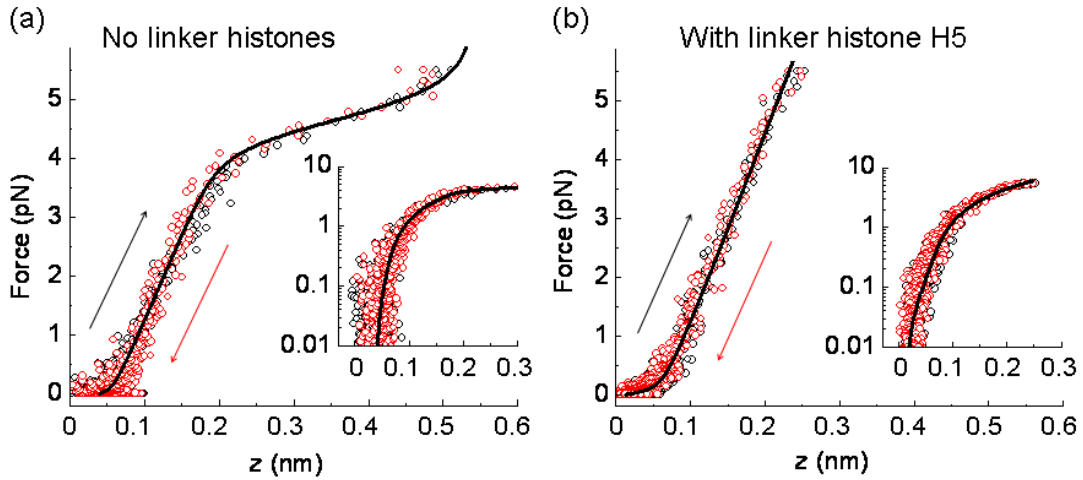


Figure 1.4: Reversible stretching of chromatin fibers folded in a 30 nm fiber. a) Fibers without linker histones feature a force plateau at 4.5 pN that could be attributed to unstacking of nucleosomes. No hysteresis was observed. At smaller forces the fiber stretches linearly. Black dots: forward trace, Red dots: backward trace. Solid black line: fit to a linear combination of springs representing DNA described by a WLC, a stacked array of nucleosomes described by a Hookean spring and a beads-on-a-string fiber described by a WLC. Inset: Same data on a logarithmic scale emphasizing the excellent fit in the force range between 10 fN and 5 pN. b) Fibers with stoichiometric amounts of linker histones resist unstacking up to at least 5 pN. Black dots: forward trace, Red dots: backward trace. Solid black line: fit to a linear combination of springs representing DNA described by a WLC and a stacked array of nucleosomes described by a Hookean spring. The three-fold extension of the fiber without disruption of the stacked nucleosomes that was found in both FE traces indicates of a one-start solenoid structure. Adapted from [64].

1.4a). Importantly, all curves were reversible and reproducible in successive FE experiments. DNA unwrapping was shown to occur only at forces exceeding 7 pN. The nucleosome interaction energy of several $k_B T$ found by Cui and Bustamante could be reproduced in absence of Mg^{2+} , but in conditions known to induce folding into a 30 nm fiber, the internucleosomal interaction energy was as large as $17 k_B T$. We argued that the 3-fold linear extension of the fiber, while the nucleosomes remain stacked onto each other, indicates a solenoidal folding for the 30 nm fiber. Importantly, when the linker length was decreased from 50 to 20 bp, a longer and stiffer fiber was obtained, hinting at a two-start arrangement. The inclusion of stoichiometric amounts of linker histone surprisingly did not affect the length nor the stiffness of the fiber (Figure 1.4b), but stabilized nucleosome stacking up to 7 pN.

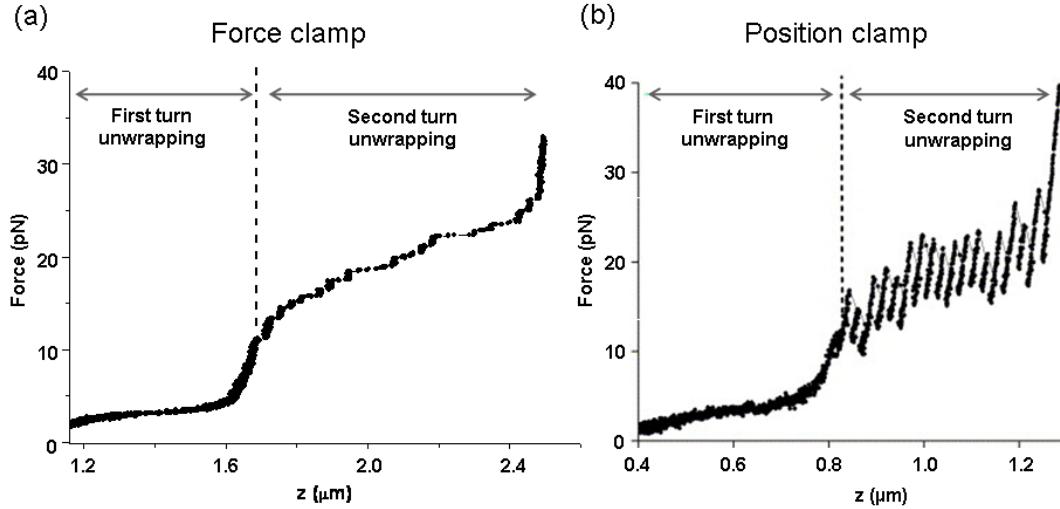


Figure 1.5: FE traces of reconstituted chromatin fibers showing unwrapping events (a) A chromatin fiber reconstituted with chicken histones and 27 repeats of the 601 positioning element measured with MT. The length of fiber below 10 pN converges to the length expected for 27 nucleosomes with only a single turn of DNA. The events above 10 pN show a stepwise length increase corresponding to the unwrapping of DNA of the second turn. Original data, conditions as described in[64]. (b) A reconstituted chromatin fiber with chicken histones and 17 repeats of the 5S rDNA positioning element measured with OT. Adapted from[41], with permission. Though the overall shape of the FE trace differs between the force-clamp and the position-clamp, similar signatures are observed.

1.7 DNA unwrapping in chromatin

Seemingly in contrast to the results reported on single nucleosomes, nucleosome arrays can bear much higher loads before unwrapping DNA from the histone core occurs. On reconstituted arrays based on 5S rDNA positioning elements Brower-Toland *et al.* reported a gradual extension of the fiber between 6 and 20 pN[41], up to a length that is consistent with the first turn unwrapping of DNA in all nucleosomes. Our MT results on 601 based arrays also indicate a gradual, reversible unwrapping of the first turn of DNA between 7 and 10 pN. In the presence of NAP-1 however, Bancaud *et al.*[65] observed a stepwise unwrapping event of the first turn DNA in the some force region. These studies show that when incorporated into an array, the rupture force for DNA unwrapping increases from approximately 3 pN to 7 pN. As a result, nucleosome unstacking occurs in a distinctly lower force regime than DNA unwrapping, allowing separation of these events.

Reconstituted fibers display unwrapping of the second turn of DNA at forces

between 10 and 25 pN, corresponding to a stepwise length increase of 23-25 nm[40, 44]. Figure 1.5b shows the distinctive peaks that appear in a position-clamp. We reproduced similar results with MT, acting as a force-clamp. In the latter case rupture events result in a stepwise increase in length instead of a sudden drop in tension, which reduces the rates of successive unwrapping events as shown in Figure 1.5a. Nevertheless, in both cases very similar step sizes and rupture forces are observed, that are characteristic for forced unwrapping of DNA in reconstituted nucleosome arrays.

In nucleosome arrays based on heterogeneous DNA the unwrapping events of the second turn of DNA yielded a very similar rupture length but the unraveling force varied between ~ 5 and 65 pN, with the majority of events at lower force[60]. This is the only study with heterogeneous DNA and purified histone proteins, showing that DNA sequence is an important factor in determining the force dependent stability of nucleosomes.

By performing dynamic force spectroscopy, Brower-Toland *et al.*[40] measured an activation-barrier for unwrapping of the second turn of DNA of 36-38 $k_B T$ and a distance between the barrier and the wrapped state of 3.2 nm. The large activation barrier provides a strong resistance against forced unwrapping and subsequent histone dissociation. In this study, the nucleosome arrays showed unwrapping and rewrapping in successive FE cycles up to 50 pN. However, the number of characteristic peaks gradually decreased, indicating irreversible dissociation of the histones at higher forces. Thus even fully unwrapped, the histone octamer has a finite life time to remain bound, probably on the location of dyad axis, before dissociation. The complete dissociation of histones was observed after stretching the fiber up to 60 pN, close to the melting transition of DNA.

In typical single molecule experiments the concentration of chromatin fibers is small. In an extensive study of nucleosome stability under single molecule experimental conditions Claudet *et al.*[44] showed that linker histone dissociation and subsequent dissociation of the H2A-H2B dimer can readily occur in force spectroscopy experiments. In fact, the rupture of the second wrap of DNA from the histone octamer, which is most characteristic in these type of experiments, can not be distinguished from unwrapping of the DNA from a tetramer consisting of $(H3-H4)_2$ only. The absence of a distinctive signature in the unwrapping of the first turn makes it hard to unequivocally prove octamer integrity. In our studies of higher-order structure however we observed a very distinct length and stiffness of the 30 nm fiber and under Mg^{2+} free conditions a WLC behavior of the beads-on-a-string conformation with a contour length that indicated fully wrapped nucleosomes[64]. Together with the reversible two-state unwrapping in single nucleosomes[52, 53, 57], it is therefore clear that histone octamers can

be stable under single molecule conditions, but octamer dissociation should be carefully considered.

1.8 Nucleosome dynamics in cell-extract assembled chromatin

Chromatin assembled using cell extracts showed three major disruption step sizes of ~ 65 nm, ~ 130 nm, and ~ 195 nm[42]. The (multiples of) 65 nm steps exceed of the length of DNA wrapped around a single histone octamer. Though somatic linker histones were absent in these extracts, other proteins like embryonic linker histone B4[66] and High Mobility Group (HMG) proteins[67] were abundantly present. Such proteins stabilize additional DNA on the nucleosome, which could explain the larger step size and the all-in-one release of the DNA without sub steps. This is also consistent with the larger spread in rupture forces, between 20 and 50 pN that was reported. The number of opening events dropped in the successive stretch-relax cycles, indicating that DNA unwrapping was not reversible in the abstract-free buffer. In the solutions containing cell extracts FE traces were reproducible. In a later study with similar material rupture lengths of ~ 30 and ~ 60 nm were reported[68] and attributed to ruptures that include linker DNA and linker histones. Analysis of the loading rate revealed three barrier heights between 20 and $28 k_B T$. The highest barrier was observed less frequently after repeated pulls, possibly due to the release of linker histone B4.

Using similar lambda chromatin fibers, Yan *et al.* studied the assembly and disassembly of chromatin fibers in real time at constant force using MT[69]. In the absence of ATP the compaction of DNA into chromatin followed first order kinetics up to a load of 3.5 pN. Above 3.5 pN, the chromatin fiber started to rupture with the step size of ~ 50 nm, which would correspond to two full turns of DNA wrapping but may also indicate the rupture of internucleosomal contacts or simultaneous rupture events. At 3.5 pN assembly and disassembly occurred at the same rate, yielding no net compaction of the fiber. In the presence of ATP and at forces below 4.2 pN, the chromatin fiber showed 200 to 400 nm length changes that occurred with a velocity of 6 to 42 nm/s for forces of 3.5 down to < 1 pN. Appreciable assembly was only reported below 1 pN. Though the identity of the ATPases was not known, the ATP-dependent chromatin reorganization was attributed to processive ATPases that remove and transport nucleosomes in chromatin. As both ATP and ATPases prevail *in vivo*, this study shows that the dynamics of chromatin organization will be far more complex than what can be captured in regular stable fibers.

1.9 Structural influences of histone modifications

A major source of diversity in chromatin is the abundant presence of histone variants and post translational modifications of histones. Especially the histone tails, and acetylation of these tails, have been implicated to play an essential role in chromatin organization[70]. Chromatin fibers containing tailless histones, obtained by digestion with trypsin[41] revealed three major differences compared to untreated fibers: i) 60% of the first turn of DNA appeared unwrapped at small forces, ii) the integrity of the second turn of DNA was not affected but iii) the rupture forces for unwrapping the second turn of DNA were reduced by several pN. The tails of the H2A-H2B dimer contributed more to these effects than the tails of the tetramer. An increase in the fluidity of native chromatin upon digestion by trypsin that was reported by Roopa and Shivashankar seems consistent with these findings[71].

A more specific local effect can be expected for the acetylation of lysines. Brower-Toland *et al.* tested the effect of global acetylation of histones by p300[41]. The addition of $\sim 15-19$ acetyl groups per nucleosome resulted in similar but less extensive effects as found for histone tail removal: 9-23% of the first turn was unwrapped, the second turn remained stable, but displayed a $\sim 0.6-1.8$ pN reduction of the rupture force. Based on these data, a model of the contributions of histone tails was proposed in which H2A/H2B tails predominantly, but not exclusively, regulate the strong off-dyad interactions. It is clear that histone modifications, like acetylation, are highly regulated *in vivo*, and tail removal or global acetylation is only the first step in deciphering the structural changes of that defines the histone code[72].

1.10 Diversity in experimental conditions

A major challenge in comparing the various results from chromatin force spectroscopy is the large number of parameters that define the composition and structure of chromatin. Though this reflects the wide variety of structures and components that can be expected *in vivo*, it complicates the interpretation and comparison of the reported data. This is especially persistent in force spectroscopy studies as only two coupled parameters, i.e. force and extension, are measured. Structurally different events can result in the same increase in end-to-end distance, making it non-trivial to unequivocally attribute changes in length to specific transitions. For example a length increase of ~ 22 nm at 7 pN was at-

Chapter 1: Diversity in experimental conditions

Table 1.1: The comparison of experimental conditions. *Principal results refer to the diagram sketched in Figure 1.6

type	DNA	Histone	Na ⁺ or K ⁺ (mM)	Mg ²⁺ (mM)	proteins	Principal results*	Technique	ref.
reconstituted fiber	5S	chicken	0, 25	none	none	a	MT	[65]
			100	1.5	none	de	OT	[40]
			100	1	none	d	OT	[44]
		chicken (tailless) (acetylated)	100	1.5	none	cd	OT	[41]
	chicken (tetramer)	100	none	none	d	OT	[44]	
	601	chicken	100	2	none, H5, H1	ab	MT	[64]
purified fiber	chicken	chicken	5, 40, 150	none	linker histones	b	OT	[43]
			5, 100	none	linker histones	d	OT	[44]
assembled fiber	Lambda	Xenopus	150	none	non-histones	cde	OT	[42]
mononucleosome	601	chicken	10	2	none	cd	MT	[53]
			10	10	none	cd	OT	[52]

tributed to second turn unwrapping in the study of single nucleosomes[52], while ~ 24 nm length increase at the same force was reported for first turn unwrapping in nucleosome arrays[65]. Given the setting of both experiments there is no doubt that these events were interpreted correctly, but this example clearly shows that FE traces should be assessed in the context of their experimental setup. The various studies on chromatin that feature different approaches to force spectroscopy, like force clamps and position clamps, result in strikingly different FE traces, as shown in Figure 1.5, but the magnitudes of the rupture forces, rupture lengths and life times are comparable.

In Table 1.1 we summarized the different experimental conditions used in the papers reviewed here. Despite the differences a number of conclusions can be drawn based on these results, of which many were previously revealed by bulk techniques: i) Reconstituted fibers are more regular than than purified chromatin fibers. ii) The stronger the positioning element, the better the reconstitution result. iii) Histone tails modulate nucleosome stability. iv) Monovalent salt screens the electrostatic interactions that stabilize DNA folding into nucleosomes. v)

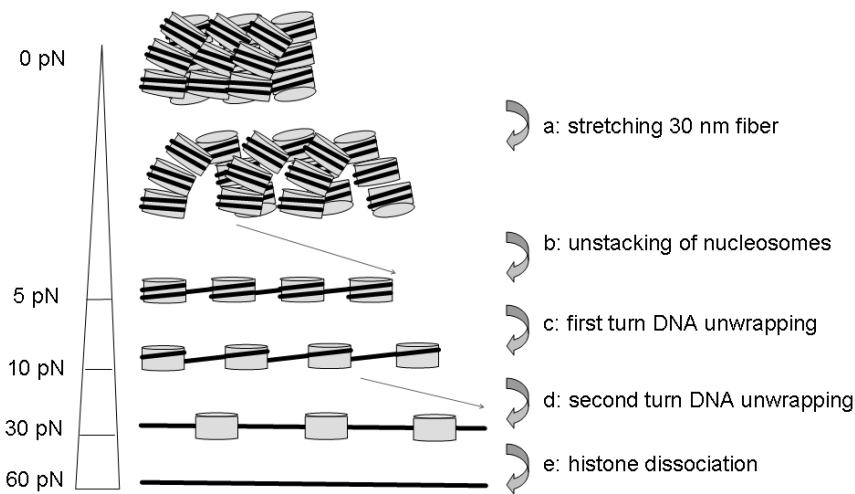


Figure 1.6: Schematic representation of chromatin fiber unfolding with the increasing force

Mg^{2+} is required for higher-order folding vi) Linker histones stabilize a few tens of bp of DNA onto the nucleosome. vii) Chromatin is a dynamic structure that can provide other proteins access to the DNA. These observations are not merely verifications of known properties of chromatin; in many cases force spectroscopy provides the most direct measurements on these structures. Furthermore force spectroscopy does not expose chromatin to staining, freezing, electrophoresis, surface deposition or crystallization. In the light of the various treatments that are necessary for those types of experiments, the differences between the experimental conditions of the studies reviewed here are not very large.

1.11 Structural transitions in chromatin under force

A unique feature of single-molecule force spectroscopy is the ability to directly resolve the dynamics of structural changes. From the combined studies it is possible to extract a global picture of force induced chromatin unfolding, as schematically depicted in Figure 1.6. With increasing force the folded fiber stretches, nucleosome-nucleosome interactions are broken, resulting in a beads-on-a-string fiber, the first turn of DNA is unwrapped, the second turn follows, and at 50 pN the histone octamer dissociates from the DNA. It is fortunate that these stages can sometimes be separated. However, especially the first stages of unraveling are likely to occur spontaneously, even in the absence of force, which will result

in concurrent unfolding of different stages. In fact the clear separation of fiber stretching and nucleosome unstacking was only reported in our recent study with highly regular fibers based on arrays of 601 positioning elements and in the presence of Mg^{2+} [64]. In the regular arrays on random DNA studied by Gemmen *et al.* [60] the second turn unwrapping occurred in a large range of rupture forces. If the same variance occurs for the first turn unwrapping, by stretching chromatin fibers with OT/MT, it will be difficult to make a clear distinction between nucleosome unstacking and first turn unwrapping that was possible with nucleosome arrays reconstituted on arrays of positioning elements. Therefore much more variation is also to be expected in more irregular fibers at low force.

One of the challenges in resolving the first stages of chromatin unfolding with force spectroscopy is the very small stiffness of the fiber itself. Most studies report a persistence length of ~ 15 - 20 nm for the beads-on-a-string fiber [43, 60, 64], i.e. three times shorter than that of DNA. The folded 30 nm fiber has a stiffness of ~ 0.025 pN/nm [64], which is more than 1000 times smaller than the stiffness of a typical optical trap. Following the equipartition theorem, such flexible tethers will feature relatively large fluctuations in extension, in the case of a 30 nm fiber consisting of 25 nucleosomes these fluctuations amount up to 30% of its length, i.e. 15 nm. Rupture length changes of similar size will be hard to resolve, though Hidden Markov analysis may partially relieve this problem [53]. The stiffness of a WLC increases significantly at higher forces, which is one of the reasons why second turn unwrapping is easier to resolve than earlier transitions in unfolding. The longer the fiber, the smaller the tether stiffness which will result in a larger amplitude of thermal length fluctuations. This explains why more detail can be resolved in shorter than in longer fibers.

Second turn unwrapping features a very high activation barrier, making this transition virtually irreversible at high force. All other structural transitions have a smaller activation barrier, which yields higher folding and unfolding rates. The resulting shorter lifetimes in combination with the larger amplitude of thermally induced length fluctuations at low force, as discussed in the previous paragraph, further complicates distinguishing separated states of (un-)folding. The resulting gradual changes superimposed on thermal fluctuations are more difficult to analyze. Most studies have so far focused on the high force transitions which are easier to resolve and interpret.

When the transitions are reversible, analysis of the FE trace using equilibrium thermodynamics can be an alternative approach. We successfully applied this for the stacking-unstacking transition shown in Figure 1.4a. The absence of hysteresis is a clear indication of thermodynamic equilibrium. The entire trace could be modeled as a force induced transition between stacked nucleosomes

and unstacked nucleosomes[64]. In this model the chromatin fiber was treated as two springs in series, one corresponding to the DNA flanking the chromatin fiber and one to the chromatin itself. When all nucleosomes were stacked, the extension of the folded fiber fitted well to a Hookean spring(Chapter 2). The array of unstacked nucleosomes fitted well to a WLC. Force induced unstacking of nucleosomes was included by using a force dependent linear combination of these springs. The resulting fit parameters matched well with the known dimensions of the chromatin fiber. Interestingly, from the obtained stiffness of the fiber we estimated a Young's modulus that indicates that the high compliance of the structure originates from the disordered histone tails(Chapter 2).

The accumulating amount of data on pulling on chromatin provides the necessary input for computer modeling. In these studies coarse graining was necessary because of the large size of the fibers. Various schemes based on Monte Carlo (MC) algorithms[73–76] or geometrical constraints[77, 78] have been tested. Many different structures have been proposed but the lack of detailed structural data has up to now made it difficult to put these simulations to the test. What is clear from many of these simulations is that the length of the linker DNA has a critical role in organizing chromatin. The length of the linker DNA varies between 10 bp and 90 bp[79, 80] and the mechanical properties of DNA at these length scales however are currently heavily debated[81]. New force spectroscopy experiments on chromatin with controlled linker lengths have the potential to resolve the structural effects of changes in linker length. For a detailed interpretation it will become important to combine such results with computer modeling and iterate between experiments and modeling.

1.12 More tension on chromatin

After almost 10 years of single molecule force spectroscopy on chromatin, the outlines of force induced chromatin unfolding and refolding have been sketched. Despite the large variety of experiments, chromatin composition, structures and transitions, it appears that a hierarchical unfolding pathway, as sketched in Figure 1.6, can globally describe the data reviewed here. The force regime in which these transitions occur is highly relevant for *in vivo* conditions and single molecule force spectroscopy is the only experimental tool available to probe force induced unfolding pathways. In conclusion, the manipulation of chromatin fibers one-at-a-time has contributed significantly in our understanding of DNA organization in the eukaryotic cell.

Many unresolved issues in chromatin folding however remain. As mentioned

before, the relation between linker length and chromatin folding requires more attention as well as the effect of DNA sequence on nucleosome stability. The effect of linker histones on chromatin stability has almost exclusively been tested with cell extract reconstituted chromatin in which little detail can be resolved at low forces. It is likely that fibers reconstituted from pure components will yield more detailed information on this issue. Post-translational histone modifications are a major focus of current research and provide an enormous challenge in terms of understanding its structural effects on chromatin. Brower-Toland *et al.*[41] have exclusively addressed this issue, with the relatively crude methods of global digestion or acetylation of histone tails that were available at the time. Recent developments in synthetic biology have made it possible to produce histones with site-specific modifications in sufficient amounts to incorporate these into chromatin fibers[82, 83]. Before using these modified fibers it will be essential to resolve the differences between recombinant, non-modified histones and chicken erythrocyte histones that have predominantly been used so far.

With a comprehensive understanding of the force response of chromatin fibers, it will become possible to investigate the interactions of other proteins with chromatin. Complexes especially relevant in this respect are known to affect chromatin structure, such as ATP-dependent chromatin remodellers, helicases, RNA and DNA polymerases, hormone receptors and many others. The molecular mechanisms involved at the nucleosomal level in these processes remain largely obscure and single molecule force spectroscopy may contribute to shedding light on these issues. Though the ATP-dependent length fluctuations of cell extract assembled chromatin that were reported by Yan[69] provide some insight, it will be far more illuminating when purified components are used to which specific effects can then be attributed. In a pioneering study of the Bustamante group it was shown that the ATP-dependent remodellers SWI/SNF and RSC can create DNA loops of a broad range of sizes (20-1200 bp) in a nucleosome-dependent manner[16]. It is likely that more such studies will become available in the near future. In conclusion, ten years of tension on chromatin has been fruitful for understanding its structure and dynamics. Now that this branch of single molecule studies has matured many important questions related to eukaryotic chromatin organization can be addressed at the single molecule level.

1.13 Scope of this thesis

This thesis presents a progressing understanding of chromatin structure and dynamics, using magnetic tweezers as a tool to manipulate force-dependent con-

formational changes at the single molecule level. Each chapter is written as a research article on the experimental methodology and presents specific perspectives on rupture of higher-order folding of chromatin.

Chapter 1 gives an overview of force-dependent chromatin unfolding. Comparing general features and properties of chromatin fibers under tension in a variety of experimental conditions, we found that detailed mechanisms of the events occurring above 15 pN have been thoroughly examined. The lack of understanding the events in the low force regime motivates the investigations as described in the following chapters.

Chapter 2 reports the quantification of mechanical properties of chromatin higher order folding. Stretching chromatin fibers reconstituted with defined components, such as linker histones and linker DNA, we examined how those intrinsic components contribute to the mechanics of chromatin fibers. With a 2-state model, we analyzed force-extension traces and discuss the possible origin of the structural change occurring between 2 and 4 pN.

Chapter 3 further explores the structural change in chapter 2 and quantifies the intrinsic heterogeneity in our chromatin fibers. Benefiting from the method developed in this chapter, we measured the absolute extension of chromatin fibers more accurately. Expanding the 2-state model used in the previous chapter, we re-examine the mechanical properties of chromatin fibers and quantify its dependence on buffer conditions.

Chapter 4 describes the dynamics of single nucleosomes in chromatin unfolding. We combined dynamic force spectroscopy and constant force measurements to resolve the behavior of individual nucleosomes. Using the 2-state model and a parameterized Hidden Markov model, we extracted the kinetics of single nucleosomes from the extension of chromatin fibers. Our findings quantify for the first time delicate nucleosome-nucleosome interactions and first turn DNA unwrapping within chromatin higher order folding.

Bibliography

- [1] Luger, K., Mader, A., Richmond, R., Sargent, D. & Richmond, T. *Nature* **389**, 251–260 (1997).
- [2] Sheng, S., Czajkowsky, D. & Shao, Z. *Biophys. J.* **91**, L35–L37 (2006).
- [3] Finch, J. T. & Klug, A. *Proc. Natl. Acad. Sci. U.S.A.* **73**, 1897–1901 (1976).
- [4] Thoma, F., Koller, T. & Klug, A. *J. Cell Biol.* **83**, 403–427 (1979).

Bibliography

- [5] d'Erme, M., Yang, G., Sheagly, E., Palitti, F. & Bustamante, C. *Biochemistry* **40**, 10947–10955 (2001).
- [6] Strick, R., Strissel, P., Gavrilov, K. & Levi-Setti, R. *J. Cell Biol.* **155**, 899–910 (2001).
- [7] Mller, W. G. *et al.* *J. Cell Biol.* **177**, 957–967 (2007).
- [8] Conconi, A. *DNA Repair (Amst)* **4**, 897–908 (2005).
- [9] Roca, J. *Nucleic Acids Res.* **37**, 721–730 (2009).
- [10] Chaban, Y. *et al.* *Nat. Struct. Mol. Biol.* **15**, 1272–1277 (2008).
- [11] Gerlich, D., Hirota, T., Koch, B., Peters, J.-M. & Ellenberg, J. *Curr. Biol.* **16**, 333–344 (2006).
- [12] Milne, T. A., Zhao, K. & Hess, J. L. *Methods Mol. Biol.* **538**, 1–15 (2009).
- [13] Lavelle, C. *Biochem. Cell Biol.* **87**, 307–322 (2009).
- [14] Wang, M. D. *et al.* *Science* **282**, 902–907 (1998).
- [15] Hamdan, S. M., Loparo, J. J., Takahashi, M., Richardson, C. C. & van Oijen, A. M. *Nature* **457**, 336–339 (2009).
- [16] Zhang, Y. *et al.* *Mol. Cell* **24**, 559–568 (2006).
- [17] Leschziner, A. *et al.* *Proc. Natl. Acad. Sci. U.S.A.* **104**, 4913–4918 (2007).
- [18] Hansen, J. C. *Annu. Rev. Biophys. Biomol. Struct.* **31**, 361–392 (2002).
- [19] Tremethick, D. *Cell* **128**, 651–654 (2007).
- [20] Horn, P. & Peterson, C. *Science* **297**, 1824–1827 (2002).
- [21] van Holde, K. & Zlatanova, J. *Semin. Cell Dev. Biol.* **18**, 651–658 (2007).
- [22] Robinson, P. & Rhodes, D. *Curr. Opin. Struct. Biol.* **16**, 336–343 (2006).
- [23] Widom, J. & Klug, A. *Cell* **43**, 207–213 (1985).
- [24] Woodcock, C. L., Frado, L. L. & Rattner, J. B. *J. Cell Biol.* **99**, 42–52 (1984).
- [25] Woodcock, C., Grigoryev, S., Horowitz, R. & Whitaker, N. *Proc. Natl. Acad. Sci. U.S.A.* **90**, 9021–9025 (1993).
- [26] Olins, A. L., Carlson, R. D. & Olins, D. E. *J. Cell Biol.* **64**, 528–537 (1975).
- [27] Olins, A. L., Senior, M. B. & Olins, D. E. *J. Cell Biol.* **68**, 787–793 (1976).
- [28] Leuba, S., Bennink, M. & Zlatanova, J. *Meth. Enzymol.* **376**, 73–105 (2004).
- [29] Robinson, P., Fairall, L., Huynh, V. & Rhodes, D. *Proc. Natl. Acad. Sci. U.S.A.* **103**, 6506–6511 (2006).

- [30] Felsenfeld, G. & McGhee, J. D. *Cell* **44**, 375–377 (1986).
- [31] Schalch, T., Duda, S., Sargent, D. & Richmond, T. *Nature* **436**, 138–141 (2005).
- [32] Dorigo, B. *et al.* *Science* **306**, 1571–1573 (2004).
- [33] Bednar, J. *et al.* *Proc. Natl. Acad. Sci. U.S.A.* **95**, 14173–14178 (1998).
- [34] Ausi, J. *Biophys. Chem.* **86**, 141–153 (2000).
- [35] Butler, P. J. & Thomas, J. O. *J. Mol. Biol.* **140**, 505–529 (1980).
- [36] Ausio, J., Borochoy, N., Seger, D. & Eisenberg, H. *J. Mol. Biol.* **177**, 373–398 (1984).
- [37] Rabbani, A., Iskandar, M. & Ausi, J. *J. Biol. Chem.* **274**, 18401–18406 (1999).
- [38] Dorigo, B., Schalch, T., Bystricky, K. & Richmond, T. J. *J. Mol. Biol.* **327**, 85–96 (2003).
- [39] Shogren-Knaak, M. *et al.* *Science* **311**, 844–847 (2006).
- [40] Brower-Toland, B. *et al.* *Proc. Natl. Acad. Sci. U.S.A.* **99**, 1960–1965 (2002).
- [41] Brower-Toland, B. *et al.* *J. Mol. Biol.* **346**, 135–146 (2005).
- [42] Bennink, M. *et al.* *Nat. Struct. Biol.* **8**, 606–610 (2001).
- [43] Cui, Y. & Bustamante, C. *Proc. Natl. Acad. Sci. U.S.A.* **97**, 127–132 (2000).
- [44] Claudet, C., Angelov, D., Bouvet, P., Dimitrov, S. & Bednar, J. *J. Biol. Chem.* **280**, 19958–19965 (2005).
- [45] Kruithof, M., Chien, F., de Jager, M. & van Noort, J. *Biophys. J.* **94**, 2343–2348 (2007).
- [46] Strick, T. R., Allemand, J. F., Bensimon, D. & Croquette, V. *Biophys. J.* **74**, 2016–2028 (1998).
- [47] Ladoux, B. *et al.* *Proc. Natl. Acad. Sci. U.S.A.* **97**, 14251–14256 (2000).
- [48] Fotiadis, D., Scheuring, S., Mller, S. A., Engel, A. & Mller, D. J. *Micron* **33**, 385–397 (2002).
- [49] Leuba, S. H. & Zlatanova, J. *Arch. Histol. Cytol.* **65**, 391–403 (2002).
- [50] Moffitt, J. R., Chemla, Y. R., Smith, S. B. & Bustamante, C. *Annu. Rev. Biochem.* **77**, 205–228 (2008).
- [51] Neuman, K. C. & Nagy, A. *Nat. Methods* **5**, 491–505 (2008).

Bibliography

- [52] Mihardja, S., Spakowitz, A., Zhang, Y. & Bustamante, C. *Proc. Natl. Acad. Sci. U.S.A.* **103**, 15871–15876 (2006).
- [53] Kruithof, M. & van Noort, J. *Biophys. J.* **96**, 3708–3715 (2009).
- [54] Kulic, I., Mohrbach, H., Lobaskin, V., Thaokar, R. & Schiessel, H. *Phys. Rev. E* **72**, 041905–1–041905–5 (2005).
- [55] Poirier, M. G., Bussiek, M., Langowski, J. & Widom, J. *J. Mol. Biol.* **379**, 772–786 (2008).
- [56] Koopmans, W., Brehm, A., Logie, C., Schmidt, T. & van Noort, J. *J. Fluoresc.* **17**, 785–95 (2007).
- [57] Hall, M. A. *et al.* *Nat. Struct. Mol. Biol.* **16**, 124–129 (2009).
- [58] Shundrovsky, A., Smith, C. L., Lis, J. T., Peterson, C. L. & Wang, M. D. *Nat. Struct. Mol. Biol.* **13**, 549–554 (2006).
- [59] Laskey, R. A., Mills, A. D. & Morris, N. R. *Cell* **10**, 237–243 (1977).
- [60] Gemmen, G. *et al.* *J. Mol. Biol.* **351**, 89–99 (2005).
- [61] Huynh, V., Robinson, P. & Rhodes, D. *J. Mol. Biol.* **345**, 957–968 (2005).
- [62] Thstrm, A. *et al.* *J. Mol. Biol.* **288**, 213–229 (1999).
- [63] Lowary, P. & Widom, J. *J. Mol. Biol.* **276**, 19–42 (1998).
- [64] Kruithof, M. *et al.* *Nat. Struct. Mol. Biol.* **16**, 534–40 (2009).
- [65] Bancaud, A. *et al.* *Nat. Struct. Mol. Biol.* **13**, 444–450 (2006).
- [66] Dworkin-Rastl, E., Kandolf, H. & Smith, R. C. *Dev. Biol.* **161**, 425–439 (1994).
- [67] An, W., van Holde, K. & Zlatanova, J. *J. Biol. Chem.* **273**, 26289–26291 (1998).
- [68] Pope, L. *et al.* *Biophys. J.* **88**, 3572–3583 (2005).
- [69] Yan, J. *et al.* *Mol. Biol. Cell* **18**, 464–474 (2007).
- [70] Robinson, P. J. J. *et al.* *J. Mol. Biol.* **381**, 816–825 (2008).
- [71] Roopa, T. & Shivashankar, G. V. *Biophys. J.* **91**, 4632–4637 (2006).
- [72] Strahl, B. D. & Allis, C. D. *Nature* **403**, 41–45 (2000).
- [73] Langowski, J. & Heermann, D. W. *Semin. Cell. Dev. Biol.* **18**, 659–667 (2007).
- [74] Langowski, J. *Eur. Phys. J. E* **19**, 241–249 (2006).

- [75] Mergell, B., Everaers, R. & Schiessel, H. *Phys. Rev. E* **70**, 011915–1–011915–9 (2004).
- [76] Ren Stehr, K. R., Nick Kepper & Wedemann, G. *Biophys. J.* **95**, 3677–3691 (2008).
- [77] Depken, M. & Schiessel, H. *Biophys. J.* **96**, 777–784 (2009).
- [78] Wong, H., Victor, J. & Mozziconacci, J. *PLoS ONE* **2**, e877 (2007).
- [79] Kornberg, R. D. *Annu. Rev. Biochem.* **46**, 931–954 (1977).
- [80] Widom, J. *Proc. Natl. Acad. Sci. U.S.A.* **89**, 1095–1099 (1992).
- [81] Garcia, H. *et al. Biopolymers* **85**, 115–130 (2006).
- [82] McGinty, R. K., Kim, J., Chatterjee, C., Roeder, R. G. & Muir, T. W. *Nature* **453**, 812–816 (2008).
- [83] Neumann, H. *et al. Mol. Cell* **36**, 153–163 (2009).

Chromatin: A Highly Compliant Helical Folding

The compaction of eukaryotic DNA into chromatin has been implicated in the regulation of all cellular processes whose substrate is DNA. To understand this regulation, it is essential to reveal the structure and mechanism by which chromatin fibers fold and unfold. Here, we have used magnetic tweezers to probe the mechanical properties of a single, well-defined array of 25 nucleosomes. When folded into a 30 nm fiber, representing the first level of chromatin condensation, the fiber stretched like a Hookean spring at forces up to 4 pN. Together with a nucleosome-nucleosome stacking energy of $14 k_B T$, four times larger than previously reported, this points to a solenoid as the underlying topology of the 30 nm fiber. Surprisingly, linker histones do not affect the length or stiffness of the fibers, but stabilize fiber folding up to forces of 7 pN. Fibers with a nucleosome repeat length of 167 bp instead of 197 bp are significantly stiffer, consistent with a two-start helical arrangement. The extensive thermal breathing of the chromatin fiber that is a consequence of the observed high compliance provides a structural basis for understanding the balance between chromatin condensation and transparency for DNA transactions.

This chapter is based on the article: *Single molecule force spectroscopy reveals a highly compliant helical folding for the 30 nm chromatin fiber*, M. Kruithof, F.T. Chien, A. Routh, C. Logie, D. Rhodes and J. van Noort, *Nature Structural and Molecular Biology* **16**, 534-540 (2009)

2.1 Introduction

The eukaryotic genome is organized into chromatin, a highly compacted structure that is now recognized to be a key regulator of all nuclear processes whose substrate is DNA, such as transcription and replication. The lowest level of DNA organization in chromatin is well known: an octamer of histone proteins wrapped by 146 bp of DNA in 1.65 super helical turns [1]. The linker histone organizes an additional 20 bp of DNA and is located at the entry/exit site of the DNA protruding from the nucleosome core[2]. Nucleosome cores are connected by linker DNA, typically 10 - 90 bp in length, forming nucleosomal arrays. Under physiological conditions, including divalent cations, nucleosome arrays fold into compact chromatin fibers with a diameter of about 30 nm[3, 4]. Biochemical and structural data suggest that nucleosome array folding is driven by nucleosome-nucleosome interactions, but that the path of the DNA linking adjacent nucleosomes is unknown. Therefore the structure of the 30 nm chromatin fiber remains controversial, despite three decades of intense research, with the consensus viewpoint see-sawing back and forth between a one-start solenoidal and a two-start zig-zag architecture [5-7].

One of the parameters that defines the architecture of the chromatin fiber is the length of the linker DNA, as expressed in terms of the nucleosome repeat length (NRL). *In vivo*, NRLs vary between 165-212 bp, but NRLs of 188 and 196 bp are by far the most common[8]. Short NRLs are less abundant and generally associated with transcriptionally active chromatin, found for example in yeast[9] and in neuron cells[10]. Long NRLs can be found in transcriptionally silent chromatin from chicken erythrocytes [11]. The presence or absence of the linker histone is a second parameter that affects chromatin folding and has also been implicated in transcription repression. Stoichiometric amounts of linker histone can be found in highly condensed chromatin. In yeast chromatin linker histones are relatively rare. In fact, longer NRLs correlate well with a higher abundance of linker histones[12]. Both the NRL and the presence of the linker histone control the relative positioning of successive nucleosomes in an array and hence direct the formation of higher-order chromatin structures.

Recently major progress in the characterization of higher-order chromatin folding has been obtained using arrays of 601 nucleosome positioning DNA [13, 14]. A 9 Å crystal structure of a tetramer of nucleosome cores, based on a 167 bp NRL array without the linker histones, [15] clearly showed the folding of the two-start helix type. These measurements were supported by crosslinking experiments[16]. Electron Microscopy (EM) on fibers with NRLs between 177 and 217 bp however revealed a well-defined constant diameter of 33 nm [7]. The

dimensions of these fibers, which were independent on the NRL, implied an interdigitated one-start solenoid structure. Thus, in spite of these breakthroughs, the controversy over the structure of the 30 nm fibers and the role of linker histones has not been resolved.

Here we address the question of the structure of the 30 nm chromatin fiber using single molecule force spectroscopy, which probes the extension of single chromatin fibers in solution with nm and sub-pN resolution. Previous force spectroscopy studies have focused on the high force regime, demonstrating the force induced unwrapping of all DNA from the octamer of histones at 15-25 pN[17–19]. Cui and Bustamante[20] did look into the chromatin compaction of long native chromatin fibers at low forces and showed that chromatin fibers unfold at several pNs. In this study we used highly homogeneous chromatin fibers of known composition whose folding has previously been carefully characterized by both sedimentation velocity and EM analyses[21, 22]. This ensures that the fibers analyzed by force spectroscopy are fully compacted and allow us to capture and to quantitatively interpret the initial stages of the unfolding pathway of chromatin fibers in much more detail. Furthermore, we explicitly take the presence and absence of stoichiometric amounts of linker histones into account and demonstrate that linker histones increase the mechanical stability of chromatin fibers. Finally, we compare 197 bp NRL arrays with 167 bp NRL arrays and show, based on their compaction and compliance, that these fibers fold into different structures consistent with a one-start and two-start helical folding.

2.2 Results

2.2.1 Reconstitution of 601 arrays yields regular 30 nm chromatin fibers

Chromatin fibers were reconstituted using salt dialysis from chicken erythrocyte histone octamers and DNA arrays consisting of 25 tandem repeats of 167 or 197 bp 601 DNA, as described[14]. In each reconstitution, the histone DNA stoichiometry was titrated in 8 steps and analyzed using gel electrophoresis[14]. Optionally, stoichiometric amounts of linker histones were reconstituted in a second titration.

Though gel electrophoresis clearly resolves the optimal reconstitution stoichiometry, resulting in the highest level of condensation (Figure 2.1), it does not have the resolution to confirm full saturation of the DNA arrays with histone octamers. To resolve the number of nucleosomes per fiber, which is necessary for

quantitative interpretation of the force spectroscopy data, individual chromatin fibers were imaged with Atomic Force Microscopy (AFM) under denaturing conditions, i.e. in the absence of Mg^{2+} (Figure 2.2a).

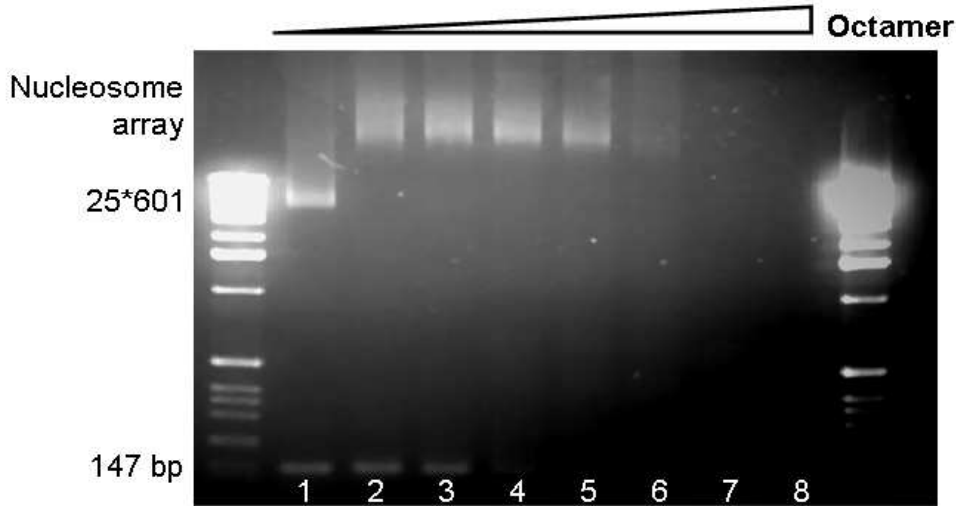


Figure 2.1: Reconstitution of nucleosomal arrays. DNA arrays containing 25*601 nucleosome positioning elements were titrated in 8 steps with chicken erythrocyte histone octamers and mixed sequence 147 bp competitor DNA. Arrays were double-bag dialyzed overnight in reconstitution buffer. 5 μ l of each sample was run on 0.9% agarose gel in 0.2 X TB buffer and stained with EtBr. Except for the experiments in Figure 2.3, which were done with the material from lane 3, all experiments were done with batches that showed the narrowest band for the nucleosomal array, in this case lane 5, pointing at optimal reconstitution.

By counting the number of nucleosomes per fiber we observed a high cooperativity in nucleosome binding on the 601 arrays which was previously also reported on 5S RNA arrays[23]. The distribution of the nucleosome occupancy per fiber (Figure 2.2b) at sub-saturating histone DNA ratios (lane 3 in Figure 2.1) shows a bimodal distribution with populations of sparsely and densely decorated fibers. Reconstitution with a higher histone to DNA ratio (lane 5 in Figure 2.1) yielded 99% of all 601 positioning sites in the fibers being occupied with a histone octamer. In the presence of Mg^{2+} EM inspection confirmed folding of the fibers into regular 30 nm fibers with dimensions that agree well with previously reported experiments [22]. The high regularity, known contour length, and the confirmed folding into 30 nm fibers makes this reconstituted chromatin uniquely suited for probing the forces that drive higher-order chromatin folding.

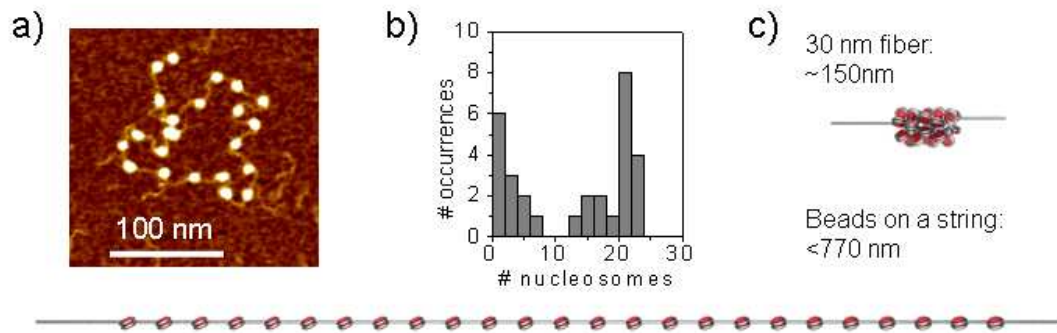


Figure 2.2: Characterization of reconstituted chromatin fibers a) AFM image of a reconstituted fiber under denaturing conditions. b) The distribution of nucleosomes per fiber of a sub-stoichiometric reconstitution shows a bimodal distribution. c) The end-to-end length of an array containing 25 nucleosomes, folded into the 30 nm fiber and flanked by in total of 300 bp of DNA, is approximately 150 nm. When unfolded in a beads-on-a-string conformation it measures 782 nm.

2.2.2 197 bp NRL fibers stretch like a Hookean spring

A quantitative understanding of chromatin compaction requires a detailed comparison with the known dimensions of the fiber components. A single nucleosome core wraps 147 bp of DNA in a cylinder with a diameter of 11 nm and a height of 5.5 nm. The nucleosomes in a 197 bp NRL fiber without linker histones are connected by 50 bp of DNA resulting in a spacing between nucleosomes of 16.6 nm. In the absence of higher order folding the contour length of a fully reconstituted 25*197 bp NRL beads-on-a-string fiber would be approximately 682 nm. For the total contour length of the used fibers an additional 100 nm of flanking DNA must be added, resulting in a contour length of 782 nm (Figure 2.2c). When folded in a 30 nm fiber with a nucleosome line density of 1.5 to 2.1 nm/nucleosome [7] the fiber adopts a length of 38 to 53 nm, resulting in a total contour length of approximately 150 nm.

Magnetic tweezers based dynamic force spectroscopy[24] were used to measure the extension of the fibers with nm resolution. In short, single chromatin fibers are tethered between the bottom slide of a flow cell and a 1 μm paramagnetic bead. The height of the tethered bead is obtained from video microscopy and image processing and represents the end-to-end distance z of the fiber (Figure 2.3a). In a typical Force-Extension (FE) experiment a pair of external magnets is moved down towards the flow cell in 20 s and up again, after which the experiment is repeated. Under folding conditions (100 mM KAc, 2 mM MgAc_2 , 10 mM Hepes

pH 7.6, room temperature) the fibers remained stable upon repeated pulling, sometimes for up to 30 FE cycles.

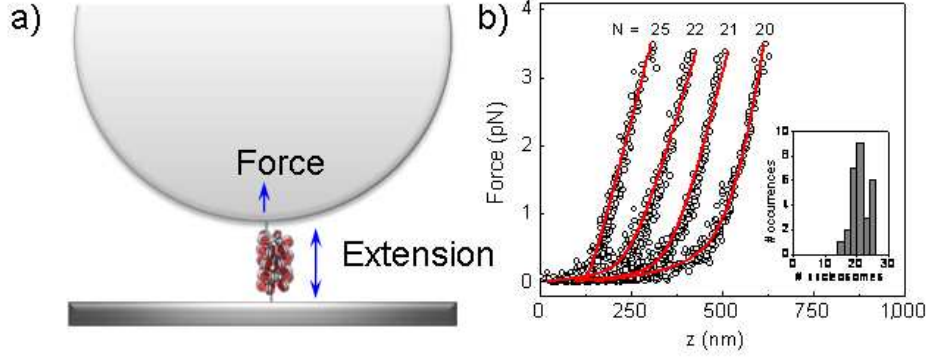


Figure 2.3: Force spectroscopy on chromatin fibers. a) Schematic drawing of a force spectroscopy experiment, not to scale. A 1 μm paramagnetic bead is tethered with a chromatin fiber to a microscope slide. The height of the bead represents the end-to-end distance of the fiber and is obtained from video microscopy and image processing. The force on the fiber is varied by changing the position of a pair of external magnets. b) Force-Extension traces of fibers with different occupations, the solid red lines were fits to Equation 2.2. Inset: distribution of nucleosomes per fiber. Note that we discarded fibers containing small numbers of nucleosomes in this analysis.

At low forces, between 0.5 and 3.5 pN, all folded nucleosomal arrays that we measured, including the sub-saturated fibers that were reconstituted with low histone/DNA ratios, exhibited a linear extension (Figure 2.3b). The FE traces represent the stretching of both the chromatin fiber and the flanking DNA. For a more quantitative interpretation of the tether extension the contributions of the chromatin and the DNA should be separated. The mechanical properties of DNA have been well established. The force $F(z)$, needed to stretch a bare DNA molecule to an end-to-end distance, z , follows a Worm Like Chain (WLC) [25, 26]:

$$F(z) = \frac{k_B T}{p} \left[\frac{1}{4(1 - z/L_0)^2} - \frac{1}{4} + \frac{z}{L_0} \right], \quad (2.1)$$

with thermal energy $k_B T$, contour length L_0 and persistence length p . The compliance of the chromatin fiber on the other hand has not been described before. The linear part of the FE traces (Figure 2.3b) suggests a Hookean extension of the chromatin part of the fiber. We therefore modeled the chromatin fiber as having a rest length L_{30} and a force-induced extension that is inversely proportional to a characteristic spring constant k . This results in a total end-to-end

distance of the tether is

$$z(F) = z_{WLC}(F, L_{DNA}, p_{DNA}) + L_{30} + \frac{F}{k} \quad (2.2)$$

in which z_{WLC} represents the inverse of Equation 2.1, using the contour length L_{DNA} and persistence length p_{DNA} of the flanking DNA. The Hookean approximation proved to fit the data well (Figure 2.3b). The large differences in the contour length of the fibers shown in Figure 2.3b should be attributed to variations in the number of nucleosomes per fiber which was also revealed by AFM imaging of this sub-saturated chromatin batch. It was possible to relate the number of nucleosomes present in each fiber to the fitted length of the flanking DNA, which increases by 197 bp for each missing nucleosome. The resulting nucleosome density distribution (Figure 2.3b, inset) shows good agreement with the distribution obtained by AFM imaging of the same batch (Figure 2.2b). Even in reconstitutions with a histone octamer-DNA stoichiometry that corresponded to the highest compaction we found that 20% of the fibers missed one or two nucleosomes, consistent with a reconstitution yield of 99% of the 601 positioning sites. However, it was possible to discard all sub-saturated fibers based on the fitted length of the flanking DNA, resulting in a more homogeneous data set. Note that even without this selection all fibers feature a very similar slope in the FE trace that is independent of the number of nucleosomes in the particular fiber.

In this chapter we focus on the extensive stretching in the low force regime that provides information on the first steps in 30 nm fiber unfolding. In the low force regime all extensions of the folded chromatin fiber appeared linear. In contrast to previous force spectroscopy studies on nucleosomal arrays[19, 27, 28], which were performed at higher forces, we did not see indications of DNA unwrapping from the nucleosome. Indeed, only at forces exceeding 7 pN we observed hysteresis in the FE traces and extensions beyond the length of the beads-on-a-string conformation (Figure 2.4). Both non-linear features indicate concurrent fiber unfolding and DNA unwrapping. In order to preserve the higher order folding, we not only limited the maximal force to 6 pN, we also carefully optimized experimental conditions and sample handling to minimize disorder in chromatin folding. This resulted in a reproducible stiffness of the chromatin fibers, as exemplified by the very similar slopes in the FE traces in Figure 2.3b. We therefore conclude that the large range over which chromatin fibers exhibit Hookean extension is characteristic for the compliance of the 30 nm fiber.

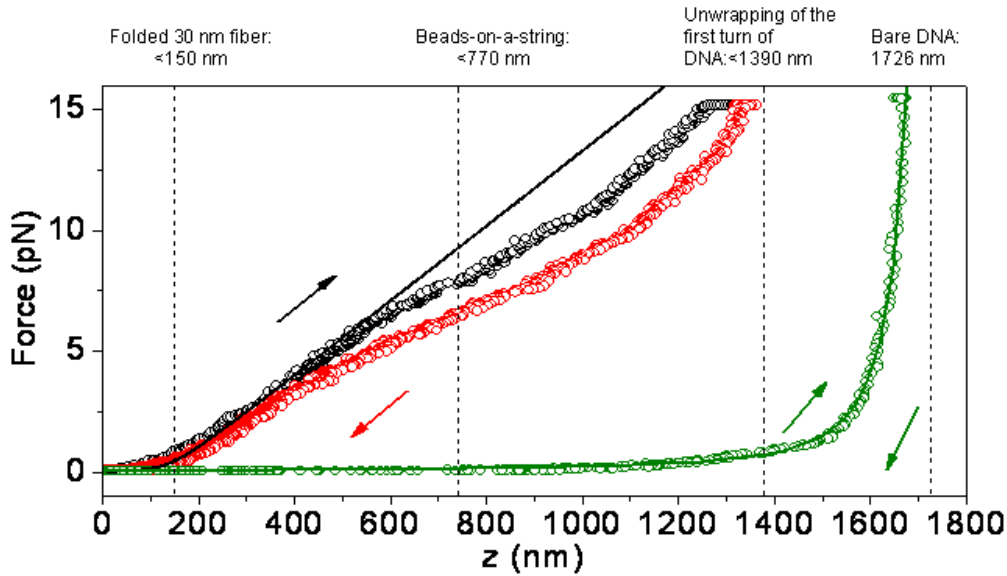


Figure 2.4: Stretching of chromatin fibers at high forces reveals DNA unwrapping. When $2.8 \mu\text{m}$ beads were used the maximum force in our FE experiments increased to approximately 15 pN. Green dots show FE trace on the DNA template alone, green line represents fit to WLC. Up to 7 pN the chromatin fiber containing H5 stretched linearly, following Hookean extension (Equation 2.2). Subsequently, a non-linear length increase was observed, stretching the fiber beyond 782 nm, the contour length of a beads-on-a-string fiber. This excess length must have resulted from DNA unwrapping from the nucleosomes. The relatively high compliance of the fiber points to incomplete stacking of the nucleosomes in the fiber. This is probably due to an extended exposure to high forces during rinsing the flow cell prior to the measurement, which is inherent to the use of larger beads. At 15 pN the end-to-end distance converges to the contour length of a fiber in which one super helical turn of DNA has been unwrapped from each nucleosome. Upon reduction of the force the fiber refolded. The hysteresis in the forward and backward trace indicated that the unfolding and subsequent refolding were not in thermodynamic equilibrium. Nevertheless, folding and refolding were reversible, and could be repeated over 10 times for a single chromatin fiber.

2.2.3 Linker histones do not affect the stiffness of a chromatin fiber

When comparing the mechanical parameters of the folded nucleosome arrays with and without linker histones (H1 or H5) we find, surprisingly, that both the stiffness and the length were unaffected by the presence or type of linker histones (Figure 2.5 and Table 2.1). As shown in Figure 2.5a-c, the simple Hookean model accurately follows the experimental FE relation of the chromatin fibers

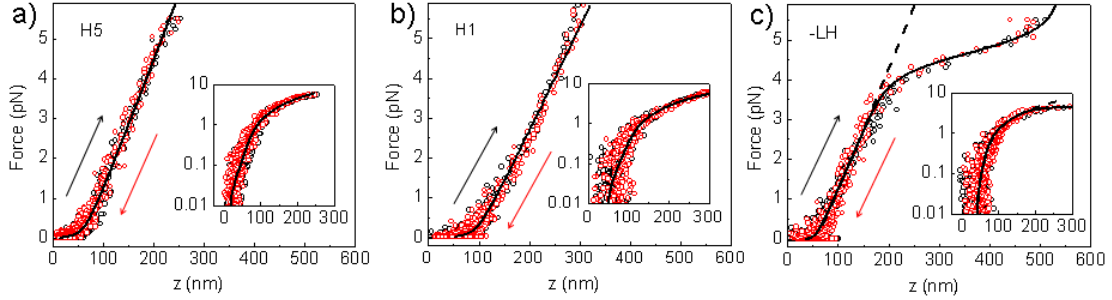


Figure 2.5: Chromatin fibers stretch like a Hookean spring, independently of the presence of linker histones. Forward (black circles) and backward (red circles) FE traces of a) chromatin fibers containing stoichiometric concentrations of H5, b) chromatin fibers containing stoichiometric concentrations of H1. The absence of hysteresis indicated that the fibers were in thermodynamic equilibrium during the entire FE cycle. Data were fitted to Equation 2.2. The average fit results on multiple chromatin fibers are listed in Table 1. c) FE traces of a fiber without linker histones, dashed line: fit to Equation 2.2, only data up to 3 pN were included. Solid line fit to Equation 2.5 resulting in $\Delta G = 13.2 \pm 0.7 k_B T$ and $\Delta z = 12.1 \pm 0.5$ nm. Insets show good fits at small forces.

over 3 orders of magnitude of force. The obtained nucleosome line density varied between 1.6 ± 0.2 and 2.0 ± 0.2 nm/nucleosome, in good agreement with recent EM measurements [7] on this chromatin material and confirms that the nucleosome arrays were properly folded into 30 nm fibers. Importantly, the absence of hysteresis indicates thermodynamic equilibrium of all conformational changes in the time of each FE cycle. It also appears that the interactions driving chromatin folding are not affected by the presence of linker histones, as additional contacts between the linker histones can be expected to increase the stiffness of the fiber, a feature that we did not observe. Fibers with and without linker histones could be stretched extensively, up to at least three times more than their rest length. Fibers with linker histones could be stretched in a linear fashion up to more than 6 pN (Figure 2.5a and b). Thus, the presence of the linker histone stabilizes the fibers under external forces, which may relate to our earlier sedimentation velocity results that showed an increased compaction of the fiber upon inclusion of linker histones [14].

The striking difference with fibers lacking linker histones is the appearance of a force plateau at 4.5 pN (Figure 2.5c). Contrary to high-force measurements in which concomitant DNA unwrapping from the histone core occurred [19], this transition did not show hysteresis and thus was fully in thermodynamic equilibrium. The end-to-end distance remained well within the length that can be expected for a beads-on-a-spring conformation, indicating that the nucleosome

core particles remained fully intact. Therefore the plateau in the FE trace of the chromatin fiber lacking linker histones should be explained by disruption of nucleosome-nucleosome interactions which are stabilized by the linker histones.

2.2.4 The nucleosomes in a 30 nm fiber are arranged in a solenoidal structure

How do the measured stiffness and extension relate to the structure of the 30 nm chromatin fiber? The stiffness of an isotropic solid cylinder is defined by its Young's modulus E [29]:

$$E = \frac{kL_{30}}{2\pi R^2}. \quad (2.3)$$

Using the appropriate radius $R = 15$ nm for a 30 nm fiber and the experimentally obtained stiffness $k = 0.025$ pN/nm and $L_{30} = 50$ nm results in a Young's modulus of $0.9 \cdot 10^{-6}$ GPa, which is 6 orders of magnitude smaller than typical tabulated values of structured proteins. Furthermore, we are not aware of any bulk material that has a tensile strength that allows for stretching more than 3 times its rest length in a linear fashion, like the fibers shown in Figure 2.5a-c that exhibit stretching from 50 nm up to more than 160 nm. Hence, it must be the *structure* of the fiber, rather than its *isotropic elasticity* that provides its extraordinary high compliance.

Most proposed structures of chromatin folding are based on one-on-one stacking of nucleosomes [7, 30], as suggested from crystal structures [1, 15], cross linking studies [16] and EM on nucleosome core particles[31] and natively assembled nucleosome arrays [32]. The two prevailing models of the 30 nm fiber are a one-start and a two-start helix. In both models fiber folding is driven by nucleosome stacking. The order of stacking however makes the difference between the two alternative folding conformations. In the one-start helix neighboring nucleosomes interact forming a single super helical ribbon, whilst in the two-start helix even and odd number nucleosomes stack into two parallel ribbons. A one-start helical spring composed of a single ribbon of stacked nucleosomes can be modeled as a simple helical spring yielding a stiffness of[29]:

$$k = \frac{1}{4N} \frac{Gr^4}{R^3}, \quad (2.4)$$

with N turns of a ribbon of radius r and shear modulus G defined as $G = E/2(1 + \sigma)$. The Poisson ratio σ depends on the compressibility of the material and is typically between 0.2 and 0.5. With $\sigma = 0.2$, $r = 5.5$ nm, $N = 25/6$

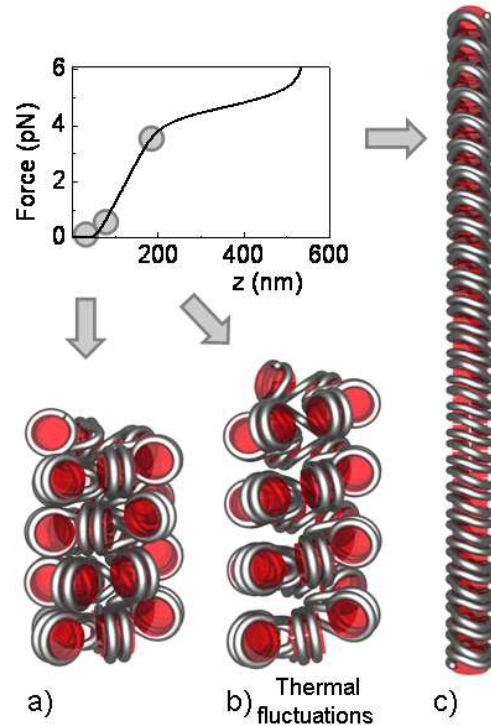


Figure 2.6: Schematic representations of chromatin fiber conformations at different forces a) $F = 0$ pN, representing the most condensed conformation of the fiber. b) The extension at 0.4 pN is equivalent to the expected average extension due to thermal fluctuations. c) Fully extended chromatin fiber at 4 pN. The height of 25 stacked nucleosomes matches the observed maximum extension of the fiber before rupture.

and $k = 0.025$ pN/nm a Young's modulus of $3 \cdot 10^{-3}$ GPa was obtained. This is smaller than reported for typical proteins, but similar to the Young's modulus of elastin, a protein that has a very high elasticity due to the disordered structure of its polypeptide chains. Thus, the measured stiffness of the chromatin fiber is consistent with the elasticity of disordered proteins that act as entropic springs. Indeed the histone tails, which are disordered polypeptide chains, have been shown to be responsible for the nucleosome-nucleosome interactions [7], and may thereby determine the flexibility of the fiber.

Whereas the small stiffness that we obtained is indicative of a helical structure of the chromatin fiber, its value does not have the accuracy to discriminate between one or two start configurations. The total length of the Hookean regime in the FE trace is more informative in this respect. Fibers containing 25 nucleosomes without linker histones could be stretched up to 160 nm (Figure 2.5), corresponding to 6.4 nm per nucleosome. The stretching of a solenoidal structure of 25 nucleosomes is schematically depicted in Figure 2.6a and b. Upon

pulling, a solenoidal structure can stretch into a continuous stack of nucleosomes, represented by the stack-of-coins structure of the maximally extended fiber (Figure 2.6c). The distance between the nucleosomes in such an arrangement can easily be spanned by the protruding histone tails that add to the 5.5 nm height of the nucleosome core[1]. If the nucleosomes in the fiber were to be arranged in a two-start structure[15], stretching of the two parallel ribbons up to 160 nm would exceed the height of a nucleosome by a factor of over 2, prohibiting physical contacts between nucleosomes even when their extruding tails would be fully stretched. Thus the Hookean behavior of the fiber, its length, its compliance and its transition to a beads-on-a-string structure provide quantitative support for the 30 nm chromatin fiber to be organized in a solenoidal, one-start topology[22].

2.2.5 Quantification of the nucleosome-nucleosome interaction energy

Because chromatin higher order folding is driven by nucleosome stacking, the high tensile strength that we obtained can only be provided by strong interactions between the nucleosomes. To understand chromatin higher-order folding it is therefore essential to obtain an accurate number on the interaction energy between stacking nucleosomes. In the previous force spectroscopy study Cui and Bustamante[20] reported a nucleosome-nucleosome interaction energy of $3.8 k_B T$, which seems rather low to maintain stacking at forces of several piconewtons. However, this value was obtained in the absence of Mg^{2+} , which is known to be required for the folding and stability of chromatin higher-order structures[33, 34]. We therefore tested whether Mg^{2+} depletion would affect the force required to disrupt the higher order structure by flowing in a buffer lacking magnesium acetate. Fibers without linker histones exhibited a significant decondensation after depletion of Mg^{2+} , as shown in Figure 2.7a. The decondensation of the fibers was reversible upon replenishment with buffer containing Mg^{2+} . Upon repeated unfolding and refolding of the fibers we observed a gradual decrease in both condensation and hysteresis (Figure 2.7b). The hysteresis represents the total work involved with the ruptures that occur in the fiber during the FE cycle and was quantified by numerical integration. Interestingly, the hysteresis only decreased when the fiber was held in an extended conformation and we therefore plotted the interaction energy as a function of the time when the chromatin fiber was held in a stretched conformation. The resulting mono-exponential decay of the hysteresis is characteristic of first order reaction kinetics. This reaction, having an off-rate of $0.01 s^{-1}$, might be attributed to the dissociation of Mg^{2+} from the fiber. Independent of its physical origin however, it is clear that Mg^{2+} depletion

gradually decreases the interactions that maintain higher order folding and that an accurate assessment of the interaction strength should therefore include the transient effects related to stretching the fiber.

What is the interaction energy when partial rupture of the fiber is taken into account? From the first FE trace after Mg^{2+} depletion we estimated, based on the extension at low force, that approximately half of the fiber already unfolded during buffer exchange. Taking this partial unfolding into account yields a free energy of nucleosome stacking of approximately $15 k_B T$ per nucleosome pair. After a large number of FE cycles the hysteresis entirely disappears, which is indicative of the absence of any higher-order structure. The resulting beads-on-a-string fiber is expected to follow a single WLC with a reduced contour length L_{BoS} due to DNA wrapping around the histone core and a reduced persistence length p_{BoS} due to the sharp kinks in the trajectory of the DNA path [35]. We obtained a good fit with $p_{BoS}=17.6\pm 2.0$ nm, approaching the value previously reported[20]. The obtained contour lengths $L_{BoS} = 691\pm 70$ nm and $L_{DNA} = 125\pm 72$ nm show good agreement with the expected dimensions of the fiber as schematically depicted in Figure 2.2. Not only these contour lengths but also the reduced apparent persistence length relative to DNA demonstrate that no DNA unwrapping from the nucleosome cores has occurred as a reduced apparent persistence length points at kinks in the DNA trajectory[35]. DNA exits in an angle of approximately 50 degrees from the core particle. Unwrapping leads to a much larger opening angle and as a result the apparent persistence length approaches that of DNA[36]. In conclusion, these experiments both explain the low value for nucleosome-nucleosome interaction energy reported previously[20] and highlight the essential role of Mg^{2+} ions in stabilizing nucleosome-nucleosome stacking interactions.

2.2.6 Mg^{2+} stabilizes nucleosome stacking under physiological conditions

Can the overstretching in the presence of Mg^{2+} also be attributed to nucleosome unstacking? After having established that the beads-on-a-string fiber accurately follows a WLC, we can now quantify the changes in fiber length during forced disruption under more physiological conditions that include Mg^{2+} . The interaction energy can be calculated in a straight forward manner[20] by multiplying the length increase at the force plateau (from 200 to 500 nm) with the force (4.5 pN), which are both obtained from Figure 2.5c and dividing it by the number of nucleosome pairs (24), resulting in $14 k_B T$. For a more accurate assessment we need to take the compliance of both the folded fiber and the flanking DNA into

account by expanding Equation 2.2 with an expression for the extension of the ruptured fiber. Using the length of the flanking DNA and a linear combination of the fraction of unstacked nucleosomes α , in equilibrium with the fraction of stacked nucleosomes $(1 - \alpha)$ the FE trace should follow:

$$z(F) = z_{WLC}(F, L_{DNA}, p_{DNA}) + [1 - \alpha(F)] z_{30}(F, L_{30}, k) + \alpha(F) z_{WLC}(F, L_{BoS}, p_{BoS}), \quad (2.5)$$

with

$$\alpha(F) = \left[1 + \exp\left(\frac{\Delta G - F\Delta z}{k_B T}\right) \right]^{-1}, \quad (2.6)$$

in which ΔG represents the free energy of nucleosome stacking, and Δz the length increase upon nucleosome unstacking. A similar expression was recently derived for force induced structural transitions in polysaccharides[37].

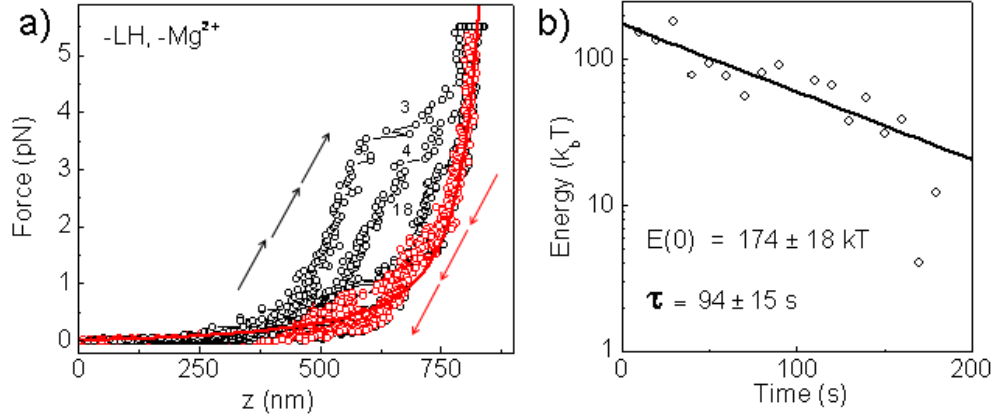


Figure 2.7: Mg^{2+} stabilizes nucleosome stacking. a) Upon depletion of Mg^{2+} hysteresis was observed in FE traces of chromatin fibers without linker histones. Multiple FE cycles obtained from a single fiber are shown, their order indicated by the numbers next to the curves. The fibers without linker histones initially ruptured at 3.5 pN and did not fully refold upon repeated FE cycles. Backward traces (red dots) were fitted with two WLC in series i.e. Equation 2.2 with α set to 1 and p_{DNA} fixed to 50 nm (red line). Fitting the three remaining free parameters resulted in $p_{BoS} = 17.6 \pm 2.0$ nm, $L_{BoS} = 691 \pm 70$ nm, $L_{DNA} = 125 \pm 72$ nm and $R^2 = 0.97$. b) The hysteresis in successive FE cycles decreased exponentially with the time the fiber was held in an extended conformation.

To reduce the number of free variables p_{BoS} and L_{BoS} were fixed to the values obtained from fitting fibers lacking higher order structure, as shown in Figure 2.7a and that are consistent with those reported by Cui and Bustamante[20]. p_{DNA} is

well documented and was fixed to 50 nm, which was reproduced in the FE trace of bare DNA, shown in Figure 2.4. The remaining five variables i.e. L_{DNA} , L_{30} , k , ΔG and Δz were used to fit the FE trace shown in Figure 2.5c. Equation 2.5 and Equation 2.6 accurately describe the full FE cycle, including the transition observed at 4.5 pN. The length increase of 13.4 nm approaches the expected length of 50 bp of linker DNA that should be added upon unstacking of a pair of nucleosomes. The free energy of nucleosome stacking corresponded to $13.8 k_B T$, matching the value obtained from extrapolation of the non-equilibrium disruption of chromatin fibers in absence of Mg^{2+} . It is also in close agreement with our previous measurements on the interaction energy between individual nucleosomes in a DNA fiber sparsely decorated with nucleosomes[24]. The large interaction energy and the excellent fit to a two state model further support interpretation of our data in terms of one-on-one stacking of nucleosomes. Thus, all the details of the FE profile of the chromatin fibers can be quantitatively understood in terms of the rupture of stacked nucleosomes in a solenoidal chromatin fiber.

2.2.7 167 bp NRL chromatin fibers are longer and stiffer, consistent with a two-start helix

The most compelling evidence for a two-start helical organization of chromatin fibers comes from cross linking[16] and crystallography[15] data on 167 bp NRL chromatin arrays. Visualization by EM revealed however that such fibers have a smaller diameter and a significantly larger length compared to 197 bp NRL fibers. This suggests a different folding, i.e. a two-start helix[21]. To test this hypothesis we reconstituted 25*167 NRL fibers, and measured their compliance (Figure 2.8). Compared to the 25*197 bp NRL fibers all 25*167 bp NRL fibers were longer at 0.5 pN and stretched less at 6 pN force. Thus, independent of any structural interpretation, the slopes of the FE traces were all higher than those of the 25*197 bp NRL fibers. Though the fibers exhibited more heterogeneity and non-specific sticking to the flow cell, indicating more disorder, the FE traces also feature a linear extension that was fitted to Equation 2.2. The average stiffness of the 25*167 bp NRL fibers appeared to be 2.7 times larger than the stiffness of the 25*197 bp NRL fibers (Table 2.1). Like the EM data we find an increased length of 25*167 bp NRL fibers[21]. The increase in stiffness is consistent with the nucleosomes being arranged into two twisted ribbons of half the length, which would quadruple the stiffness. We found a relative increase of only 2.7 together with a smaller R^2 of the fit and a larger rest length of the fiber. All these observations hint at increased disorder relative to the 25*197 bp NRL fibers. Further quantification, however, requires more advanced analysis (Chapter 4).

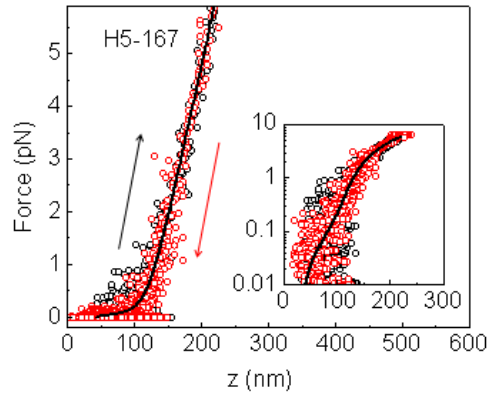


Figure 2.8: 167 bp repeat length fibers are longer and stiffer. FE trace of a 167 bp repeat length nucleosome array. The fiber behaves qualitatively similar to 197 bp repeat length fibers, showing Hookean extension in both the forward (black) and the backward trace (red). The fit to Equation 2.2, black line, however reveals less condensation and a higher stiffness.

Importantly, if the stiffness that we report would originate from stretching an isotropic rod instead of a double helical stack, pulling the longer and thinner 125*67 bp NRL fibers would yield a decreased instead of an increased stiffness. Therefore the FE measurements on the 25*167 bp NRL chromatin fibers confirm that these fibers are arranged in two twisted stacks, consistent with a two-start helix.

2.3 Discussion

Single molecule force spectroscopy provides an unique way to probe the interactions that drive chromatin folding. By using well-defined chromatin arrays it was possible to analyze FE traces using the framework of classical mechanics, allowing for detailed quantitative interpretation with nm and sub-pN resolution. Because chromatin fibers were not stained, dried, surface deposited or exposed to extreme buffer conditions, the fibers could adopt their thermodynamically most favorable conformation. This allowed us to probe higher order chromatin structure directly, under physiological conditions and without preparation artifacts. Furthermore, it was possible to reproduce FE traces on each individual fiber, confirming thermodynamic equilibrium, and to unequivocally verify the presence of each nucleosome in the fiber. The possibility to manipulate fibers individually and to select specific fibers is unique to single molecule techniques and warrants new possibilities for revealing the heavily debated structure of chromatin fibers.

Chapter 2: Discussion

Table 2.1: The mechanical parameters that define chromatin structure. Average and standard error of mean of the fitting parameters to Equation 2.2 for chromatin fibers containing H5, H1 and lacking linker histones, selected to contain 25 nucleosomes. ^aFit was limited to the Hookean range i.e. $F < 3$ pN. ^bFE traces of fibers without linker histones fitted to Equation 2.5 using $p_{BOS} = 17$ nm, as obtained from Figure 2.7a and $p_{DNA} = 50$ nm

Linker histone	NRL (bp)	k (pN/nm)	L_{30} (nm)	L_{DNA} (nm)	ΔG ($k_B T$)
H5	197	0.019 ± 0.004	50 ± 6	50 ± 6	-
H1	197	0.028 ± 0.001	40 ± 4	60 ± 8	-
none ^a	197	0.023 ± 0.003	66 ± 16	54 ± 12	-
none ^b	197	0.021 ± 0.003	72 ± 17	40 ± 10	13.8 ± 0.5
H5	167	0.052 ± 0.013	79 ± 21	78 ± 23	-
Linker histone	NRL (bp)	Δz (nm)	N	$\langle R^2 \rangle$	
H5	197		10	0.88	
H1	197		7	0.85	
none ^a	197		3	0.80	
none ^b	197	13.4 ± 0.7	3	0.93	
H5	167		7	0.77	

The single molecule force spectroscopy experiments agree well with recent EM and sedimentation velocity data that established a linker histone-dependent compaction of 197 bp NRL arrays into a 30-nm chromatin fibers[21]. 167-bp NRL arrays displayed a limited linker histone-dependent compaction, resulting in thinner fibers. All methods indicate that the linker histone stabilizes the higher-order structure, which in the case of force spectroscopy shows as a higher rupture force. The current data go beyond the sedimentation velocity and EM analysis since they provide direct evidence for the topology of both types of fibers. Furthermore, by fitting the FE traces to a Hookean model we show that the presence of linker histones does not result in more compact fibers in the absence of force, but instead increases the tensile strength of the fiber. The high compliance and the rupture of nucleosome stacking at 4 pN that we report here may translate into differences in overall compaction when measured by sedimentation velocity or EM as the centrifugal forces and the forces involved with surface deposition may be sufficient to induce partial unstacking of the nucleosomes. Since single molecule force spectroscopy can separate force induced extension from differences in rest length it can give a more accurate value for the nucleosome packing density of the highly compliant chromatin fibers.

By looking at the total contour length of the fiber under conditions with and

without Mg^{2+} we showed that no DNA was unwrapped from the histone core at forces below 7 pN. The latter may seem surprising when compared to pulling experiments on single nucleosomes which feature unwrapping of 60 bp at 3 pN and full unwrapping at 6 pN[38]. It appears however that the embedding of a nucleosome in an array of nucleosomes stabilizes the wrapped conformation. This is consistent with the finding that full unwrapping in the context of a nucleosomal array requires 15-25 pN[17–19], significantly more than in the mono-nucleosome experiment. *In vivo*, nucleosomes are always flanked by neighboring nucleosomes, which stresses the relevance of this higher tensile strength.

Does the high compliance of the condensed chromatin fiber have any physiological relevance? Even these highly regular, strongly condensed fibers featured an extraordinary small stiffness, which results in large thermal fluctuations in their extension, following equipartition theorem:

$$\frac{1}{2}kz^2 = \frac{1}{2}k_B T \quad (2.7)$$

The root-mean-squared amplitude of these fluctuations at room temperature exceeds 10 nm for a fiber consisting of 25 nucleosomes. Thus the low stiffness of the 30 nm fiber allows for thermal fluctuations of about 20% of its length, but larger fluctuation will also occur. Figure 2.6b shows that the nucleosomal DNA in fibers stretched to such extensions is relatively well exposed. Thus the breathing of the folded structure without unstacking of the nucleosomes that is the consequence of the observed high compliance can be of biological importance since it provides eukaryotic cells with the opportunity to combine structural transparency with a high compaction of chromatin.

In recent work Poirier *et al.* [39] studied the enzymatic accessibility of nucleosomal DNA in homogeneous arrays similar to the arrays used here but with a 177 bp NRL. By comparison of the digestion rates of target sites in a mononucleosome with the same sites within a nucleosomal array they found that nucleosome organization into chromatin fibers changes the accessibility of nucleosomal DNA only modestly. The relative accessibility varied from ~ 3 -fold decreases to ~ 8 -fold increases. Linker DNA however was severely occluded compared to bare DNA. The relatively open structure of the fiber that we report here is clearly required for this surprising finding. The increase in accessibility, that points to enhanced unwrapping of the nucleosomal DNA, may reduce the bending of the linker DNA that is characteristic for one-start helical folding of the fiber. The amplitude of the thermal fluctuations is however insufficient to render enzymatic access to the linker DNA that remains in the central region of the fiber. Hence both studies support the picture of a dynamic, flexible chromatin fiber that has a relatively open structure.

How do our findings on reconstituted model fibers relate to the structure of native chromatin? Although for any species and cell type linker DNA length is variable, it varies around a characteristic distinct length. Analysis of nucleosome repeat lengths found in nature showed broad maxima at 167, 177, 188, 197 bp [8, 40], providing evidence that linker lengths are quantized and satisfy the equation $147 \text{ bp} + 10n$, where n is an integer number. Recent genome-wide analysis of nucleosome positions in the yeast genome[41] also provides evidence for well defined linker DNA lengths. Our model fibers reflect the dominant NRL distributions found in nature. Previous studies [14, 21] confirmed that the model fibers used in our study have the same folding pathway and dimensions as native chromatin fibers. Furthermore, EM analysis has shown that model fibers with NRLs of 177, 187, 197 and 207 bp form the same structure, tolerating a wide range of linker DNA lengths. The 167 NRL nucleosome array of which a tetramer was crystallized and was shown to fold in a two-start helix[15], features different dimensions [21]. This finding is substantiated by our current data comparing 167 and 197 bp fibers. It is likely that *in vivo* a number of structures will coexist because of heterogeneity in NRL. However, to decipher what these structures are requires model fibers with defined NRLs and histone content as used in this study.

Another important finding in our experiments is that the nucleosome-nucleosome interaction energy is 4 times higher than reported before[20]. It is known that not only Mg^{2+} but also an ionic strength of at least 50 mM is required for the stability of chromatin folding[14, 42]. The experiments of Cui and Bustamante were performed at 40 mM NaCl and in the absence of Mg^{2+} and it is therefore likely that under those conditions only partially compacted fibers were measured. We have shown that in the absence of Mg^{2+} we could reproduce this smaller interaction energy in the entire fiber, but that it is indeed accompanied by defects in nucleosome stacking. A higher ionic strength and the presence of Mg^{2+} is also expected to better approach the ionic conditions *in vivo* and our findings underscore the necessity to study chromatin structure under conditions that are representative of its natural environment.

The high interaction energy also has implications for the values used in computational chromatin fiber modeling. A small interaction energy has been the basis to model the higher order structure of chromatin, which generally favors zig-zag conformations[43–45]. A net free energy of nucleosome-nucleosome interaction of $14 k_B T$, as we report here, implies that the interactions between nucleosomes can accommodate much more DNA bending than previously thought. This will yield very different outcomes in structural computations and may favor helical folding over a zig-zag structure. Whereas in the zig-zag model the linker length directly

determines the diameter of the fiber, EM measurements show that this is not the case[22]. Thus the question remains, what determines the diameter of the fiber? Recent theoretical modeling suggests tight packing of nucleosomes as the mechanism determining the diameter of 30 nm fibers [46]. The high interaction energy that we report here definitely supports such a suggestion, but we also show that the stacking of nucleosomes is quite flexible. From our measurements on different NRLs it is clear though that the length of the linker DNA remains a major parameter in organizing chromatin.

A nucleosome-nucleosome interaction of $14 k_B T$ corresponds to an equilibrium constant for unstacking of 10^{-6} , i.e. in equilibrium one of every million nucleosomes is unstacked. An interaction this strong implies that an active mechanism to disrupt nucleosome-nucleosome interactions is required if DNA is to be unpacked. One such mechanism can be the specific modification of histone residues. A prime candidate for such a modification is acetylation of K16 in the N-terminal tail of H4[47] which is located in a region of the H4 tail that makes specific contacts with the surface of H2A-H2B on an adjacent nucleosome, as seen in the crystal structure of nucleosome cores[1]. This provides a physical mechanism for epigenetic control of transcription.

A possibly equally important physical mode of control is the variation of linker length between the nucleosomes. Our results confirm that the topology of the fiber, but not the mode of stacking the nucleosomes, is dependent on the NRL. It is well established that transcriptionally active nuclei, found for example in yeast and neurons, often feature short linker lengths[48]. The relatively high disorder that we found in 167 bp NRL fibers, in combination with the previously reported smaller condensation, may be intrinsic to the chromatin structure of short NRLs as a consequence of increased bending of the linker DNA compared to 197 bp NRL fibers. The free energy of nucleosome stacking in the 197 bp NRL fibers that we report here represents the net free energy in the context of a chromatin fiber. It is the sum of the attractive stacking interaction between the nucleosomes and the energetic penalty for bending the linker DNA between them. Because the histone composition and the buffer conditions were identical in the two different NRL arrays that we measured, it must be the linker DNA that changed the interactions that drive overall fiber folding. An increased DNA bending in short NRL fibers would explain a decrease of the free energy of nucleosome stacking which in turn results in a more open chromatin structure. It may therefore be the decreased stacking probability rather than the alternative topology of short NRL chromatin that is functionally relevant for transcription control.

The physical origin and the extension of distorted stacking of nucleosomes are currently under investigation. The highly regular chromatin fibers used in this

study provide a reference for comparison with fibers that bear the wide variety of histone composition, NRL, post-transcriptional modifications and other marks that are abundantly present in native chromatin. On top of these variations in chromatin composition, chromatin *in vivo* is continuously subject to forces that are generated by chromatin remodelers, RNA and DNA polymerases and other DNA based molecular motors. The magnitude of these forces is hard to estimate but these DNA based molecular motors typically have a stalling force of 10-25 pN[19, 49]. Thus it is clear that all the force induced structural rearrangements reported here are within the realm of the nuclear DNA machinery. Overall, our findings not only provide strong evidence for a one-start helical topology of the 30 nm fiber but also provide quantitative parameters that characterize the highly dynamic organization of chromatin.

2.4 Methods

2.4.1 DNA and chromatin fibers

25 repeats of a 197 bp 601 DNA sequence were produced in several cloning steps, using the low-copy-number vector pETcoco-1 (Novagen). DNA was linearized by XhoI and NheI digestion, and filled in dUTP-digoxigenin at the XhoI end and dUTP-biotin at the NheI end. Chromatin fibers were reconstituted through salt dialysis with competitor DNA (147 bp) and histone octamers purified from chicken erythrocytes. A second salt dialysis was performed for incorporating linker histones H5 or H1 [14].

2.4.2 Flow cell

A clean cover slip was coated with poly-d-lysine (Sigma), and then with a mixture of polyethyleneglycol (PEG) containing 20% w/v mPEG-Succinimidyl Propionic Acid (SPA)-5000 and 0.2% biotin-PEG-N-Hydroxysuccinimide (NHS)-3400 (Nektar). The coverslip was then mounted on a poly-di-methylsiloxane (PDMS, Dow Corning) flow cell containing 10x40x0.4 mm flow channel. Further surface preparation was performed inside the channel with specific binding of 0.1 mg/ml streptavidin (Sigma) for 10 minutes.

2.4.3 Sample preparation

The flow cell was flushed with 1 ml measurement buffer (MB) (10 mM HEPES pH 7.6, 100 mM KAc, 2 mM MgAc₂, 10 mM NaN₃ , 0.1% (v/v) Tween-20, (+)

0.02% (w/v) BSA), followed by 0.1 μg chromatin fibers diluted in 250 μl MB for 10 min, and subsequently with 1 ml MB, then 40 μg 1 μm paramagnetic beads (DYNAL MyOne) coated with anti-digoxigenin (Roche) and diluted in 250 μl MB (+). After 10 min incubation, the cell was rinsed by 1 ml MB (+) at flow rate of 5 $\mu\text{l/s}$.

2.4.4 Magnetic tweezers

Chromatin fiber-tethered paramagnetic beads were imaged in a home built inverted microscope. Force extension curves were generated using dynamic force microscopy as described[24]. Contrary to previous experiments on chromatin fibers with optical tweezers that act as a position clamp [19, 20, 27], magnetic tweezers are operated as a force clamp. Rupture events will thus appear as an increase in extension rather than a decrease in force, which produces the characteristic spikes in FE traces obtained with optical tweezers.

2.5 Acknowledgments

We would like to thank T. Richmond, H. Schiessel, T. Schmidt, and J. Widom for helpful discussions and I. de Boer-Tuyn for technical support. This work was financially supported by the “Nederlandse Organisatie voor Wetenschappelijk Onderzoek” (NWO) and the European Science Foundation (ESF)

Bibliography

- [1] Luger, K., Mäder, A. W., Richmond, R. K., Sargent, D. F. & Richmond, T. J. *Nature* **389**, 251–60 (1997).
- [2] Simpson, R. T. *Biochemistry* **17**, 5524–5531 (1978).
- [3] Thoma, F., Koller, T. & Klug, A. *J. Cell. Biol.* **83**, 403–427 (1979).
- [4] Widom, J. & Klug, A. *Cell* **43**, 207–213 (1985).
- [5] Widom, J. *Annu. Rev. Biophys. Biophys. Chem.* **18**, 365–395 (1989).
- [6] Tremethick, D. J. *Cell* **128**, 651–654 (2007).
- [7] Robinson, P. J. J. & Rhodes, D. *Curr. Opin. Struct. Biol.* **16**, 336–343 (2006).
- [8] van Holde, K. E. *Chromatin* (Springer-Verlag, New York, 1989). Chromatin.
- [9] Freidkin, I. & Katcoff, D. J. *Nucleic Acids Res.* **29**, 4043–4051 (2001).

Bibliography

- [10] Pearson, E. C., Bates, D. L., Prospero, T. D. & Thomas, J. O. *Eur. J. Biochem.* **144**, 353–360 (1984).
- [11] Bates, D. L. & Thomas, J. O. *Nucleic Acids Res.* **9**, 5883–5894 (1981).
- [12] Woodcock, C. L., Skoultchi, A. I. & Fan, Y. *Chromosome Res.* **14**, 17–25 (2006).
- [13] Lowary, P. T. & Widom, J. *J. Mol. Biol.* **276**, 19–42 (1998).
- [14] Huynh, V. A. T., Robinson, P. J. J. & Rhodes, D. *J. Mol. Biol.* **345**, 957–968 (2005).
- [15] Schalch, T., Duda, S., Sargent, D. F. & Richmond, T. J. *Nature* **436**, 138–141 (2005).
- [16] Dorigo, B. *et al.* *Science* **306**, 1571–1573 (2004).
- [17] Bennink, M. L. *et al.* *Nat. Struct. Biol.* **8**, 606–610 (2001).
- [18] Claudet, C., Angelov, D., Bouvet, P., Dimitrov, S. & Bednar, J. *J. Biol. Chem.* **280**, 19958–19965 (2005).
- [19] Brower-Toland, B. D. *et al.* *Proc. Natl. Acad. Sci. U.S.A.* **99**, 1960–1965 (2002).
- [20] Cui, Y. & Bustamante, C. *Proc. Natl. Acad. Sci. U.S.A.* **97**, 127–132 (2000).
- [21] Routh, A., Sandin, S. & Rhodes, D. *Proc. Natl. Acad. Sci. U.S.A.* **105**, 8872–8877 (2008).
- [22] Robinson, P. J. J., Fairall, L., Huynh, V. A. T. & Rhodes, D. *Proc. Natl. Acad. Sci. U.S.A.* **103**, 6506–6511 (2006).
- [23] Solis, F. J., Bash, R., Yodh, J., Lindsay, S. M. & Lohr, D. *Biophys. J.* **87**, 3372–3387 (2004).
- [24] Kruithof, M., Chien, F., de Jager, M. & van Noort, J. *Biophys. J.* **94**, 2343–2348 (2008).
- [25] Marko, J. F. & Siggia, E. *Macromolecules* **28**, 8759–8770 (1995).
- [26] Bustamante, C., Marko, J. F., Siggia, E. & Smith, S. *Science* **265**, 1599–1600 (1994).
- [27] Bennink, M. *et al.* *Nat. Struct. Biol.* **8**, 606–610 (2001).
- [28] Bednar, J. *et al.* *Proc. Natl. Acad. Sci. U.S.A.* **95**, 14173–14178 (1998).
- [29] Howard, J. *Mechanics of Motor Proteins and the Cytoskeleton* (Sinauer Associates Inc, Massachusetts, 2001).
- [30] Wong, H., Victor, J.-M. & Mozziconacci, J. *PLoS ONE* **9**, e877 (2007).

- [31] Dubochet, J. & Noll, M. *Science* **202**, 280–286 (1978).
- [32] Dubochet, J., Adrian, M., Schultz, P. & Oudet, P. *EMBO J.* **5**, 519–528 (1986).
- [33] d’Erme, M., Yang, G., Sheagly, E., Palitti, F. & Bustamante, C. *Biochemistry* **40**, 10947–10955 (2001).
- [34] Strick, R., Strissel, P. L., Gavrilov, K. & Levi-Setti, R. *J. Cell. Biol.* **155**, 899–910 (2001).
- [35] Kulić, I. M., Mohrbach, H., Lobaskin, V., Thaokar, R. & Schiessel, H. *Phys. Rev. E* **72**, 041905–041910 (2005).
- [36] Kruithof, M. & van Noort, J. *Biophys. J.* **96**, 3708–3715 (2009).
- [37] Haverkamp, R. G., Marshall, A. T. & Williams, M. A. K. *Phys. Rev. E* **75**, 021907–021914 (2007).
- [38] Mihardja, S., Spakowitz, A. J., Zhang, Y. & Bustamante, C. *Proc. Natl. Acad. Sci. U.S.A.* **103**, 15871–15876 (2006).
- [39] Poirier, M. G., Bussiek, M., Langowski, J. & Widom, J. *J. Mol. Biol.* **379**, 772–786 (2008).
- [40] Widom, J. *Proc. Natl. Acad. Sci. U.S.A.* **89**, 1095–1099 (1992).
- [41] Wang, J.-P. *et al.* *PLoS Comput. Biol.* **4**, e1000175 (2008).
- [42] Bates, D. L., Butler, P. J., Pearson, E. C. & Thomas, J. O. *Eur. J. Biochem.* **119**, 469–476 (1981).
- [43] Wedemann, G. & Langowski, J. *Biophys. J.* **82**, 2847–2859 (2002).
- [44] Sun, J., Zhang, Q. & Schlick, T. *Proc. Natl. Acad. Sci. U.S.A.* **102**, 8180–8185 (2005).
- [45] Kepper, N., Foethke, D., Stehr, R., Wedemann, G. & Rippe, K. *Biophys. J.* **95**, 3692–3705 (2008).
- [46] Depken, M. & Schiessel, H. *Biophys. J.* **96**, 777–84 (2008).
- [47] Robinson, P. J. J. *et al.* *J. Mol. Biol.* **381**, 816–825 (2008).
- [48] Thomas, J. O. & Thompson, R. J. *Cell* **10**, 633–640 (1977).
- [49] Wang, M. D. *et al.* *Science* **282**, 902–907 (1998).

Chapter 3

Quantification of force induced structural changes

Nucleosomal arrays fold into 30 nm chromatin fibers but the structure and the mechanics of such fibers remain highly disputed. Nevertheless, higher-order folding of chromatin has been implied to play a strong regulatory role in all eukaryotic processes involving DNA. A fundamental understanding of these processes requires insight in the folding properties with molecular detail. Single molecule force spectroscopy experiments have the potential to provide such insight but interpretation of the data has been hampered by the large variations in experimental force-extension traces. Here we show that a simple two-state model of stacked and unwrapped nucleosomes accurately describes the force-extension relation of a range of fiber compositions and buffer conditions. Using the model we could recover the composition as well as the mechanical properties of heterogeneous chromatin fibers. At 3-4 pN nucleosomes unstack and only a single turn of DNA remains wrapped around the histone core. Extended exposure to such forces induces dimer dissociation. We found no indications of cooperativity in nucleosome unstacking. The current model not only provides insight in the mechanisms of chromatin higher-order folding, it also allows for detailed, quantitative assessment of the factors that influence chromatin structure, like for example post-translational modifications.

This chapter is based on the article: *Rigorous quantification of force induced structural changes in heterogeneous 30 nm chromatin fibers*, F.T. Chien, A. Routh, T. van der Heijden, D. Rhodes and J. van Noort, to be submitted

3.1 Introduction

Chromatin fibers are composed of strings of nucleosome core particles (NCPs) that are connected by several 10s of base pairs (bp) of linker DNA. The NCP consists of an octamer of histone proteins and 147 bp of DNA[1]. The tails of the histone proteins mediate the nucleosome-nucleosome interactions that stabilize folding into higher-order structures, like the 30 nm fiber[2]. Despite 30 years of intensive research, the structure of the 30 nm chromatin fiber is still poorly defined. Although 30 nm fibers can be reconstituted *in vitro* from DNA and purified histone proteins[3], as well as extracted and imaged from natively assembled chromatin fibers[4], there is a lack of evidence that they actually exist in a nucleus of a eukaryotic cell. Nevertheless, insight in the physical mechanisms that drive chromatin higher-order folding is essential for understanding the role of chromatin organization in all processes involved in the maintenance, transcription and replication of the eukaryotic genome.

In vivo chromatin structure can be regulated by DNA-sequence[5], ATP-dependent chromatin remodelers[6], post-translational modifications[2], linker histones[7] and other factors that bind to DNA or histones. The possible variations in size, composition, chemical and mechanical properties of chromatin fibers make native chromatin fibers challenging substrates for obtaining structural information. Reconstitution from purified histones and arrays of DNA positioning elements results in highly regular, stoichiometric chromatin fibers[8]. However, even these fibers display enough structural heterogeneity to preclude averaging as used in various high-resolution structure determination techniques. An exception to this forms the X-ray structure of a tetranucleosome, featuring nucleosomes arranged in two stacks, forming a two-start zig-zag structure[9]. However, it is not clear whether the structure of the 30 nm fiber that was deduced from a short-linker tetramer represents chromatin folding in larger fibers and under physiological conditions. In fact, careful analysis of the dimensions of such fibers as a function of the linker length indicated a one-start solenoidal folding for linker lengths exceeding 20 bp[10].

In order to fully characterize the structure and dynamics of chromatin fibers, one needs to take into account all variations in structure and composition that are present in a population of chromatin fibers. Even in single nucleosomes, a variety of structural changes have been described, such as transient release of part of the DNA from the core particle, known as DNA breathing, and dissociation of H2A-H2B histone dimers [11, 12]. Single-molecule Fluorescence Resonance Energy Transfer (FRET)[13, 14], as well as bulk studies using restriction enzyme accessibility, indicate that DNA breathing occurs at the time scale of milliseconds

and can extend up to several tens of bp into the nucleosome. DNA breathing has been shown to be strongly regulated by post-translational modifications[15] and may be linked to dimer dissociation. FRET-based experiments on trimers of nucleosomes suggested at least four distinct states of chromatin folding, that were characterized by time constants ranging from microseconds to seconds[16]. The delicate balance in nucleosomal dynamics depends strongly on buffer conditions. Such intricate dynamic behavior of the nucleosomes in a chromatin fiber impedes a generic structural description and calls for a single-molecule approach in order to fully understand its folding and dynamics.

Single molecule force spectroscopy has been successful in resolving force induced transitions in chromatin fibers[17–19]. Especially the transition from partially unwrapped to fully unwrapped nucleosomes, at forces above 10 pN, has been studied extensively. Such transitions result in 25 nm steps of contour length increase, that corresponds to ~ 75 bp of unwrapped DNA. Claudet et al. reported that H2A-H2B dimers easily dissociate from the nucleosome at these forces and at the very low chromatin concentration (< 0.5 nM) in which such experiments are typically conducted, leaving a fiber of H3-H4 tetramers[20].

The higher-order folding of chromatin has been studied less extensively [17, 21]. It is only stable at forces below 5 pN. At such small forces the combination of a high flexibility, a small extension and the stickiness of the nucleosomes on the surface complicate quantitative interpretation of Force-Extension (FE) traces. Previously, we have measured the compliance of well-defined, reconstituted chromatin fibers using magnetic tweezers (MT) and reported, based on the FE traces of these fibers, that the topology of chromatin fibers depends on the linker DNA length. Despite the careful control over the composition of the fibers, we observed a large variety in the mechanical properties of these fibers, which we resolved by selection of the most condensed fibers.

Here we present a rigorous physical model of the FE behavior of reconstituted fibers, which includes all datasets. The model links the extension of the fiber to its three dimensional structure and includes the stoichiometry and mechanical properties of different nucleosome conformations as well as the transitions between these conformations. Using this model, we attribute the force induced transition below 4 pN to a non-cooperative extension that results from unwrapping and unstacking of the nucleosomes, leading to a fiber with octamers that contain a single wrap of DNA. We show that extended exposure to forces as small as 4 pN leads to progressive dissociation of dimers. Importantly, establishing the parameters that define the mechanical properties of chromatin fibers allows for comparison between heterogeneous fibers and is a prerequisite for understanding the role of post-translational histone modifications in regulating chromatin structure. Since

forces of a few pNs can be expected *in vivo*, such structural changes are likely to play an important role in the regulation of chromatin structure in living cells.

3.2 Theory

In our description of the force dependent extension of the chromatin fiber, we separate three types of structures, i.e. (i) DNA, (ii) a nucleosome connected to neighboring nucleosomes by linker DNA, like in a beads-on-a-string(BoS) fiber, and (iii) a nucleosome stacked onto neighboring nucleosomes in a folded 30 nm fiber. Each has a characteristic contour length L , which can be related to its extension z using an appropriate mechanical model. The FE relation of DNA at forces below 10 pN follows the well-established Worm-Like-Chain (WLC) model in which the flexibility of the tether is defined by its persistence length p_{DNA} [22]. Here we use the inverse expression for a WLC:

$$z_{DNA}(f_0) = \Re[L_{DNA} \left(\frac{3}{4} + \frac{f_0}{3} - \frac{1}{24} \left[A(f_0)^{\frac{1}{3}} + B(f_0)^{\frac{1}{3}} + i\sqrt{3} \left(A(f_0)^{\frac{1}{3}} - B(f_0)^{\frac{1}{3}} \right) \right] \right)], \quad (3.1)$$

with the reduced force $f_0 = \frac{F p_{DNA}}{k_B T}$, thermal energy $k_B T$, $A(f_0) = C(f_0) - 12\sqrt{D(f_0)}$, $B(f_0) = C(f_0) + 12\sqrt{D(f_0)}$, $C(f_0) = (4f_0 - 3)^3 - 216$ and $D(f_0) = -3(4f_0 - 3)^3 + 324$.

Each fully wrapped nucleosome contains 147 bp of DNA folded in 1.7 turns, which reduces the contour length of the DNA by approximately 50 nm. Partial unwrapping of the DNA will increase the contour length of the nucleosome. The folding of DNA in the nucleosome also induces an effective kink in the trajectory of the DNA. Kulic and Schiessel have shown that a kink in the trajectory of a WLC results in a reduction of its persistence length and that the force-extension relation follows a WLC as long as $f_0 > 1$ [23]. We therefore model the BoS fiber as a WLC with contour length L_{BoS} and persistent length p_{BoS} .

In previous force spectroscopy experiments we reported a linear extension of the fiber z_{30} , up to its force-induced rupture, that is well described by Hooke's law (Chapter 2):

$$z_{30}(F) = L_{30} + \frac{F}{k_{30}}, \quad (3.2)$$

where L_{30} is the rest length of the 30 nm fiber per nucleosome and k_{30} is the stiffness of the 30 nm fiber per nucleosome. Electron microscopy measurements

have shown a compaction of the 30 nm fiber corresponding to 1.5-2 nm per nucleosome in the absence of force[8]. In thermodynamic equilibrium the ratio between nucleosomes in a BoS fiber and nucleosomes in a 30 nm fiber follows a Boltzmann equation:

$$\frac{N_{BoS}(F)}{N_{30}(F)} = \exp\left(-\frac{\Delta G - F [z_{BoS}(F) - z_{30}(F)]}{k_B T}\right), \quad (3.3)$$

with ΔG , the difference in free energy between the nucleosome in a 30 nm fiber and the nucleosome in a BoS fiber. In a non-equilibrium situation the distribution between BoS and 30 nm nucleosomes may deviate from this. In particular, we observed a significant number of the nucleosomes N_{BoS}^0 that did not fold in a 30 nm fiber at 0 pN. The total number of nucleosomes N in the reconstituted fibers equals the number of nucleosome positioning elements and is the sum of all types of conformations:

$$N = N_{30}(F) + N_{BoS}(F) + N_{BoS}^0. \quad (3.4)$$

Thus, the total extension of the fiber composed of sections of DNA, N_{BoS} nucleosomes in a BoS fiber and N_{30} nucleosomes embedded in a 30 nm fiber is the sum of the force-dependent extensions of each segment:

$$z(F) = z_{DNA}(F) + N_{30}(F) \cdot z_{30}(F) + [N_{BoS}(F) + N_{BoS}^0] \cdot z_{BoS}(F). \quad (3.5)$$

3.3 Results

3.3.1 Accurate contour length measurements on small tethers with magnetic tweezers

Our initial measurements on bare DNA molecules with a known length, showed a variation of contour lengths (Figure 3.1a), analogous to previous reports. Here we show that these variations can be attributed to off-center attachment of the DNA to the bead. Because of the magnetic anisotropy of the super paramagnetic beads, we cannot control where the DNA attaches to the bead. In other words, the attachment point of the DNA could be on the side instead of the bottom of the bead[24]. In this case the height of the bead is smaller than the extension of the molecule. By applying a geometric correction to this offset we were able to converge all force-extension curves (Figure 3.2a) onto the trace that matches the

size and persistence length of the DNA (Figure 3.2b). Note that this anisotropic effect becomes relatively more evident as the length of the molecule approaches the radius of the bead. Tethers that are significantly smaller than the bead radius however are not competent to span the distance between bead attachment point and the surface and consequently appear as a bead that is directly attached to the surface.

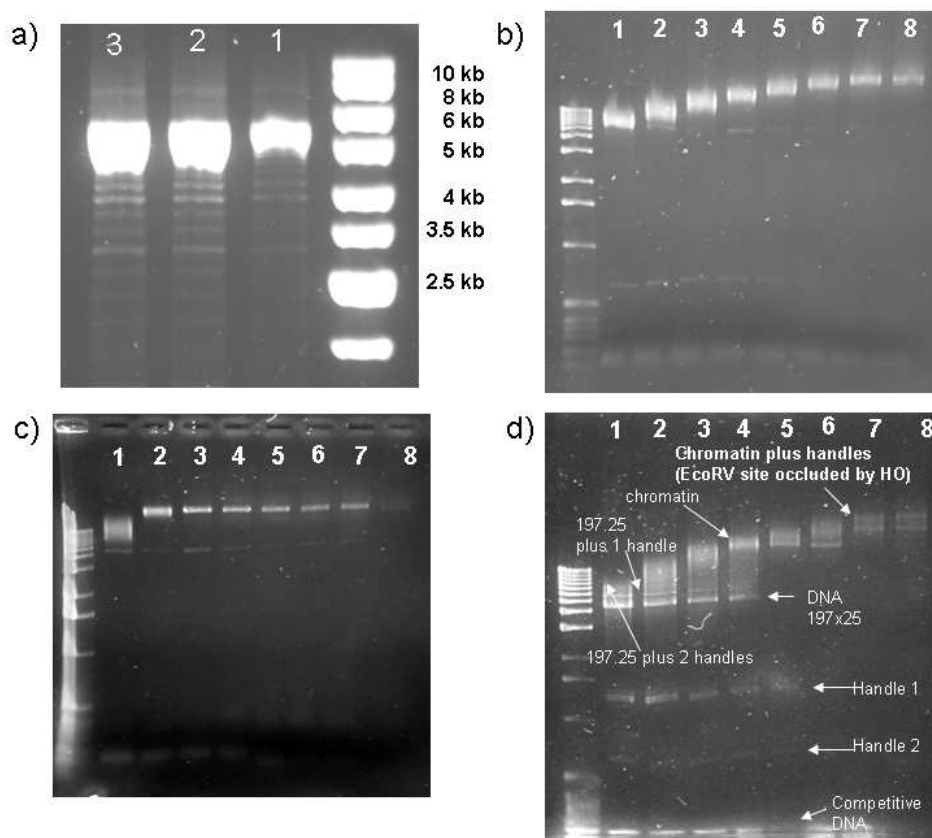


Figure 3.1: Biochemical preparations examined with gel electrophoresis. (a) 200 ng, 100 ng, and 50 ng 601 DNA arrays were loaded in lane 1, 2, and 3 respectively. The majority displays the size between 5 kb and 6 kb. The overexposed gel image exhibits few minor bands below the major band. (b) 601 DNA arrays with handles of 2035 bp were titrated in 8 steps with purified histones and mixed with 147 bp competitor DNA. (c) 601 DNA arrays with handles of 251 bp were titrated in 8 steps with the materials described in (b). (d) Chromatin fibers in 8 titrations shown in (c) were digested with EcoRV restriction enzymes. The digested handles have the size 1362 bp and 673 bp respectively. Lane 4 displays the narrowest band of chromatin fibers without handles.

Figure 3.2c shows a set of corrected FE traces measured on arrays of 601 positioning elements. The corresponding distribution of contour length of 601 DNA

arrays agrees well with the values obtained from counting nucleosome unwrapping at high force and qualitatively matches the electrophoresis results. Thus, despite of the different geometries of tethering a molecule to a paramagnetic bead, we can accurately obtain the contour length of individual molecules.

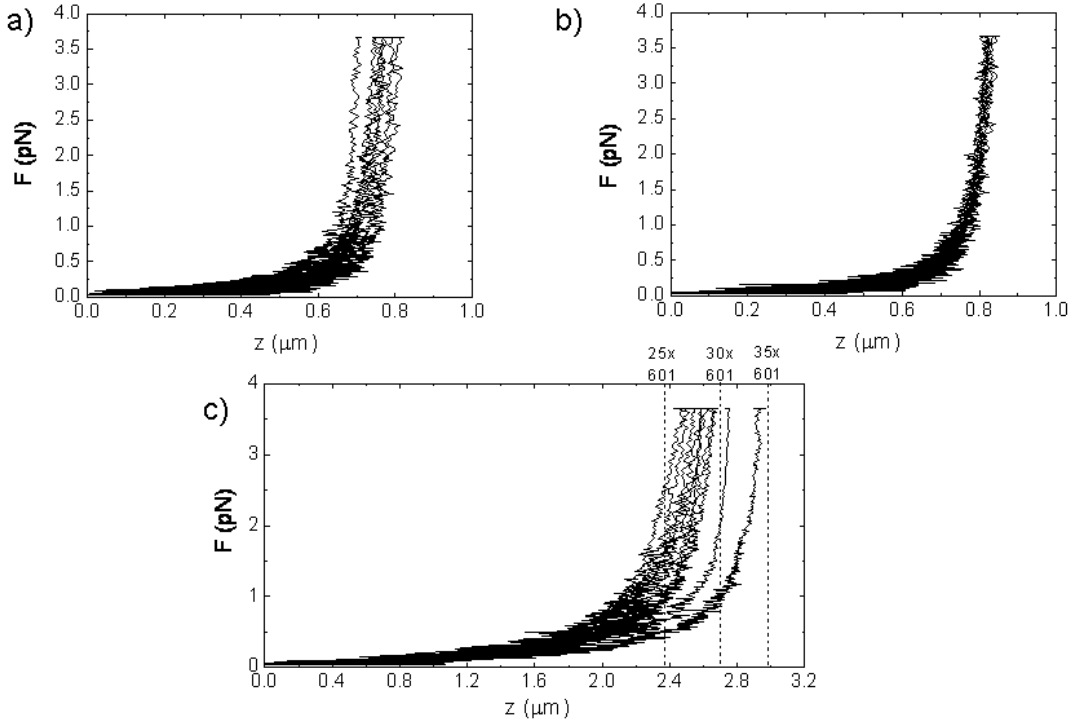


Figure 3.2: The variation of the size of 601 DNA arrays with 2035 bp handles displayed in FE traces. (a) FE traces of 2411 bp DNA fragments made with PCR without correcting anisotropic effects. (b) FE traces in (a) converge after the correction. The spread in length at 3.8 pN is within 50 nm. (c) The FE traces of the 601 DNA arrays with 2035 bp handles display 0.6 μm spread in length at 3.8 pN, indicating various numbers of 601 repeats.

3.3.2 Nucleosomes do not reconstitute on DNA handles

Compared to our previous report (Chapter 2) we increased the length of the handles, sum of the two DNA fragments on both sides of the chromatin fiber, from 251 bp to 2035 bp, in order to identify fibers in which nucleosomes are directly attached to the surface of the coverslip or to the bead through non-specific interactions. All fibers that had an extension smaller than 700 nm at 2 pN were discarded because the DNA handles extend to 700 nm following equation 3.1. After reconstitution, the chromatin fibers with the long handles appeared as two bands (lane 1 and lane 6 to lane 8)(Figure 3.1b) and a gradual transition

in lane 2 to lane 5 in the native gel (Figure 3.1b) as opposed to chromatin fibers with relatively short handles of 251 bp, that appear as a narrow band in the native gel (Figure 3.1c). Both the short handles and the long handles did not contain nucleosome positioning sequences so the formation of nucleosomes on these handles was not expected. To rule out reconstitution of nucleosomes on the long handles and to further characterize the properties of the fiber we did a post-reconstitution digestion of the handles. The subsequent native gel electrophoresis showed that the EcoRI restriction sites were well accessible and that the resulting DNA fragments did not contain nucleosomes (Figure 3.1d). We therefore conclude that the observed variation in the number of nucleosomes in individual fibers results from the variation in the number of 601 repeats in the DNA.

3.3.3 Low force analysis of chromatin stretching recovers the composition of single chromatin fibers

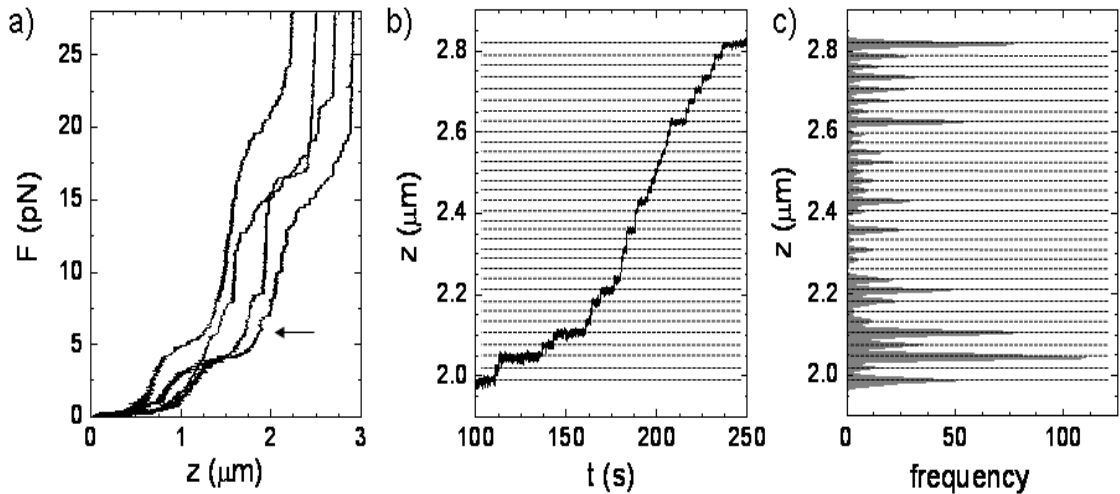


Figure 3.3: FE traces obtained from stretching individual chromatin fibers reconstituted with 197 bp 601 DNA arrays and histone octamers purified from chicken erythrocytes. (a) The chromatin fibers were tethered to $2.8 \mu\text{m}$ super paramagnetic beads, allowing magnetic tweezers to exert forces upto 28 pN. The FE traces display four representative characteristics: an entropic extension below 1 pN, a Hookean spring like extension, a plateau, and stepwise rupture events. (b) A representative time trace of a chromatin fiber indicated with an arrow in (a). The distance between adjacent dash lines is 25 nm. Above 7.5 pN, 33 steps with 25 nm step size are counted according to the number of the peaks shown in the histogram (c), revealing the number of nucleosomes on the fiber.

The number of nucleosomes in an individual chromatin fiber can be assessed straightforwardly at high forces (> 10 pN) by counting the number of distinct stepwise extensions that correspond to the unwrapping of the second turn of DNA from a single nucleosome, as shown in figure 3.3a. These traces are similar to the results obtained from optical tweezers experiments operated in position-clamp mode[18]. Due to the high stiffness of DNA at these forces, Brownian fluctuations of the tether length are small compared to the 25 nm steps in extension. For this batch of reconstituted fibers we observed a distribution of nucleosomes with $N=30\pm 5$ (Figure 3.3a), in accordance with the heterogeneity in the number of 601 repeats in the DNA that was used for this reconstitution.

Though high force measurements unequivocally resolve the number of nucleosomes in a fiber, these forces also induce histone dissociation [18]. In order to resolve the fiber composition in a potentially less-destructive manner we used Equation(3.5) to fit the FE traces between 1 pN and 5 pN, fixing $L_{DNA}= 2035$ bp, $p_{DNA} = 52$ nm and $L_{30} = 1.5$ nm (Figure 3.4a). From the fit we obtained $N= 35\pm 9$, which agrees with the number of second turn unwrapping events observed at high forces ($N = 33$, Figure 3.3b). Data points below 1 pN were discarded in this analysis because in the case of $2.8 \mu\text{m}$ beads and at such small forces, the extension of the fiber in a dynamic force spectroscopy experiment is dominated by the viscous drag on the bead[25]. The poor accuracy of N in the fit is a consequence of the use of a rather large bead for pulling on a very flexible tether, which results in a large amplitude of the Brownian fluctuations. Nevertheless, within the accuracy of the fit, the number of nucleosomes is consistent with the number of unwrapping events in this fiber at high forces.

Using $1 \mu\text{m}$ magnetic beads significantly reduces both the Brownian fluctuations, as shown in fig. 3.4b, and the viscous drag at small forces. However, in our magnetic tweezers setup $1 \mu\text{m}$ beads allow for a maximum force of about 4 pN. Therefore we cannot obtain the number of nucleosomes in the fiber from the number of second-turn unwrapping events. The FE traces of 15 different reconstituted chromatin fibers display significant variations, as shown in Figure 3.5a. All traces were fitted to Equation 3.5 and the distribution of the fit parameters is shown in Figures 3.5b-3.5g. Overall, the model yielded good fits with $R^2 \geq 0.95$. The number of nucleosomes varied between fibers, as expected based on the distribution of 601 position elements, but the values that define the stiffness of the BoS fiber, p_{BoS} as well as $k_{30}, \Delta G$, and L_{BoS} , are narrowly distributed suggesting that all variations between the fibers can be captured in the two-state model description for fiber extension.

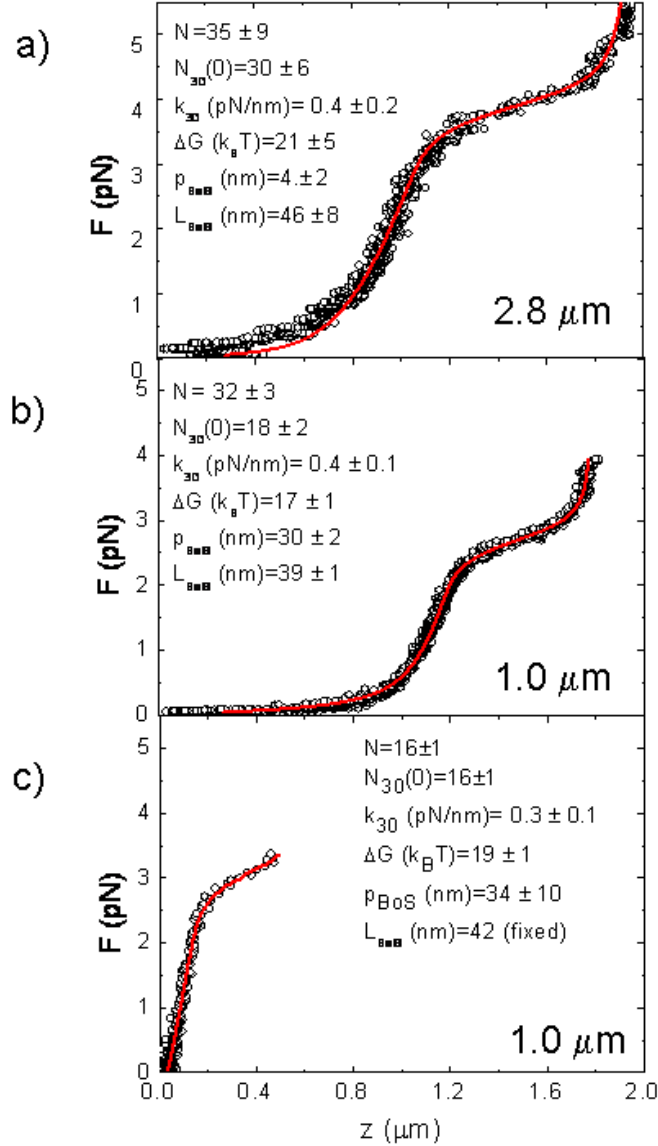


Figure 3.4: Comparison of FE traces obtained with 1 μm and 2.8 μm magnetic beads. (a) The fiber was tethered to a 2.8 μm magnetic bead and the FE trace was shown as black circles. The fit of 2-state model between 1 pN and 5 pN is displayed as a overlaid solid line. The fit below 1 pN was simulated according to the parameters yielded in the fit. (b) With a 1 μm bead, the FE trace shown as black circles is fitted to the model, yielding the fit shown as a overlaid solid line. Compared to the results of the fit in (a), the resulted parameters have reduced standard deviations. (c) The FE trace of a chromatin fiber with 251 bp DNA handles (black circles)[21] was fitted to the model containing fixed L_{BoS} 42 nm (the overlaid red line). The results are in a good agreement with the results obtained from chromatin fibers with 2035 bp DNA handles in (a) and (b). The reason why there was not initially a significant flat part to the curve at low force, as in parts in (a) and (b), is that the fiber in (c) did not contain a BoS fiber and the maximum extension of 251 bp DNA handles is 50 nm.

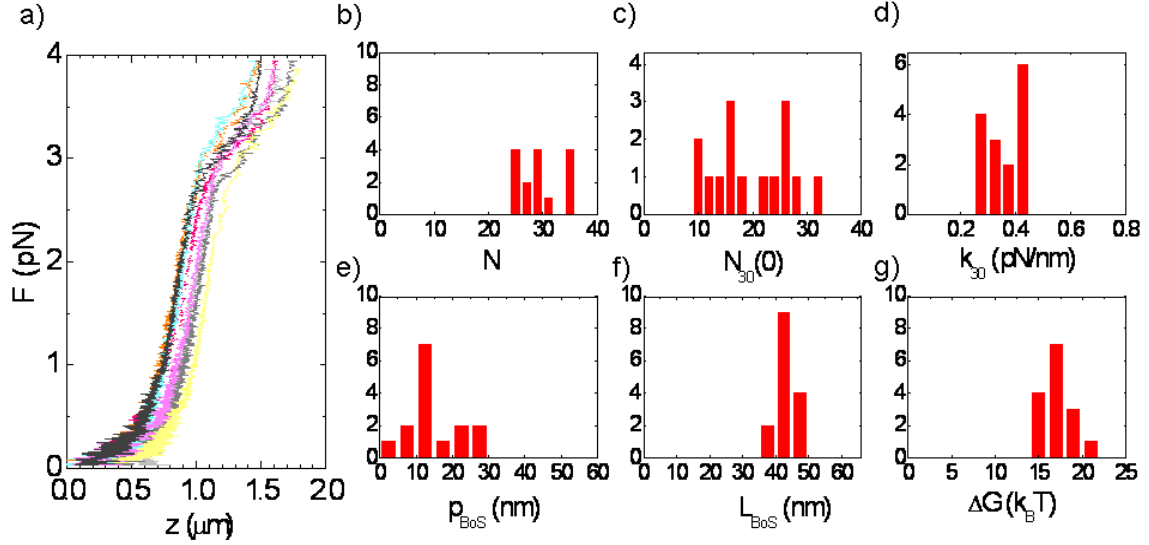


Figure 3.5: Reproducible mechanical properties of chromatin fibers with 2035 bp DNA handles. (a) FE traces obtained from 15 chromatin fibers tethered to $1 \mu\text{m}$ magnetic beads. (b) Quantified mechanical properties with 2 state model display narrow distributions of k_{30} , p_{BoS} , L_{BoS} , and ΔG . The variation of N is between 25 and 35 nucleosomes. $N_{30(0)}$ display a wide distribution between 9 and 32.

3.3.4 The force plateau at 3-4 pN represents simultaneous unstacking and unwrapping of nucleosomes

The fit of the FE trace to Equation 3.5 reveals, next to the number of nucleosomes, a second source of heterogeneity between fibers, which is that only part of the nucleosomes fold into a higher-order structure. All pulling traces were repeated three times on the same fiber, yielding overlapping FE traces. This indicates that the observed variation is intrinsic to the specific fiber and does not represent alternative conformations within each fiber. The contour length per nucleosome in the BoS fiber, L_{BoS} , is 43 ± 3 nm, which matches the sum of the contour length of linker DNA (17 nm) and the contour length of one turn wrapped DNA (25 nm). The narrow distribution of this parameter shows that it is a generic property that reproduces between fibers. If the nucleosomes in the BoS fiber would be fully wrapped, the maximum contour length per nucleosome would be the sum of the diameter of the nucleosome and the length of the linker DNA and would thus not exceed 26 nm. Unwrapping of one turn of the DNA, as previously demonstrated in single nucleosomes at forces of several pN[26, 27], adds additional 20 nm. This suggests that the BoS fiber conformation, on which the WLC description of the unfolded chromatin fiber was based, does not consist

of fully wrapped nucleosomes, but rather histone cores with only a single turn of DNA. Importantly, in all of the experimental traces we observed a fraction of this BoS conformation that was independent of force. Therefore, it seems that all fibers are only partially folded into 30 nm fibers in the experimental conditions that we used.

The force-dependent rupture of the folded chromatin fiber, as described by Equation 3.5, should not depend on the size of the DNA handles that tether the fiber between the surface and the bead. Here we extended the DNA handles, relative to our previous experiments, to several thousands of bp in order to directly recognize and discard non-specific sticking of chromatin to either the bead or the surface. Figure 3.4c shows a FE trace of a chromatin fiber with short DNA handles (251 bp). Again the fit reproduces the parameters that we obtained from the fibers connected with longer DNA handles. Thus the model that we present here captures FE behavior of a variety of chromatin fibers in a consistent manner.

3.3.5 Irreversible unfolding points to H2A-H2B dimer dissociation

The partial unwrapping of DNA from the histone core is likely to affect the stability of octamers. Because the unwrapping of the DNA exposes the H2A-H2B dimers, dimer-DNA interactions will not contribute to the stability of the octamer in a partially unwrapped state, which may drive dimer dissociation. The excellent reproducibility of the FE traces within a fiber demonstrates that the transient force-induced unwrapping is not necessarily detrimental to the nucleosomes in the fiber. Figure 3.6a shows 15 successive FE cycles on the same chromatin fiber, featuring a gradual shift towards a more extended structure. The successive traces were fit to Equation 3.5 and the resulting fit parameters are displayed in Figure 3.6b-3.6g. Again we obtained good fits yielding parameters that reproduced in successive FE traces, except for $N_{30}(0)$. The gradual increase of the number of nucleosomes that do not fold into a 30 nm fiber points to an irreversible change in the fiber composition towards nucleosomes with 43 nm contour length.

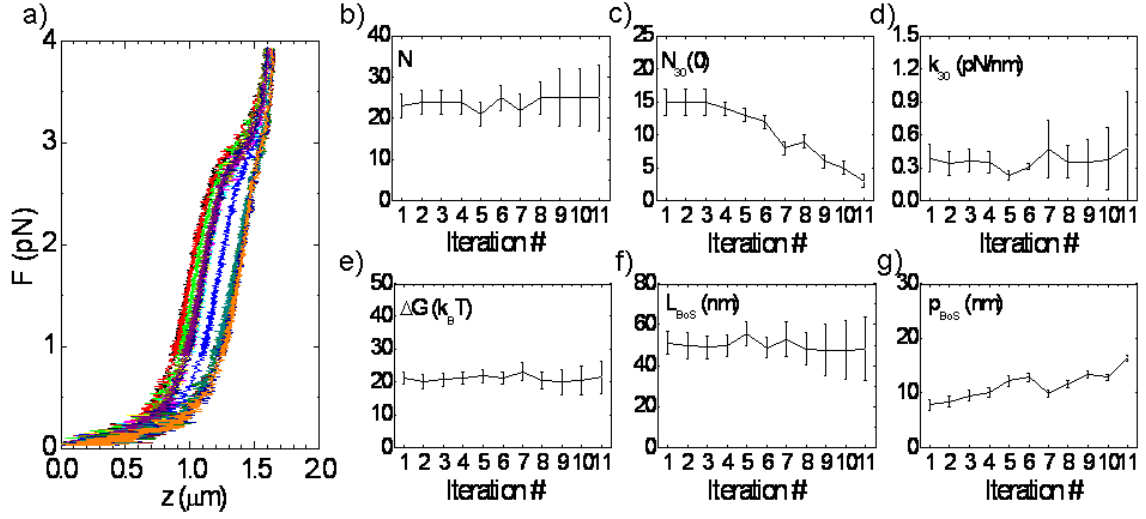


Figure 3.6: The change of the number of fully wrapped nucleosomes ($N_{30}(0)$) in repeated pulling experiments. (a) An identical chromatin fiber was stretched for 15 times, displaying the difference of $0.4 \mu\text{m}$ between 1 pN and 2.5 pN and the convergence at 3.9 pN. By fitting those traces to two-state model, the quantified results were shown in (b) to (g) as histograms. All the parameters are narrowly distributed except $N_{30}(0)$ and p_{BoS} .

It is known that dimers readily dissociate under single molecule conditions [20, 28]. The contour length of the nucleosomes in a BoS that we obtain here, as well as the irreversible increase of the fraction of nucleosomes in this conformation, imply that dimer dissociation causes the gradual decrease in chromatin compaction that is shown in Figure 3.6c. This interpretation is in accordance with the suggestion that nucleosome stacking requires the presence of at least one dimer per nucleosome pair, based on the H4-tail interaction with an acidic patch of the H2A-H2B dimer that was observed in the structure of the nucleosome [29]. The delicate dependence on exposure to forces, the significant variation that we observed between fibers, as well as the difficulty to assess the stoichiometry of H2A-H2B dimers in chromatin fibers by other means impede alternative ways to directly confirm the force-dependent dissociation of dimers. Nevertheless, the robustness of the fits obtained on a variety of chromatin fibers supports the interpretation of N_{BoS}^0 as the number of partially dissociated nucleosomes, i.e. H3-H4 tetramers, in the chromatin fiber. Using Equation 3.5 we can resolve the number of tetramers in each individual fiber, which is not only crucial for a structural interpretation of the FE traces, but also for quantitative assessment of the interaction forces that drive chromatin folding.

3.3.6 Mono- and divalent salts change the nucleosome-nucleosome interaction energy in folded fibers

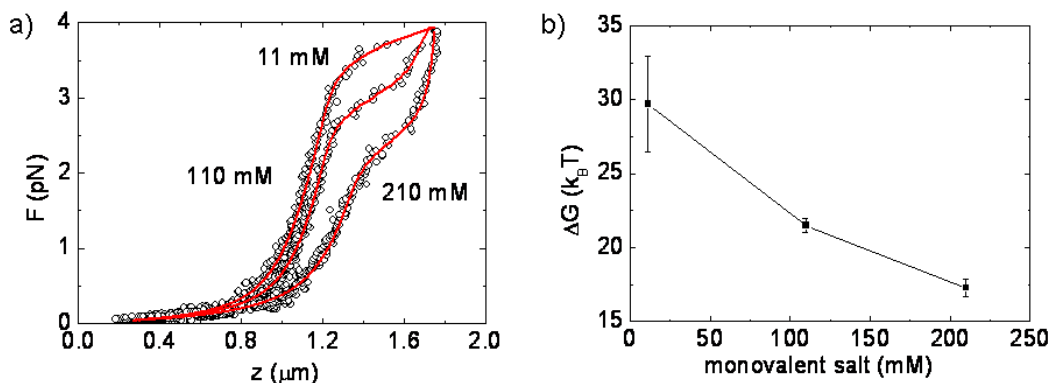


Figure 3.7: The impact of ionic strength in the interaction energy. (a) In the presence of 10 mM Na⁺, an identical chromatin fiber was stretched in 10 mM, 100 mM, and 200 mM K⁺. The extension of the chromatin fiber is shown as black cycles in FE plots. The overlaid solid lines are the fits obtained from 2-state model. (b) A plot of the interaction energy ΔG versus the concentration the total monovalent salt.

Table 3.1: A table gives the average values and deviations of all the results from the fits.

Salt (mM)	N_{30}	k_{30} (pN/nm)	$\Delta G(k_B T)$	L_0 (nm)	p_{BoS} (nm)
11	16.9 ± 0.8	0.26 ± 0.01	30 ± 3	54.6 ± 0.4	18 ± 2
110	13.8 ± 0.4	0.27 ± 0.01	22 ± 1	47.8 ± 0.7	20 ± 1
210	10.1 ± 0.4	0.19 ± 0.01	17 ± 1	50.5 ± 0.3	19 ± 1

Having established a rigorous model for describing the FE behavior of single chromatin fibers, we are now in a good position to evaluate the salt dependence of higher-order chromatin folding in detail. By measuring the same chromatin fiber we minimized heterogeneities in terms of fiber composition. Figure 3.7a shows three FE traces at increasing concentration of K⁺. After measuring three curves that all overlapped and did not show hysteresis, a new buffer was introduced in the flow cell and the measurement was repeated. When the salt concentration increased from 11 mM to 210 mM, the force plateau at which the 30 nm fiber ruptured decreased from 3.5 pN to 2.3 pN. We also observed a decrease in the condensation of the folded fiber. From the fits to Equation 3.5 we can attribute the reduced condensation of the fiber to a dissociation of nucleosomes into tetramers. Furthermore, the interaction energy dropped from 30 ± 3 $k_B T$ at

11 mM to $17 \pm 1 k_B T$ at 210 mM. All other mechanical parameters remained constant and within the range that we observed under standard conditions (Table 3.1). Thus the two-state description of nucleosome pairs, being either stacked or unstacked *and* unwrapped, holds over a wide range of salt conditions. This is an important finding because it shows that stability of the interactions rather than the conformation and the mechanical properties of the folded 30 nm fiber itself are sensitive to changes in salt conditions.

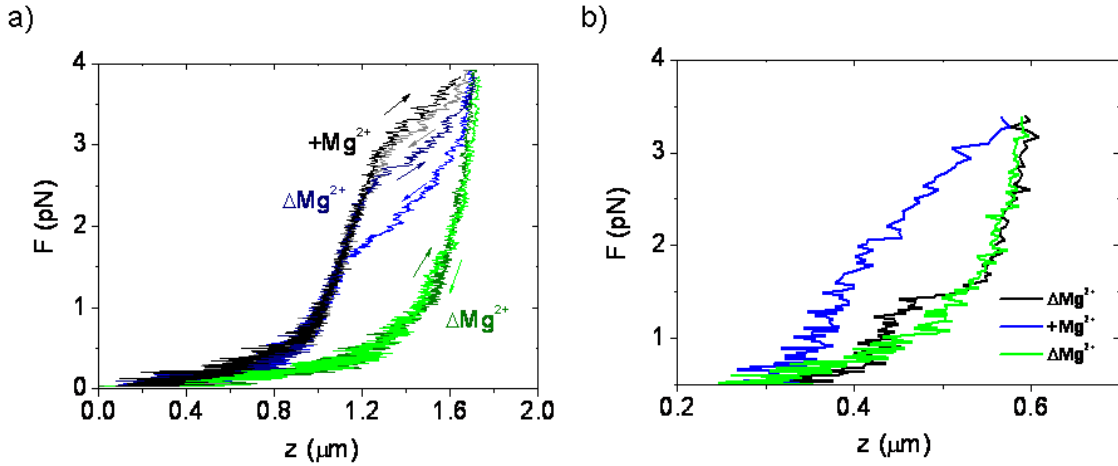


Figure 3.8: The role of Mg^{2+} in stabilizing fully wrapped nucleosomes. (a) The black and gray traces labeled with $+Mg^{2+}$ display the FE traces of a chromatin fiber stretched in the presence of Mg^{2+} . The arrows indicate the black trace as the forward trace and the dark gray trace is the backward trace. Subsequently, the Mg^{2+} was depleted by changing with 500 μl buffer without Mg^{2+} at the flow rate 2 $\mu l/s$, following a pulling experiment which results, the navy trace (forward) and the blue trace (backward), are labeled with blue ΔMg^{2+} . Finally, 500 μl buffer without Mg^{2+} was used to rinse the flow cell. The forward trace (olive) and the backward trace (green) were measured in the final buffer condition labeled with green ΔMg^{2+} . (b) A chromatin fiber was stretched in the absence of Mg^{2+} and the backward FE trace is labeled as ΔMg^{2+} (black line). Subsequently, we added Mg^{2+} by changing 250 μl buffer containing Mg^{2+} and performed one pulling experiment, yielding the backward FE trace labeled with $+Mg^{2+}$ (blue line). Then, we depleted Mg^{2+} again by flowing 250 μl buffer with Mg^{2+} at the flow rate 10 $\mu l/s$. The backward FE trace in the final buffer condition is labeled with ΔMg^{2+} (green line). In all these measurements, the forward traces are overlaid on the blue line and are not shown in the plot.

A few mM Mg^{2+} is required for chromatin folding into higher order structures. Upon depletion of Mg^{2+} we observed a large hysteresis between the pulling and release FE traces, indicating non-equilibrium behavior (Figure 3.8a). After multiple pulling experiments the data collapsed onto a trace that represents a partially

unwrapped BoS fiber. The fit parameters of the traces obtained from the same fiber before and after depletion of Mg^{2+} showed that the properties of the BoS fiber do not depend on the presence of Mg^{2+} within the accuracy of our measurements. The irreversible nature of the unstacking and unwrapping that together define higher-order folding indicates that restacking of nucleosome pairs is inhibited in absence of Mg^{2+} . Replenishment of Mg^{2+} however, partially recovers fiber folding, as shown in Figure 3.8b. Thus, as opposed to repeated and/or extended exposure to several pNs of force, Mg^{2+} depletion does not induce dimer dissociation by itself. In these experiments we replaced the buffer by flowing in new buffer. Though we tried to find a balance between minimizing the time necessary for replacing the buffer and minimizing the drag force generated by the flowing buffer, we cannot exclude that drag forces induced the dissociation of a few H2A-H2B dimers. Nevertheless, it is clear from these experiments that unstacking and unwrapping of nucleosomes do not necessarily lead to dimer dissociation, even in highly diluted conditions that are typical for single-molecule experiments. In conclusion we have shown that the FE behavior of chromatin fibers at low forces and in a range of buffer conditions follows a two-state equilibrium between stacked and unwrapped states of nucleosome pairs in which the interaction energy is modulated by salt conditions.

3.4 Discussion

Single-molecule force spectroscopy is unique in its ability to probe the mechanical properties of individual chromatin fibers, including their higher-order folding. Here we have shown that the rich variety in FE behavior that we measured can be attributed to heterogeneity in the number of nucleosomes and in the fraction of nucleosomes that are stacked. We have shown that all FE traces follow a simple force-dependent equilibrium of two states, representing a folded fiber in which nucleosomes are stacked, and an unfolded fiber in which nucleosomes, with one turn wrapped DNA only, interact through their linker DNA. The excellent fit to such a two-state system reveals that there is no cooperativity in the unfolding of the chromatin fiber. Thus it is sufficient to consider the interactions between two nucleosomes in the chromatin fiber, without the need to take non-neighboring nucleosomes into account. Our analysis also shows that, like single nucleosomes[26, 27], nucleosomes in a chromatin fiber unwrap in two distinct steps in response to increasing stretching forces. This is confirmed by the notion that even FE traces of fibers that only contain a few stacked nucleosomes, in which non-neighbor interactions are less likely to occur, follow the same me-

chanical model with the same mechanical parameters that define stretching and unstacking.

Quantitative analysis of the extension of nucleosomes in a BoS conformation reveals that these nucleosomes only contain a single turn of DNA. We separated nucleosomes that, depending on the force, reversibly change from a stacked to an unstacked *and* unwrapped conformation and nucleosomal particles that do not stack and remain unwrapped even at very small forces. The gradual and irreversible increase of this fraction after extended exposure to forces of only a few pN suggests that these particles have lost one or two H2A-H2B dimers. This finding confirms earlier reports that in typical force spectroscopy experiments only tetramers remain bound to the DNA[28]. By measuring at forces below 4 pN the fibers can be kept intact for sufficient time to probe their mechanical properties. These findings have important ramifications both for the interpretation of chromatin structure from various bulk techniques and for our understanding of chromatin structure *in vivo*.

Sedimentation velocity analysis is perhaps the most commonly used method for measuring chromatin condensation. Using sedimentation analysis a gradual dependence of chromatin condensation on salt concentration has been reported[10]. Several computational efforts have interpreted this as a subtle overall swelling of the fiber due to changes in electrostatic screening by the counterions[30]. In our current experiments we show that this is not the case: instead it is a change in the interaction energy and a resulting shift in the ratio between stacked and unwrapped nucleosomes that causes the fiber to decondense. Though it is not trivial to estimate the forces involved in sucrose gradient centrifugation, these forces may be in the same order of magnitude as the forces that we apply in our force spectroscopy experiments. Thus changes in sedimentation velocity can still be interpreted as changes in chromatin condensation, but here we suggest that these represent changes in the equilibrium between stacked and unwrapped states rather than a global swelling of the fiber.

Contrary to our initial interpretations[21], we have no evidence for an intermediate state consisting of fully wrapped nucleosomes in a BoS conformation (Figure 3.9a). The absence of any indications for such unfolded fibers could be either because unstacking (Figure 3.9d to Figure 3.9a) is rate-limiting, and is directly followed by unwrapping of the DNA from the histone core (Figure 3.9a to Figure 3.9b), or because in the folded fiber part of the nucleosomal DNA is partially unwrapped (Figure 3.9e). Force spectroscopy measurements on single nucleosomes shows reversible unwrapping at 2.5 pN [26, 27], at the same level as the force plateau for unstacking *and* unwrapping that we report here, indicating that unwrapping may be rate-limiting. The equal, or slightly increased,

enzymatic accessibility of nucleosomal DNA in a folded array[31], as compared to individual NCPs, on the other hand may point to sustained DNA unwrapping in folded chromatin arrays. Such partial unwrapping may significantly reduce the energetic cost for bending the linker DNA, which has been a strong argument against folding into a solenoidal structure.

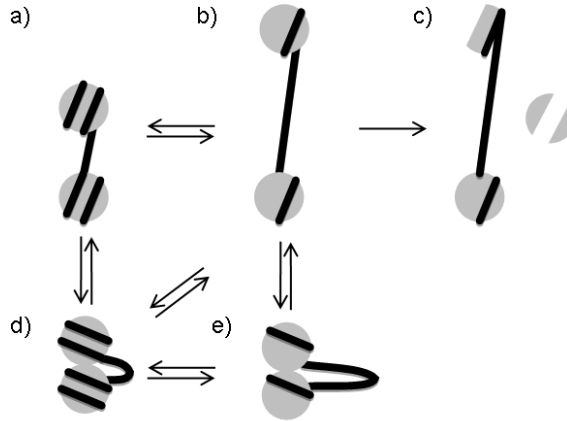


Figure 3.9: Schematic representation of the conformational changes in a chromatin fiber. The transition from fully wrapped nucleosomes (a) to nucleosomes with only one turn of DNA occurs in single nucleosomes at 2.5 pN and results in an extension of approximately 25 nm. After unwrapping we observed irreversible dimer dissociation forming tetramers (c). When pulling on folded fibers we report a stepwise extension of 42 nm, indicating a direct transition from stacked nucleosomes (d) to unstacked and unwrapped nucleosomes (b). The absence of the intermediate BoS structure (a) could be due to sustained unwrapping in the folded fiber (e) or due to a very short life time of the fully wrapped nucleosomes (a) at 2.5 pN.

Here we have shown, based on improved assessment of the tether length, by including all datasets and by explicitly allowing for the occurrence of tetramers in our analysis, that typically a small fraction of the nucleosomes don't stack at small forces (less than 1 pN) and under the conditions used. This has several consequences for our previously published interpretations of similar data[17, 21]. Based on the extension of the fiber before unstacking we argued that a 30 nm fiber with a 197 nucleosome repeat length fold into a solenoidal topology[21]. Because we now know that some of the nucleosomes may not have been in a stacked state, we underestimated the extension per stacked nucleosome before. Given the stiffness and the maximum rupture force, the maximal extension per nucleosome before rupturing is 7.8 nm, which is well within the dimensions of the nucleosome with partially stretched histone tails. The longer extension of the folded fiber before rupturing excludes alternative structures and thus further sup-

ports our previous interpretation. Because we now explicitly include a fraction of unstacked and unwrapped nucleosomes, the interaction energy that we report here is larger than the value we reported before. This energy includes unstacking and unwrapping. Given the discussion above, it is not clear whether these contributions can be decoupled. Future experiments that combine force spectroscopy with the single-molecule FRET measurements may be able to provide an even more detailed description.

What are the consequences of the described mechanism for chromatin unfolding *in vivo*? In this work we show that the force plateau at 2.5 pN represents nucleosome unstacking and DNA unwrapping, which can subsequently lead to dimer dissociation. The various DNA-based ATPases responsible for chromatin remodelling, transcription and replication, that are abundantly present in the eukaryotic nucleus, can all generate forces that exceed this threshold[32–37]. In fact, even thermal forces of the chromosome may be in this range. It is therefore likely that the dynamics that we describe here can also be found in the living cell and may play a significant role in maintaining the high mobility of dimers in that is observed in the eukaryotic nucleus[38].

Post-translational histone modifications have also been implicated to play an important role in the regulation of DNA based activities *in vivo* through the modulation of chromatin condensation[39]. Some of these modifications, in particular H4K16Ac[2] are likely to affect the interactions between nucleosomes. Others, like H3K56Ac have been shown to modulate the unwrapping of DNA within nucleosomes[15]. Here we propose that these activities may not be independent. With the current combination of low force pulling experiments and quantitative analysis it will be possible to unravel the effects of such modifications on chromatin higher-order folding, bringing us closer to a structural understanding of the regulatory role of chromatin organization.

3.5 Materials and Methods

3.5.1 Chromatin fibers

The DNA substrate in reconstituted chromatin fibers originated from pUC18 vector (Novagen) with 25 197bp repeats of the 601 nucleosome positioning sequence. After multiple generations we observed that recombination events had changed the original vector to a variety of plasmids containing 25-35 repeats. After digestion with XhoI and NheI digestion, single stranded ends were filled with a dUTP-digoxigenin at the XhoI and a dUTP-biotin at the NheI end. The linear DNA fragment was mixed with competitor DNA (-147 bp) and histone octamers

purified from chicken erythrocytes, and reconstituted into chromatin fibers using salt dialysis[8].

3.5.2 Flow cell preparation

A coverslip was sonicated in 1% RBS-50 and then 99% ethanol. Flame drying was performed afterward to remove excess of organic solvent. After one hour treatment in ozone plasma, the coverslip was coated with 1 mg/ml L-polylysine (Sigma) and then with a mixture of 20% w/v mPEG-Succinimidyl Propionic Acid (SPA)-5000 and 0.2% biotin-PEG-N-Hydroxysuccinimide (NHS)-3400 (Sunbright). Subsequently, the coverslip was mounted on a poly-di-methylsiloxane (PDMS, Dow Dorning) flow cell containing a 10x40x0.4 mm flow channel. The third coating was done in the channel by incubating with 0.1 mg/ml streptavidin (Sigma) for 10 minutes. After the channel was rinsed with 1 ml measurement buffer (MB) (10 mM HEPES pH 7.6, 100 mM KAc, 2 mM MgAc, 10 mM NaN₃, 0.1% (v/v) Tween-20, (+)0.2% (w/v)BSA), 0.1 μ g chromatin fibers were flushed in and tethered to 1 μ m paramagnetic beads (DYNAL Myone) coated with anti-digoxigenin (Roche). Excess non-tethered beads were removed with 1 ml MB (+) at a flow rate of 5 μ l/s.

3.5.3 Magnetic Tweezers

We used the same magnetic tweezers setup as described by Kruithof *et al.*[25]. We noted however a significant variation in tether length, even for DNA tethers with a known homogeneous size. We attributed this variation to attachment of the tether that was offset with respect to the bottom of the bead and corrected this offset by a rotation scheme. Figure (3.2) shows that this correction adequately recovers the correct tether length, within several nanometers.

3.6 Acknowledgements

We thank Maarten Kruithof, Peter Prinsen, and Nima Radja for helpful discussions and Ineke de Boer-Tuyn for technical support. This work was supported by HSFP.

Bibliography

- [1] Luger, K., Mader, A., Richmond, R., Sargent, D. & Richmond, T. *Nature* **389**, 251–260 (1997).

Bibliography

- [2] Robinson, P. J. J. *et al.* *J. Mol. Biol.* **381**, 816–825 (2008).
- [3] Huynh, V., Robinson, P. & Rhodes, D. *J. Mol. Biol.* **345**, 957–968 (2005).
- [4] Langmore, J. P. & Schutt, C. *Nature* **288**, 620–622 (1980).
- [5] Segal, E. *et al.* *Nature* **442**, 772–778 (2006).
- [6] Cairns, B. *et al.* *Cell* **87**, 1249–1260 (1996).
- [7] Allan, J., Mitchell, T., Harborne, N., Bohm, L. & Crane-Robinson, C. *J. Mol. Biol.* **187**, 591–601 (1986).
- [8] Robinson, P., Fairall, L., Huynh, V. & Rhodes, D. *Proc. Natl. Acad. Sci. U.S.A.* **103**, 6506–6511 (2006).
- [9] Schalch, T., Duda, S., Sargent, D. & Richmond, T. *Nature* **436**, 138–141 (2005).
- [10] Routh, A., Sandin, S. & Rhodes, D. *Proc. Natl. Acad. Sci. U.S.A.* **105**, 8872–8877 (2008).
- [11] Engholm, M. *et al.* *Nat. Struct. Mol. Biol.* **16**, 151–158 (2009).
- [12] Bohm, V. *et al.* *Nucleic Acids Res.* **39**, 3093–3102 (2011).
- [13] Li, G., Levitus, M., Bustamante, C. & Widom, J. *Nat. Struct. Mol. Biol.* **12**, 46–53 (2004).
- [14] Koopmans, W., Brehm, A., Logie, C., Schmidt, T. & van Noort, J. *J. Fluoresc.* **17**, 785–95 (2007).
- [15] Neumann, H. *et al.* *Mol. Cell* **36**, 153–163 (2009).
- [16] Poirier, M. G., Oh, E., Tims, H. S. & Widom, J. *Nat. Struct. Mol. Biol.* **16**, 938–944 (2009).
- [17] Cui, Y. & Bustamante, C. *Proc. Natl. Acad. Sci. U.S.A.* **97**, 127–132 (2000).
- [18] Brower-Toland, B. *et al.* *Proc. Natl. Acad. Sci. U.S.A.* **99**, 1960–1965 (2002).
- [19] Claudet, C. & Bednar, J. *Eur. Biophys. J. E* **19**, 331–337 (2006).
- [20] Claudet, C., Angelov, D., Bouvet, P., Dimitrov, S. & Bednar, J. *J. Biol. Chem.* **280**, 19958–19965 (2005).
- [21] Kruithof, M. *et al.* *Nat. Struct. Mol. Biol.* **16**, 534–540 (2009).
- [22] Bustamante, C., Marko, J., Siggia, E. & Smith, S. *Science* **265**, 1599–1600 (1994).
- [23] Kulic, I., Mohrbach, H., Lobaskin, V., Thaokar, R. & Schiessel, H. *Phys. Rev. E* **72**, 041905– (2005).

- [24] Klaue, D. & Seidel, R. *Phys. Rev. Lett.* **102**, 028302 (2009).
- [25] Kruithof, M., Chien, F., de Jager, M. & van Noort, J. *Biophys. J.* **94**, 2343–2348 (2007).
- [26] Kruithof, M. & van Noort, J. *Biophys. J.* **96**, 3708–3715 (2009).
- [27] Mihardja, S., Spakowitz, A., Zhang, Y. & Bustamante, C. *Proc. Natl. Acad. Sci. U.S.A.* **103**, 15871–15876 (2006).
- [28] Hagerman, T. A. *et al. Biophys. J.* **96**, 1944–1951 (2009).
- [29] Rhodes, D. *Nature* **389**, 231, 233 (1997).
- [30] Arya, G. & Schlick, T. *J. Phys. Chem. A* **113**, 4045–4059 (2009).
- [31] Poirier, M. G., Bussiek, M., Langowski, J. & Widom, J. *J. Mol. Biol.* **379**, 772–786 (2008).
- [32] Lia, G. *et al. Mol. Cell* **21**, 417–425 (2006).
- [33] Wang, M. D. *et al. Science* **282**, 902–907 (1998).
- [34] Yin, H. *et al. Science* **270**, 1653–1657 (1995).
- [35] Wuite, G. J., Smith, S. B., Young, M., Keller, D. & Bustamante, C. *Nature* **404**, 103–106 (2000).
- [36] Maier, B., Bensimon, D. & Croquette, V. *Proc. Natl. Acad. Sci. U.S.A.* **97**, 12002–12007 (2000).
- [37] Zhang, Y. *et al. Mol Cell* **24**, 559–568 (2006).
- [38] Kimura, H. & Cook, P. R. *J. Cell Biol.* **153**, 1341–1353 (2001).
- [39] Cosgrove, M. S. *Expert Rev. Proteomics* **4**, 465–478 (2007).

Force-dependent dynamics of single nucleosomes in chromatin

The accessibility of the DNA wrapped around a histone core is regulated within chromatin fibers and the detailed mechanism of the regulation is still unresolved. Here we examined the dynamics of single nucleosomes within chromatin fibers using magnetic tweezers. In constant force measurements, the extension of the stretched fiber showed reversible stepwise rupture events between multiple conformations containing different number of fully folded nucleosomes. Using a two-state model and a parameterized Hidden Markov analysis, we resolved the transition times, yielding the lifetimes of the closed and the open states. In the absence of force the lifetime of the open state is $1.2 \mu\text{s}$ and increases by 6 orders of magnitude with a few pN forces. Compared to mononucleosomes, the single nucleosomes within chromatin have significantly shorter lifetimes of the open state and the energy difference of the closed-open transition of $17 k_B T$ is 1.5-fold larger than the energy required in the first turn DNA unwrapping in mononucleosomes. Our findings show that nucleosome opening includes the rupture of nucleosome-nucleosome interactions and first turn DNA unwrapping in a single step.

This chapter is based on the manuscript: *Quantification of force-dependent dynamics of single nucleosomes in chromatin fibers*, F.T. Chien, T. van der Heijden, A. Routh, N. Radja, D. Rhodes and J. van Noort, to be submitted

4.1 Introduction

The eukaryotic genome is organized in chromatin. Chromatin consists of long arrays of nucleosomes, each made of approximately 147 base pairs (bp) of DNA wrapped around a histone octamer[1]. Nucleosome-nucleosome interactions contribute to higher-order structures of chromatin fibers[2]. Both DNA wrapping in nucleosomes and higher-order chromatin folding impose a steric barrier preventing DNA accessibility. Chromatin therefore plays an important role in the regulation of transcription, replication and other processes involving DNA[3, 4]. Exposure of nucleosomal DNA requires transient unfolding of chromatin fibers as well as partial or full unwrapping of DNA from the histone cores, and possibly histone dissociation. For a structural understanding of DNA organization in chromatin and its regulatory role, it is therefore important to reveal the kinetics of these processes.

In vitro, nucleosomal arrays fold into dense chromatin fibers that have a diameter of roughly 30 nm. Though it is not clear whether the 30 nm fiber is present in the eukaryotic nucleus, insight in its structure, dynamics, and the forces that drive 30 nm fiber folding will help to understand the mechanisms that control DNA accessibility. Extensive sedimentation analysis[5, 6], electron microscopy[7–9] and cross-linking studies[2] have shown a dependence of the condensation and stability of the fiber on ionic strength[9], Mg^{2+} concentration [8], the presence of linker histones[9], and the length of linker DNA[7]. The X-ray structure of a tetranucleosome showed two pairs of stacked nucleosomes, suggesting that 30 nm fibers fold into a zig-zag conformation[10]. However, it is not clear whether this is representative for all fiber compositions, nor is it clear how such fibers dynamically fold and unfold. Forster Resonance Energy Transfer (FRET) measurements on a trinucleosome, which were inspired by the X-ray structure, recovered a rich dynamic behavior of the interactions between the nucleosomes with at least four different states[11]. Enzymatic DNA digestion of nucleosomal arrays showed that the fiber is relatively open and accessible to restriction enzymes[12], suggesting that transiently open states are significantly populated. Thus, bulk experiments have revealed a highly dynamic open state of chromatin fibers, but neither their structure nor the kinetics have been fully resolved.

With single molecule force spectroscopy it is possible to mechanically manipulate individual chromatin fibers and study the structural transitions within chromatin fibers by analyzing the force-extension relation. For single nucleosomes within chromatin fibers, the forced unwrapping of the second turn of DNA from histone cores occurs at forces between 15 and 25 pN. A detailed energy landscape for the second turn DNA unwrapping has been constructed from the force depen-

dence of the unwrapping rates[13]. This energy landscape was shown to depend on the presence and the acetylation state of the histone tails[14]. Studying the higher-order folding of chromatin fibers however, requires a more subtle approach as 3 to 4 pN is sufficient to break the nucleosome-nucleosome interactions[15, 16]. Using reconstituted fibers we have previously shown that mechanical properties of a fiber, i.e. its rest length and its stiffness, depend on the linker DNA length, but not on the presence of linker histones, nor on ionic strength[16]. Force induced rupture of chromatin higher-order folding yields a fiber containing nucleosomes that have only one turn of DNA wrapped around the histone core (Chapter 3). This structural transition of the chromatin fiber was reversible in the time window of the experiment, i.e. several tens of seconds. Extended exposure to forces exceeding 4 pN resulted in irreversible DNA unwrapping which we attributed to dissociation of H2A-H2B dimers (Chapter 3). These dynamic force spectroscopy experiments however could not recover the kinetics of rupturing nucleosome-nucleosome interactions and DNA unwrapping events that are associated with this transition. The high transition rates, the large flexibility of the fiber with the accompanying large thermal fluctuations of the extension of the fiber, and the possibility of multiple simultaneous unfolding transitions complicate a detailed analysis of the kinetics of chromatin unfolding.

Mononucleosomes provide a relatively simple system to study nucleosome dynamics and have been successful in uncovering a rich pallet of structural transitions. FRET studies on mononucleosomes have revealed that the partial unwrapping of the first turn of DNA occurs spontaneously every 250 ms and has a life time of 25 ms[17, 18]. Post-translational histone modifications, in particular acetylation of H3K56, significantly shifts the equilibrium towards the partially unwrapped conformation[19]. Single molecule force spectroscopy on mononucleosomes revealed a two-stage unwrapping of DNA from the histone core[20, 21]. First turn unwrapping at 2.5 pN is reversible and strongly depends on the ionic strength, reflecting the electrostatic nature of DNA- histone interactions[20]. The life times of the wrapped and the unwrapped states of the first turn of DNA follow Arrhenius-like force-dependence. Kulic and Schiessel have shown that bending of linker DNA in the force spectroscopy experiments creates a strong barrier against unwrapping when forces are applied to the DNA ends[22]. Nucleosome-nucleosome interactions are likely to significantly affect the dynamics of nucleosomes. For a fair assessment of the dynamics of conformational changes in nucleosomes it is probably not sufficient to study isolated nucleosomes. It is therefore important to study nucleosome dynamics in the context of a chromatin fiber.

In a previous study we have shown that the plateau in the force extension

traces of chromatin fibers can be fully explained by a transition from a folded fiber to a fiber with nucleosomes that only contain one turn of wrapped DNA. Next to the mechanical parameters of the fibers we could also extract the difference in free energy between these two states, but the transition rates remained hidden in the data. Here, we probed the dynamics of these transitions by recording the fluctuations in the extension of single chromatin fibers at constant forces. Using a parameterized Hidden Markov analysis, inspired by the analysis of multichannel patch clamp recordings[23], we resolved the transition rates between states of each nucleosome from the extension time traces that we measured. The change in the conformation of an individual nucleosome is hidden in the variations of the overall extension because of the relatively large thermal fluctuations of the tether and possibility of simultaneous changes in a nucleosome array. By explicitly accounting for this force dependence in all parameters that affect the measurements it is possible to reduce the complexity of the HMM analysis. Thus, we obtained the lifetime of each state as a function of force. The life time of the unwrapped state, extrapolated to zero force is $1.2 \mu\text{s}$, which is three orders of magnitude smaller than the life time of the unwrapped state in free mononucleosomes. The state corresponding to fully wrapped nucleosomes within the chromatin fiber has a much longer lifetime, reflecting the stabilization of the nucleosome by embedding in the fiber.

4.2 Theory

4.2.1 A two-state model for force induced conformational changes in nucleosomes

The force dependence of the parameters that define the structure of a chromatin fiber in a magnetic tweezers force spectroscopy experiment complicates a quantitative, time-resolved interpretation of the extension traces. In our previous studies we showed that the plateau in the Force-Extension (FE) trace measured on reconstituted chromatin fibers can be well described by a two-state model, in which the nucleosomes in the fiber change from a folded conformation into an extended conformation. The detailed structure of the DNA trajectory and the nature of the nucleosome-nucleosome interactions in the folded fiber remained unresolved. The length of the extended conformation however unambiguously points to a conformation in which each nucleosome contains a single wrap of DNA and does not interact with its neighbors. Here we will refer to these states as an open (o) state and a closed (c) state, whose lifetimes τ_o and τ_c follow an

Arrhenius-like force-dependence:

$$\begin{aligned}\tau_o(F) &= \tau_o(0) \exp(+F\delta_o/k_B T), \\ \tau_c(F) &= \tau_c(0) \exp(-F\delta_c/k_B T),\end{aligned}\tag{4.1}$$

with force F , thermal energy $k_B T$ and δ_o and δ_c the distance between the barrier and the open or closed state. With video microscopy we measured the height of the bead that is tethered by the fiber in discrete time steps Δt , corresponding to the time between two frames. The probability of staying in each state after a time Δt follows a Poisson distribution:

$$\begin{aligned}P(o | o) &= \exp(-\Delta t/\tau_o(F)), \\ P(c | c) &= \exp(-\Delta t/\tau_c(F)).\end{aligned}\tag{4.2}$$

The equilibrium constant $K(F)$ depends on the force and the extension of both states, z :

$$K(F) = \frac{\tau_o(F)}{\tau_c(F)} = \exp\left(-\frac{\Delta G - F[z_o(F) - z_c(F)]}{k_B T}\right),\tag{4.3}$$

in which ΔG represents the difference in free energy between the two states in the absence of force.

4.2.2 Conformational changes of multiple nucleosomes in a fiber

Assuming there is no cooperativity of nucleosome transitions and all nucleosomes are identical, each nucleosome independently follows Equation 4.3. Thus, the fraction of open nucleosomes within the fiber, θ , equals

$$\theta(F) = \frac{\tau_o(F)}{\tau_o(F) + \tau_c(F)} = \frac{K(F)}{K(F) + 1}.\tag{4.4}$$

A fiber with N nucleosomes can have $N+1$ different states. The probability to be in a state with i closed nucleosomes is

$$P(i, F) = \binom{N}{i} (1 - \theta(F))^i \theta^{N-i}(F).\tag{4.5}$$

The total extension of the fiber z_{fiber} is the sum of the extension of the DNA flanking the fiber, z_{DNA} , and the extensions of each nucleosome:

$$z_{fiber}(i, F) = z_{DNA}(F) + i \cdot z_c(F) + [N - i + N(0)]z_o(F). \quad (4.6)$$

Here we have taken into account our previous observation that, under the conditions used in single molecule force spectroscopy, there is always a number of permanently unwrapped nucleosomes $N(0)$. These nucleosomes have an extension that is, within the accuracy of our experiment, equivalent to that of the open conformation. As reported before[16], an array of open nucleosomes follows a FE behavior that can be described by a Worm Like Chain (WLC), characterized by its persistence length p_o and contour length L_o . An explicit description of reverted WLC, WLC^{-1} , is given in Chapter 3. The folded fiber follows a Hookean extension with a characteristic stiffness per nucleosome k_c and a contour length L_c . The details of the extension of z_{DNA} , z_o , and z_c are as follows

$$\begin{aligned} z_{DNA}(F) &= WLC^{-1}(L_{DNA}, p_{DNA}) \\ z_o(F) &= WLC^{-1}(L_o, p_o) \\ z_c(F) &= L_c + F/k_c. \end{aligned} \quad (4.7)$$

Because the fiber is very flexible, thermal fluctuations are generally large and can obscure the discrete change in extension when a nucleosome switches between the closed and open states. The stiffness of the fiber k_{fiber} with i closed nucleosomes is

$$k_{fiber}(i, F) = \left(\frac{d z_{fiber}(i, F)}{dF} \right)^{-1}. \quad (4.8)$$

Thus the probability distribution for observing the bead at height z when the fiber is in state i equals

$$\begin{aligned} P(z, i, F) &= \sqrt{\frac{c^2(i, F) k_{fiber}(i, F)}{2\pi k_B T}} \times \\ &\exp\left(-\frac{c^2(i, F) k_{fiber}(i, F) \cdot (z - z_{fiber}(i, F))^2}{2k_B T}\right) P(i, F), \end{aligned} \quad (4.9)$$

where c is a correction factor for camera blurring. Here we assumed that extension of the fiber results in an immediate increase of the bead height. This is only valid

when the frame rate $(\Delta t)^{-1}$ is smaller than the corner frequency, f_c , of the bead-fiber tether:

$$f_c(i, F) = \frac{k_{fiber}(i, F)}{12\pi^2\eta R}, \quad (4.10)$$

with bead radius R and viscosity η . Though the measured average position of the bead accurately follows the extension of the fiber in this case, its variance is reduced due to blurring effects of the camera. This can be accounted for by a motion blur correction function [24]:

$$c(i, F) = \frac{2}{\Delta t f_c(i, F)} - \frac{2}{\Delta t^2 f_c^2(i, F)}(1 - \exp[-\Delta t f_c(i, F)]). \quad (4.11)$$

The overall time averaged probability distribution to observe a bead height z equals:

$$P(z, F) = \sum_{i=0}^N P(z, i, F). \quad (4.12)$$

4.2.3 A parameterized Hidden Markov Model of nucleosome dynamics

Though the above description of the tether extension quantifies parameters as a function of force, it does not include the force dependent kinetics of the nucleosome transitions in the chromatin fiber. Compared to experiments on mononucleosomes a dwell-time analysis of the different states of the fiber is more difficult because i) multiple transitions may occur within one time frame Δt , ii) the dwell times between changes in extension become shorter with more nucleosomes in the fiber, iii) relative changes in extension decrease with multiple nucleosomes and iv) the thermal fluctuations are larger due to the increase in length and the decrease in stiffness of the fiber.

Hidden Markov Models (HMMs) incorporate a Markov process describing transitions between different states and its obscuring by noise. Inspired by the multichannel patch clamp recordings[23], we use a parameterized HMM that allows the parameters of the individual nucleosomes to be extracted directly from a constant force time trace of the extension of a single chromatin fiber. As the mechanical parameters and the equilibrium constant for the conformational changes are defined above and can be fitted from the equilibrium FE trace, the only missing parameter is the life time of one of the states, and how it depends on force.

The probability distribution $P(z, i, F)$ for each state of the fiber is given by Equation 4.10. The transitions between states of the fiber at force F can be described in a transition matrix where the elements $A_{i,j}(F)$ correspond to the conditional probabilities $P(i | j)$

$$\begin{aligned}
 P(i | i) &= P(c | c)^i P(o | o)^{N-i} \\
 P(i | i - 1) &= iP(c | c)^{i-1} P(o | o)^{N-i} (1 - P(c | c)) \\
 P(i | i + 1) &= (N - i)P(c | c)^i P(o | o)^{N-i-1} (1 - P(o | o)).
 \end{aligned}
 \tag{4.13}$$

All other elements with $|i - j| > 1$ equal 0. With Equations (4.8-4.12) we can now define a parameter vector Θ that fully describes the structure and dynamics of the fiber:

$$\Theta = (L_{DNA}, p_{DNA}, L_0, p_0, L_c, k_c, \Delta G, \tau_0(F))
 \tag{4.14}$$

Using a Viterbi algorithm[25], we optimized $\tau_0(F)$ for given $L_{DNA}, p_{DNA}, L_0, p_0, L_c,$ and k_c and ΔG to maximize the likelihood of Θ to describe $z_{fiber}(i, F)$. To allow for multiple transitions to occur simultaneously, resulting in multiple steps, and transitions that cancel within one frame, we tested higher order transitions by multiplying the transition matrix. For transitions of order m this results in $A^m(F)$. We increased m until the best fit, i.e. lowest mean squared difference, was obtained. Thus, by fitting $\tau_0(F)$ and testing which order of the transitions that matched the time trace best, we obtained the lifetimes of the two states of a single nucleosome embedded in a chromatin fiber.

4.3 Results

4.3.1 Force-Extension traces capture structural transitions in a stretched chromatin fiber.

FE traces on single chromatin fibers up to forces of 4 pN are very reproducible and display no hysteresis, pointing at dynamic equilibrium of the different conformations of the chromatin fiber[16], Figure 4.1a. In a typical experiment we cycled the force on the fiber in a well-defined fashion: first the force was kept constant at 30 fN for 30 s, then the magnet position was decreased in 20 s in a linear fashion, resulting in an exponentially increasing force[21], up to a preset maximum, which was kept for a preset time before reversing the force down to 30 fN. After this we measured for another 30 s. To obtain more data points, we

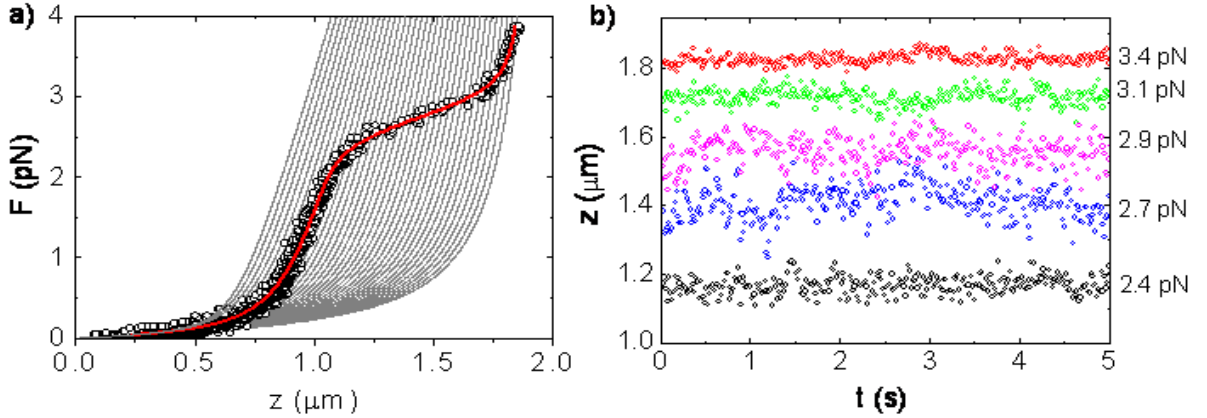


Figure 4.1: Different states of a chromatin fiber. (a) The FE trace of a stretched chromatin fiber (black circles) is fitted with 2-state model (red line). The fit parameters are $N = 28 \pm 1$, $k_c = 0.37 \pm 0.02$ pN/nm, $L_o = 40.2 \pm 0.1$ nm, $p_o = 14 \pm 1$ nm, and $\Delta G = 16.5 \pm 0.1 k_B T$. Taking the parameters obtained from the fit, we use Equation 4.4 to calculate the FE traces of each of the states within a fiber by decreasing the number of the closed nucleosomes (black lines). (b) Constant force measurements display large fluctuations of the extension of a stretched chromatin fiber. The time period of the measurements is 2 minutes. The displayed here are the first 5 seconds with a frame rate 60 Hz. The colors of the traces correspond to the exerted forces, 2.4 pN (black), 2.7 pN (blue), 2.9 pN (magenta), 3.1 pN (green), and 3.4 pN (red).

decreased the speed of shifting the magnets at forces above 1 pN. Overall, fibers were exposed to forces exceeding several pN only for a limited time. The low force measurements at the beginning and the end of the experiment allow for an accurate assessment of the offset and the drift in the FE trace. Together with absolute length measurements of sub-micro tethers (Chapter 3), this allows for a quantitative, absolute measurement of the extension of a fiber, which is required for a mechanical description of the FE trace.

The FE trace of a single chromatin fiber follows the mechanics of a complex spring, consisting in part of DNA and in part of chromatin, as described in Kruithof *et al.*[16] and Equation 4.8. The chromatin fiber changes from a folded conformation into an extended conformation at about 3 pN, resulting in a plateau in the FE trace. Fitting the FE trace to Equation 4.8 yields reproducible parameters for the mechanical properties of the fiber, p_o and k_c , as well as for the difference in free energy ΔG between the open and the closed nucleosomes in the fiber (Chapter 3). Because the composition of the fiber may vary, despite of the use of well-defined tandem arrays of 601 positioning elements(Chapter 3), we analyzed fibers individually. The fiber shown in Figure 4.1a was reconstituted with the DNA subtract containing 35 repeats of 601 sequence so it contained 35

nucleosomes. Thus, this fiber can have 36 states, depending on the conformation of each of its nucleosomes. Using fitted parameters we computed the FE traces for this fiber for each state (Figure 4.1). At forces below 2 pN the measured extension of the fiber was significantly larger than that of the fully folded fiber, indicating the loss of dimers in 8 nucleosomes, in accordance with our previous report (Chapter 3). In the force plateau the fiber switches states with an increasing amount of open nucleosomes, but the dynamics of these transitions remains hidden in the FE traces due to the limited time resolution and the relatively large thermal fluctuations of the extension of the fiber.

4.3.2 Constant force measurements reveal dynamic transitions

Figure 4.1b shows several traces of the extension of the fiber at constant force. At 2.4 pN, most nucleosomes remain in the closed state, whereas at 3.4 pN most nucleosomes remain in the open state. The expected change in the extension of the fiber due to unstacking and unwrapping of a single nucleosome between 2 pN and 4 pN is 22-25 nm (Figure 4.5a). In both extremes of the plateau the fluctuations in extension are significantly smaller than those at the intermediate states. Note that the fluctuations in the extension measurement are in all cases significantly larger than the accuracy of the bead detection, which is several nm. From the stiffness which is the slope of the FE trace of each state between 2 and 4 pN we calculate the corner frequencies f_c of the bead response (Equation 4.10), yielding at least 150 Hz. Any changes in extension transitions slower than 150 Hz will be accurately followed by the bead. However, observation of the bead with a frame rate of 60 Hz results in a reduction of the fluctuations by $c^2 = 0.69$, Equation 4.11 due to blurring. Thus, the expected standard deviation of the extension of each state is 11 nm. When further averaging is not desired, observation of individual transitions in the fiber therefore approaches the physical limits of the signal-to-noise ratio of extension measurements of the fiber.

Before analysis of the dynamics of the conformational changes in single chromatin fibers, we first tested the validity of our mechanical model at constant force by the analysis of the time averaged extension distributions. Figure 4.2a shows five FE traces obtained from the same fiber with increasing forces, along with the fit to Equation 4.8. As expected, the FE traces are highly reproducible, confirming the reversibility of the conformational changes in the force plateau. Note that the size of the force plateau is much smaller than that of the fiber shown in Figure 4.1. This indicates that a larger number of nucleosomes within this fiber had dissociated dimers. The mechanical parameters of both fibers were

however the same, within the accuracy of the measurement. Figure 4.2b shows the distribution of the extension of the fiber as measured over 30 s, along with a global fit to Equation 4.12. The global fit to the extension distributions at constant force yielded the same mechanical parameters for the chromatin fiber as those obtained from the FE trace. Though Equation 4.8 and Equation 4.6 are based on the same mechanical model, the different time dependence of the force in these experiments and the explicit inclusion of the thermal fluctuations of the fiber extension probe different aspects of the kinetics of the fiber-bead system. The good agreement of both fit results demonstrates that all relevant parameters to describe the kinetics of the force-dependent fiber mechanics are included in our analysis.

In a constant force experiment we expect the probability distribution of each state of the chromatin fiber, as well as their transition probabilities be invariant over time, following the definition of Markov processes. This is only valid if the composition of the fiber does not change over time. As in previous experiments however, we sometimes observed a gradual increase in the number of nucleosomes that stayed permanently in the open state, which we attribute to the dissociation of H2A-H2B dimers (Chapter 3). An extended exposure to forces above the rupture force increased the probability for such events. Because we measured FE traces before and after each constant force experiment we were able to verify the fiber integrity. Traces that showed hysteresis were discarded for further analysis. This limited the duration of the constant force experiments.

4.3.3 The kinetics of conformational changes of single nucleosomes embedded in chromatin fibers

Here we use a parameterized HMM to analyze the kinetics of force-induced conformational transitions in single chromatin fibers. Because the FE experiments yielded the same mechanical parameters as the constant force experiments we used the parameter set obtained from the FE fit in the HMM analysis, leaving a single free parameter that describes the kinetics of the transition. Figure 4.3 shows 2.5 s sections of 5 constant force extension traces recorded for 120 s on the same chromatin fiber. The results of the HMM analysis are overlaid. Despite the stochastic variations in the extension, the result of the HMM analysis accurately follows the experimental time trace. We obtained the best agreement when transitions of order $m = 2$ were included, indicating that the rates of the transitions in the fiber were close to the frame rate of the camera. Indeed, most of the assigned states have a life time corresponding to a few frames. Despite the relatively large thermal noise and the relatively short life times of the states of

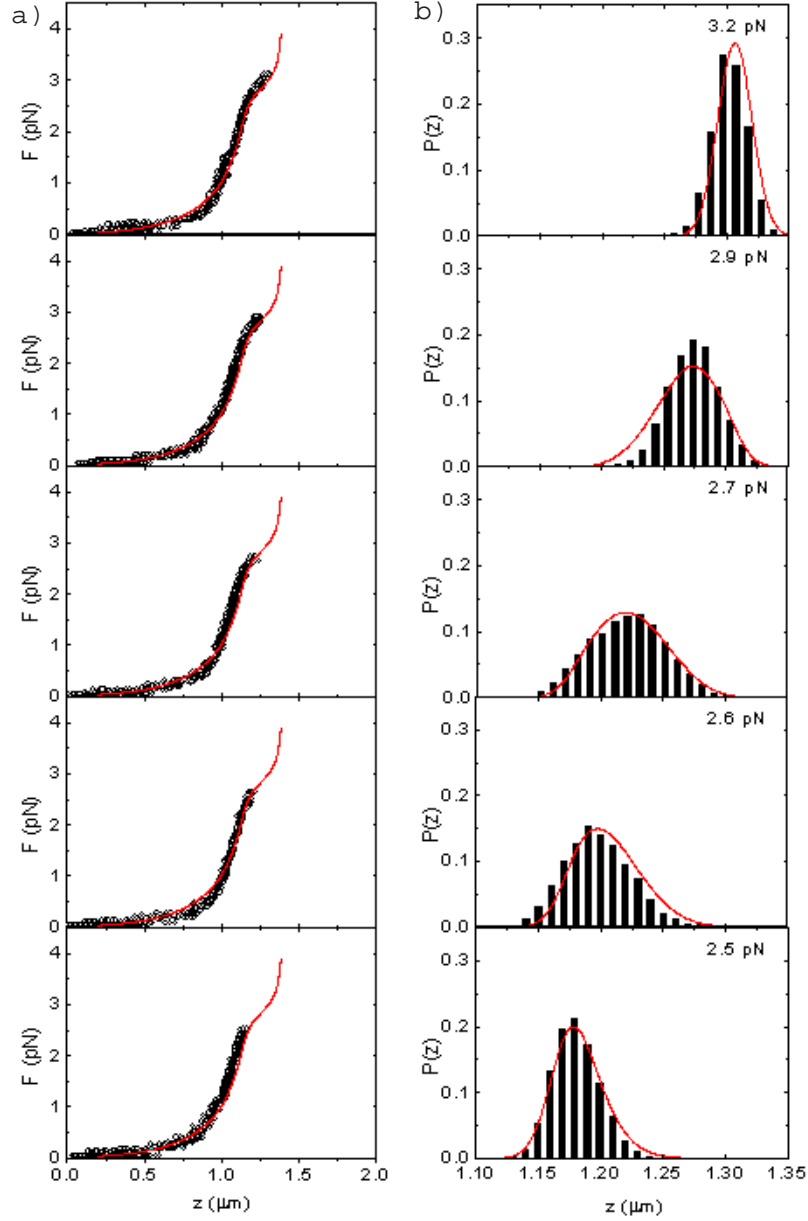


Figure 4.2: Probability distributions of the extension of a chromatin fiber. (a) Force extension traces are shown as black circles and the red solid line shows a fit to the first FE trace obtained prior to the series of constant force measurements. The fit parameters obtained from the fit to FE trace are $N = 6 \pm 2$, $k_c = 1 \pm 1$ pN/nm, $L_o = 42 \pm 1$ nm, $p_o = 7 \pm 1$ nm, and $\Delta G = 17 \pm 5 k_B T$. (b) Global fit (solid red lines) of the histograms of individual time traces obtained at the constant force (black columns). The fit parameters obtained from global fits are $k_c = 0.67 \pm 0.04$ pN/nm, $L_o = 38.6 \pm 0.2$ nm, $p_o = 7.6 \pm 0.3$ nm, and $\Delta G = 16.1 \pm 0.2 k_B T$. N was fixed to 6 as measured in the FE traces.

the fiber, the parameterized HMM can still assign the state of the fiber in each frame.

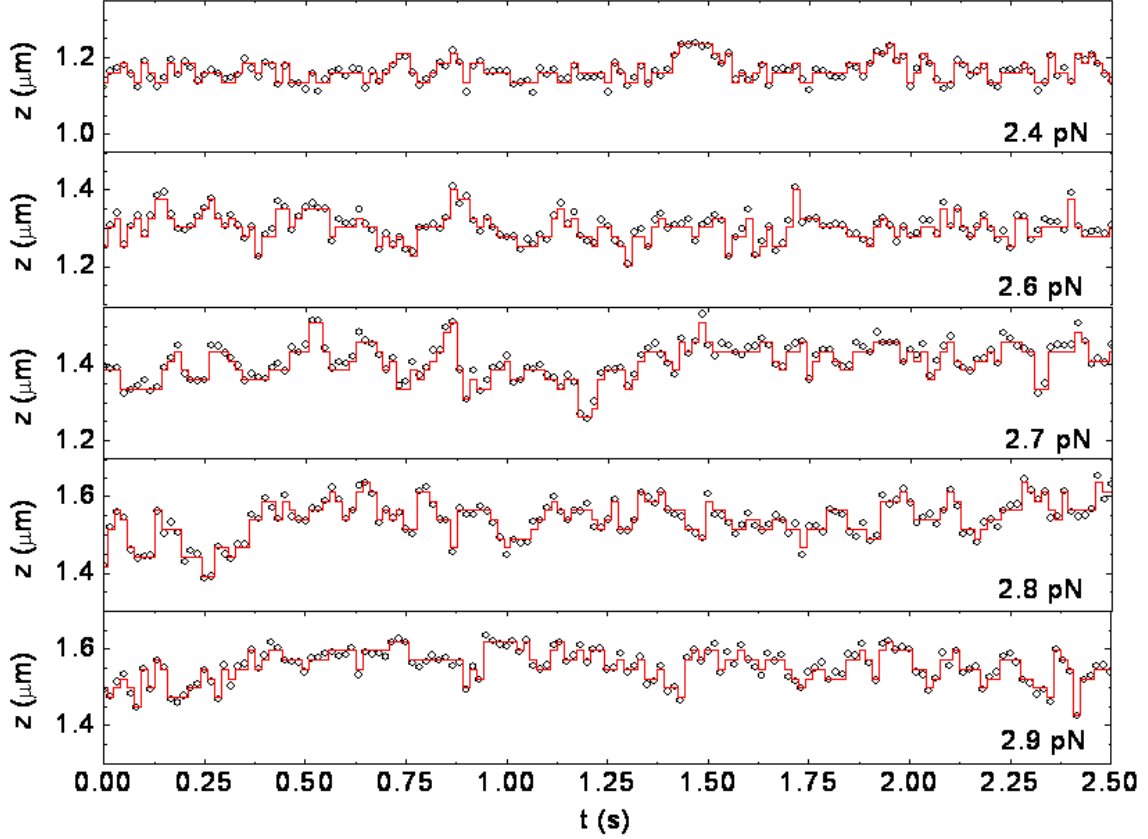


Figure 4.3: Time traces of transitions between multiple states at different forces. The extension of the states assigned by the parameterized HMM is shown as solid red line overlaid the experimental data (black circles). The standard deviation without transitions is 11 nm.

By repeating the HMM analysis at different forces we obtained the force dependence of the kinetics of single nucleosomes embedded in a chromatin fiber. Figure 4.4a shows that the open and the closed states follow an Arrhenius-like force-dependence. The good agreement with Arrhenius equation, Equation 4.1 is an independent confirmation of the accuracy of the HMM analysis. The fraction of open nucleosomes that was deduced from the FE traces is plotted in the same figure. Consistent with the plateau in the FE trace, the fraction of open nucleosomes increases from 10% at 2.3 pN to 90% at 3.3 pN.

The high force sensitivity shown in Figure 4.4a is a result of the large change in extension that is associated with the change from the open to the closed state of the nucleosome. Per nucleosome, the maximum difference in extension of the

open and the closed state is 25.3 nm, as fitted from the FE traces. From the force dependence of the lifetimes (Equation 4.1) we obtain the location of the barrier in the energy landscape describing the transition between the closed and the open state, $\delta_c = 11 \pm 1$ nm and $\delta_o = 18 \pm 1$ nm. When extrapolated to zero force, the lifetime of the closed state $\tau_c(0) = 244 \pm 7$ s and the lifetime of the open state $\tau_o(0) = 1.2 \pm 0.1 \mu\text{s}$. Thus, kinetic analysis of chromatin fiber conformational changes by the parameterized HMM uncovers all relevant details of the energy landscape for opening individual nucleosomes within the fiber.

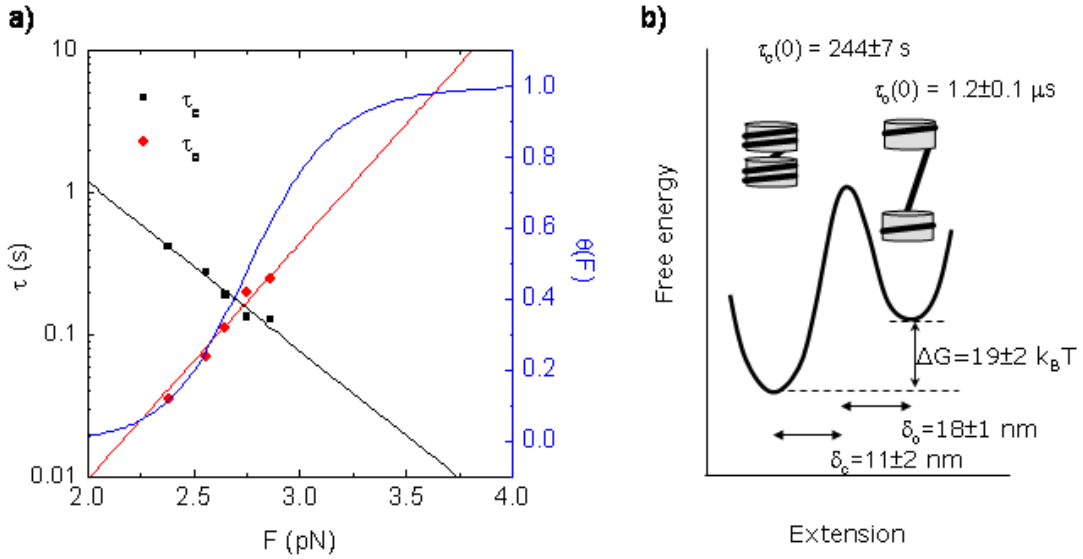


Figure 4.4: Force-dependence of the lifetimes of the open and the closed states. (a) A plot of lifetimes of the open state (red circles) and the closed state (black squares) versus force. The solid red and black lines are fits to Equation 4.1. The ruptured fraction is a function of force following Equation 4.1 and is shown as a blue line. The dash line indicates the Nyquist frequency of 30 Hz. (b) The energy landscape for unstacking and unwrapping was reconstructed with the life times of the closed and the open state, the distances from each state to the energy barrier, and the free energy difference were obtained from Equation 4.1. The fit parameters are $\Delta G = 19 \pm 2 k_B T$, $\tau_c(0) = 244 \pm 7$ s, $\tau_o(0) = 1.2 \pm 0.1 \mu\text{s}$, $\delta_c = 11 \pm 1$ nm, and $\delta_o = 18 \pm 1$ nm.

4.4 Discussion

4.4.1 HMM analysis of chromatin unfolding

The combination of constant force extension measurements and parameterized HMM analysis revealed for the first time the energy landscape of chromatin fiber structural changes at the level of single nucleosomes. For the HMM approach, we

included the force dependence of all the parameters that define chromatin structure. In this way it is possible to obtain the kinetics from constant force measurements by fitting a single parameter. We obtained a good agreement for the free energy difference between the open and the closed state of the nucleosomes from fits to FE traces $\Delta G = 16.5 \pm 0.1 k_B T$, from global fits to the extension probability distributions yielding $\Delta G = 16.1 \pm 0.2 k_B T$, and from the lifetimes extrapolated to zero force yielding $\Delta G = 19 \pm 2 k_B T$. Though these three measurements are based on the same two-state model, very different experimental and analytical procedures were used, probing different time-dependent aspects of the fiber.

Note that the window of lifetimes that can be measured is narrow due to experimental limitations. On the low force side our measurements were limited by the frame rate of the camera. With the Nyquist frequency that equals one-half of a frame rate of 60 Hz of the camera, we can only detect the fluctuations that last for at least 33 ms, which corresponds to the lifetime of the open state at 2.4 pN. With a faster camera however one would run into the regime where viscous damping of the bead is limiting, Equation 4.14. On the high force side it would be technically possible to extend the force range for these measurements until the life time of the closed state reduces to cover the Nyquist frequency. However, exposure to forces exceeding 3 pN for 120 s resulted in gradual extension of the fiber, hysteresis in the FE traces, and non-converging results in the HMM analysis. Fitting of the FE traces before and after the constant force recordings yielded a clear increase in the number of nucleosomes in a permanently open state, possibly indicating dimer dissociation (data not shown). This would point to a dimer dissociation rate of approximately 1 per min, when the nucleosome is in the open state. Clearly, at smaller forces, when nucleosomes are predominantly in the closed state, dimer dissociation proceeds much slower. Between these physical boundaries imposed by the stability of the nucleosome and the viscous damping of the fluctuations, the parameterized HMM can be used to accurately determine the kinetics of individual nucleosomes embedded in a chromatin fiber.

4.4.2 A structural interpretation of force induced chromatin unfolding

We observed an Arrhenius-like force-dependence of nucleosome opening, summarized in an energy landscape for conformational transitions of single nucleosomes in chromatin fibers shown in Figure 4.4b. As stated by Mihardja *et al.*[20] one limitation to studying nucleosomal arrays is the difficulty to distinguish between the behavior of individual nucleosomes. The good agreement and reproducibility of the data with the various forms of our two-state mechanical model for chro-

matin stretching that we report here indicate that the nucleosomes in our fibers behave identically and independently. The use of chicken erythrocyte histones, regular arrays of 601 positioning elements and careful titration and salt dialysis reconstitution are all important to yield the highly regular chromatin fibers used in this study. The absence of cooperative effects and the identity of the structural transition are important as it implies that nucleosomes interact exclusively at most with their neighbors and not with other nucleosomes within the fiber. Only then will the first and the last nucleosome follow the same opening kinetics. This rules out many proposed nucleosome-nucleosome contacts[26–28].

What does the energy landscape for nucleosome unfolding reveal about the structure and dynamics of a nucleosome embedded in a chromatin fiber[20]? Based on the contour length of the nucleosome it is clear that the open state of the nucleosome corresponds to a conformation with one turn wrapped DNA[20]. We have not been able to directly interpret the structure of the closed nucleosome in a chromatin fiber. Before, we argued that the absence of hysteresis in the FE traces, the Hookean extension of the folded fiber and a stiffness that is compatible with the elasticity that would be expected for a chain of nucleosomes linked by disordered histone tails, are compatible with a single stack of nucleosomes that are connected by their histone tails. The current analysis of the fluctuations in the extension of the fiber confirms that there are no discernible intermediate states in the fiber, prior to the changes that occur in the force plateau.

The force plateau in the chromatin FE traces is at the same level as the rupture forces that have been reported for DNA unwrapping from mononucleosomes[20, 21]. Moreover, the length increase upon nucleosome opening between 2 pN and 4 pN is 22 to 24 nm(Figure 4.5), which is the same as the reported hopping size for DNA unwrapping in mononucleosomes[20, 21]. These results might suggest that the transitions between the closed and the open state simply represent the unwrapping of the first turn of DNA. A complication in such a comparison is that the molecular interactions that stabilize the fiber together strongly depend on the buffer conditions. We reported before (Chapter 3) that the interaction energy in chromatin fibers decreases from $30 k_B T$ to $17 k_B T$ when the monovalent salt concentration increases from 11 mM to 210 mM. Furthermore, although Mg^{2+} is required for proper folding of fibers, fibers precipitate when the Mg^{2+} concentration exceeds 2 mM[9]. This makes comparisons between studies in which different buffer conditions were used non-trivial. In this study we used the same buffer conditions as we used before on mononucleosomes[21], which was different from that used by Mihardja *et al.*[20] with 10 mM Mg^{2+} and 50 mM potassium acetate. Another complication for detailed comparison is the narrow force regime that is accessible together with the strong, non-linear force dependence of the

stability of the nucleosome. This may cause large errors when extrapolating to zero force. Despite these considerations it is clear that the free energy for the unwrapping of mononucleosomes, $9-12 k_B T$ [20, 21] is significantly smaller than $\Delta G=16-19 k_B T$ that we measured for the transitions occurring at the plateau in the fiber. The difference can be attributed to the interactions that stabilize the closed nucleosome in the chromatin fiber.

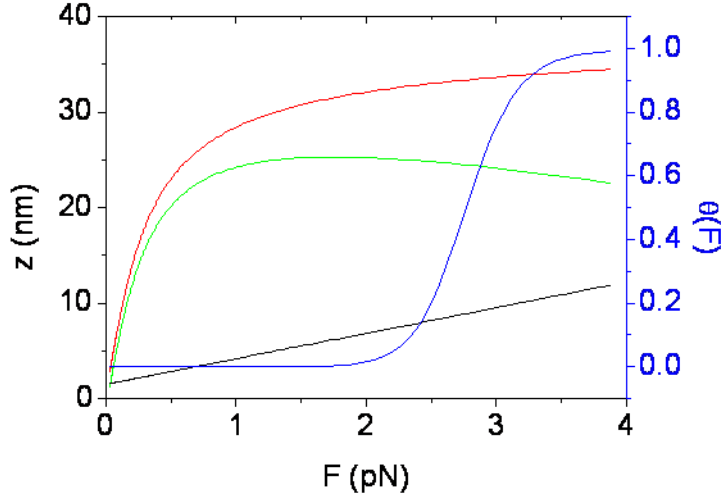


Figure 4.5: Force-extension traces of the open state (red line), the closed state (black line), and the length difference between two states (green line) of a single nucleosome within a chromatin fiber. The parameters are obtained from the fit in Figure 4.1: $L_c = 1.5$ nm, $k_c = 0.37$ pN/nm, $L_o = 40.2$ nm, $p_o = 14$ nm, and $\Delta G = 16.5 k_B T$. The force-dependent fraction of open nucleosomes is plot as a blue line.

The maximum extension of the closed state also points to a single file of stacked nucleosomes in the folded fiber. The unfolded array of nucleosomes follows a WLC and its small persistence length indicates that the extension of the fiber is only 70% of its contour length(Figure 4.5). The nucleosomes in the closed state follow a Hookean extension and the stiffness of this conformation requires a fivefold extension with respect to the rest length of the fiber before the transition. Such extensive stretching can be accommodated by unwinding of the super helix of stacked nucleosomes[16]. In fact, based on the stiffness that was fitted from the FE traces, the stretching of the stacked nucleosomes continues during the force plateau and reaches a maximum extension of 12 nm at 4 pN when the fraction of stacked nucleosomes reaches zero(Figure 4.5). For a stack of nucleosomes that have their cylindrical axis aligned with the force, this length exceeds the height of the globular part of the nucleosome by approximately 5 nm. This length could be spanned by a histone tail of at least 12 amino acids and can be

reduced when the nucleosomes are skewed. Note that interactions between non-neighboring nucleosomes would yield an extension of such nucleosome pairs that is incompatible with the values that we measured. The location of the barrier in the unfolding landscape, $\delta_c = 11 \pm 2$ nm, closely matches the extension of the maximally stretched state, confirming this interpretation. Overall, both the FE traces and the unfolding energy landscape are consistent with a closed state of the nucleosome that interacts with its neighbors by its histone tails.

The absence of a discernible intermediate between the closed state which we interpret as a stacked nucleosome and the open state which corresponds to a nucleosome with one turn wrapped DNA could be explained in different ways. First, when the resistance against force is larger for the stacking interaction than for the DNA wrapping interaction, unstacking of a nucleosome will be directly followed by unwrapping of its DNA. The limited temporal resolution of magnetic tweezers may not be able to resolve such a short-lived unstacked, but fully wrapped state. However, upon refolding it is not likely that this state would also be so short-lived that it would be overlooked in our constant force measurements. Second, when these two conformations would have the same extension, we would not observe them separately in the magnetic tweezers measurements. It is unlikely though that an array of stacked nucleosomes would have the same stiffness as an array of unstacked, fully wrapped nucleosomes. When the stiffnesses are not the same, there will be a force regime where the extension of these conformations is significantly different, which we did not observe. Alternatively, it may be possible that the nucleosomes in the folded fiber are partially unwrapped. Forced rupture of the nucleosome-nucleosome interactions will then directly yield an unwrapped nucleosome with only a single turn of DNA. FRET experiments on mononucleosomes have indicated that partial unwrapping occurs 10-40% of the time[17, 18]. Compared to these experiments, mononucleosome force spectroscopy yielded much more stable wrapping, which was attributed to the force that initially increases the stability of the nucleosome[22]. In a folded chromatin fiber the severe bending of the linker DNA, that has been an argument against solenoidal folding of 30 nm chromatin fibers[7], can be significantly relieved by partial unwrapping of the nucleosomal DNA. This interpretation would be consistent with the reported increased enzymatic accessibility of nucleosomal DNA in fibers compared to that of mononucleosomes[12]. Interestingly, a recent FRET study indicated that unwrapping may include partial dissociation of H2A-H2B dimers from the core particle, that remain bound to the DNA[29, 30]. Here we can not deduce the trajectory of the DNA in the folded fiber, but our measurements indicate that unstacked, fully wrapped nucleosomes do not significantly contribute to the dynamic structure of the chromatin fiber.

4.4.3 Consequences for chromatin organization *in vivo*

The large nucleosome-nucleosome interaction energy and the short life time of the open state show that nucleosomes are predominantly in a closed conformation in the absence of force. Extrapolation of the lifetime of the open state to zero force yields a lifetime of 1.2 μ s. Interestingly this is in the same range as the time scales for nucleosome stacking that were deduced from FRET measurements on trinucleosomes[11]. Such a short lifetime seems prohibitively small for DNA interactions with other DNA binding proteins. The very high force sensitivity of nucleosome-nucleosome interactions however offers the cell a convenient way to shift the equilibrium to the open state. Forces of several pN can easily be generated by DNA translocating enzymes such as chromatin modelers and DNA and RNA polymerases[31–34]. Perhaps thermal fluctuations of connected chromatin parts may be sufficient to induce nucleosome unstacking. Importantly, we show here that this results directly in partial DNA unwrapping and eventually in dimer dissociation. Thus the commonly used paradigm of highly condensed 30 nm fiber like fibers for inactive chromatin and the beads-on-a-string type of conformation of fully wrapped nucleosomes in active chromatin[35–37] does not match with our observation that even very small forces of several pN can induce chromatin unfolding. We have also shown here that fully wrapped non-interacting nucleosomes are not stable under conditions that resemble anticipated nuclear conditions.

Of course a cell has a much wider repertoire of strategies available for modulating chromatin condensation, like the binding of linker histones[38], addition or removal of post-translational histone modifications[19], inclusion of histone variants[8] and binding of other regulatory factors[39]. In addition, variations in linker length and DNA sequence will affect nucleosome stacking[9]. The current statistical mechanical framework provides all parameters that are necessary to evaluate the structural effects of these changes to chromatin in a quantitative manner[40]. Though the parameterized HMM currently assumes identical non-cooperative nucleosomes, it could be expanded to more elaborate models for heterogeneous chromatin. Mapping out the differences between nucleosomes in endogenous chromatin will help to establish a structural understanding of chromatin and its role in regulation of DNA based processes in the eukaryotic nucleus.

4.5 Materials and Methods

4.5.1 Chromatin fibers

A pUC18 vector (Novagen), containing 35 repeats of a 197 bp 601 sequence[41] was digested with BsaI and BseYI and filled with one dUTP-digoxigenin at the BsaI end and one dUTP-biotin at the BseYI end. The linear DNA fragment was mixed with competitor DNA (~ 147 bp) and histone octamers purified from chicken erythrocytes, and reconstituted into chromatin fibers using salt dialysis[42].

4.5.2 Experimental configuration

Pulling experiments were carried out in a buffer containing 10 mM HEPES pH 7.6, 100 mM KAc, 2 mM Mg(Ac)₂, 10 mM NaN₃, 0.1% (v/v) Tween-20, 0.2% (w/v) Bovine Serum Albumin (BSA) at room temperature. One end of a chromatin fiber was attached to the streptavidin activated surface on the surface of a coverslip coated with a mixture of 20% (w/v) mPEG-Succinimidyl Propionic Acid (SPA)-5000 and 0.2% (w/v) biotin-PEG-N-Hydroxysuccinimide (NHS)-3400 (Sunbright). The other end was attached to a 1.0 μm diameter paramagnetic beads (DYNAL MyOne) coated with anti-digoxigenin (Roche). The tethered chromatin fibers were stretched with a custom made magnetic tweezers setup[43]. The height of the tethered bead was measured using automated image processing programmed in LabView. A geometric correction was applied to obtain the absolute length of the tethered chromatin fibers. The force was calibrated from the magnet position as described in Kruithof *et al.* [43]. The tethered bead was measured at 30 fN for 30 s to define the position of the surface of the coverslip and correct the mechanical drift. Each pulling cycle included three parts: stretching with a shift rate of 0.33 mm/s, a constant force measurement at a preset force, and a relaxation with a shift rate of 0.33 mm/s. The duration of the constant force measurements was 30 s for global fit analysis and 120 s for the HMM analysis.

4.5.3 Fitting routine

A Levenberg-Marquadt routine was used to fit the force-extension traces, the global fits, and the parameterized transition matrix to the data obtained from the Viterbi algorithm. For the global fits, first the time traces obtained from constant force measurements were binned with a bin size of 10 nm in the range from 0 to 2000 nm and normalized. The weighting factor used was the squared

Bibliography

root of the amplitude of the histogram. For the HMM analysis, the transition matrix was obtained by fitting the matrix containing the assigned transition frequencies by the Viterbi algorithm to Equation 4.14. The outcome of this fit was used as an input for the next stage in the Viterbi algorithm. We systematically tested different orders of the transition matrix and calculated the mean squared difference between the experimental extension time trace and the fitted time trace based on the assigned states, yielding the second order for the optimal order.

Bibliography

- [1] Luger, K., Mader, A., Richmond, R., Sargent, D. & Richmond, T. *Nature* **389**, 251–260 (1997).
- [2] Grigoryev, S. A., Arya, G., Correll, S., Woodcock, C. L. & Schlick, T. *Proc. Natl. Acad. Sci. U.S.A.* **106**, 13317–13322 (2009).
- [3] Bcavin, C., Barbi, M., Victor, J.-M. & Lesne, A. *Biophys. J.* **98**, 824–833 (2010).
- [4] Vincent, J. A., Kwong, T. J. & Tsukiyama, T. *Nat. Struct. Mol. Biol.* **15**, 477–484 (2008).
- [5] Zhou, J., Fan, J. Y., Rangasamy, D. & Tremethick, D. J. *Nat. Struct. Mol. Biol.* **14**, 1070–1076 (2007).
- [6] Dorigo, B., Schalch, T., Bystricky, K. & Richmond, T. J. *J. Mol. Biol.* **327**, 85–96 (2003).
- [7] Robinson, P., Fairall, L., Huynh, V. & Rhodes, D. *Proc. Natl. Acad. Sci. U.S.A.* **103**, 6506–6511 (2006).
- [8] Robinson, P. J. J. *et al.* *J. Mol. Biol.* **381**, 816–825 (2008).
- [9] Routh, A., Sandin, S. & Rhodes, D. *Proc. Natl. Acad. Sci. U.S.A.* **105**, 8872–8877 (2008).
- [10] Schalch, T., Duda, S., Sargent, D. & Richmond, T. *Nature* **436**, 138–141 (2005).
- [11] Poirier, M. G., Oh, E., Tims, H. S. & Widom, J. *Nat. Struct. Mol. Biol.* **16**, 938–944 (2009).
- [12] Poirier, M. G., Bussiek, M., Langowski, J. & Widom, J. *J. Mol. Biol.* **379**, 772–786 (2008).
- [13] Brower-Toland, B. *et al.* *Proc. Natl. Acad. Sci. U.S.A.* **99**, 1960–1965 (2002).
- [14] Brower-Toland, B. *et al.* *J. Mol. Biol.* **346**, 135–146 (2005).

- [15] Cui, Y. & Bustamante, C. *Proc. Natl. Acad. Sci. U.S.A.* **97**, 127–132 (2000).
- [16] Kruithof, M. *et al. Nat. Struct. Mol. Biol.* **16**, 534–540 (2009).
- [17] Li, G., Levitus, M., Bustamante, C. & Widom, J. *Nat. Struct. Mol. Biol.* **12**, 46–53 (2004).
- [18] Koopmans, W., Brehm, A., Logie, C., Schmidt, T. & van Noort., J. *J. Fluoresc.* **17**, 785–95 (2007).
- [19] Neumann, H. *et al. Mol. Cell* **36**, 153–163 (2009).
- [20] Mihardja, S., Spakowitz, A., Zhang, Y. & Bustamante, C. *Proc. Natl. Acad. Sci. U.S.A.* **103**, 15871–15876 (2006).
- [21] Kruithof, M. & van Noort, J. *Biophys. J.* **96**, 3708–3715 (2009).
- [22] Kulic, I. M. & Schiessel., H. *Phys. Rev. Lett.* **92**, 228101 (2004).
- [23] Klein, S., Timmer, J. & Honerkamp, J. *Biometrics* **53**, 870–884 (1997).
- [24] Wong, W. P. & Halvorsen, K. *Opt Express* **14**, 12517–12531 (2006).
- [25] Rabiner, L. *IEEE* **77**, 257–286 (1989).
- [26] Schwarz, P., Felthouser, A., Fletcher, T. & Hansen, J. *Biochemistry* **35**, 4009–4015 (1996).
- [27] van Holde, K. & Zlatanova, J. *Semin. Cell Dev. Biol.* **18**, 651–658 (2007).
- [28] Blacketer, M. J., Feely, S. J. & Shogren-Knaak, M. A. *J. Biol. Chem.* **285**, 34597–34607 (2010).
- [29] Engeholm, M. *et al. Nat. Struct. Mol. Biol.* **16**, 151–158 (2009).
- [30] Bohm, V. *et al. Nucleic Acids Res.* **39**, 3093–3102 (2011).
- [31] Lia, G. *et al. Mol. Cell* **21**, 417–425 (2006).
- [32] Jin, J. *et al. Nat. Struct. Mol. Biol.* **17**, 745–752 (2010).
- [33] Kulaeva, O. I., Hsieh, F.-K. & Studitsky., V. M. *Proc. Natl. Acad. Sci. U.S.A.* **107**, 11325–11330 (2010).
- [34] Wuite, G. J., Smith, S. B., Young, M., Keller, D. & Bustamante, C. *Nature* **404**, 103–106 (2000).
- [35] Felsenfeld, G. & Groudine, M. *Nature* **421**, 448–453 (2003).
- [36] Vermaak, D., Ahmad, K. & Henikoff, S. *Curr. Opin. Cell Biol.* **15**, 266–274 (2003).
- [37] Naughton, C., Sproul, D., Hamilton, C. & Gilbert, N. *Mol. Cell* **40**, 397–409 (2010).

Bibliography

- [38] Robinson, P. & Rhodes, D. *Curr. Opin. Struct. Biol.* **16**, 336–343 (2006).
- [39] Kepert, J. F., Mazurkiewicz, J., Heuvelman, G. L., Tth, K. F. & Rippe., K. *J. Biol. Chem.* **280**, 34063–34072 (2005).
- [40] Chien, F.-T. & van Noort, J. *Curr. Pharm. Biotechnol.* **10**, 474–485 (2009).
- [41] Lowary, P. & Widom, J. *J. Mol. Biol.* **276**, 19–42 (1998).
- [42] Huynh, V., Robinson, P. & Rhodes, D. *J. Mol. Biol.* **345**, 957–968 (2005).
- [43] Kruithof, M., Chien, F., de Jager, M. & van Noort, J. *Biophys. J.* **94**, 2343–2348 (2007).

Summary

In eukaryotic cells, genomic DNA is organized in chromatin fibers composed of nucleosomes as structural units. A nucleosome contains 1.7 turns of DNA wrapped around a histone octamer and is connected to the adjacent nucleosomes with linker DNA. The folding of chromatin fibers effectively increases the compaction of genomic DNA, but it remains accessible for enzymatic reactions. This apparent paradox motivates a detailed study of the dynamics of chromatin. A structural model at the molecular level will shed light on how cells regulate the compaction and dynamics of genomic DNA. This thesis presents the results of an experimental study on the dynamics of chromatin higher-order folding. Using magnetic tweezers, we observed force-dependent structural changes within chromatin fibers at the single nucleosome level.

In *Chapter 1* we reviewed the studies of force-dependent chromatin unfolding in the past decade. Despite a variety of measurement conditions, the results on pulling chromatin fibers show consistent intermediates of chromatin unfolding. Similar to mononucleosomes, chromatin unfolding consists of the release of the outer and inner turns of wrapped DNA. Furthermore, the unfolding involves elastic stretching of chromatin higher-order folding, rupture of internucleosomal interactions, and dissociation of histone octamers. Those events have unique features in the Force-Extension traces that are measured. The linear extension of the higher-order folding below 4 pN reveals that chromatin fibers behave like a Hookean spring. The plateau between 3 and 4 pN shows the gradual release of wrapped DNA, indicating the exposure of linker DNA and outer-turn wrapped DNA. The stepwise rupture events occurring above 15 pN indicate the irreversible unwrapping of the inner turn of DNA. Resolving force induced structural changes of chromatin fibers helps to understand the processes involving chromatin that occur *in vivo* and reveals the mechanical constraints that are relevant for processing and maintenance of DNA in eukaryotes.

In *Chapter 2* we quantified the mechanical properties of the higher-order folding of chromatin fibers, particularly focusing on the linear extension behavior in the force regime below 4 pN. A fully folded chromatin fiber, representing the

first level of chromatin condensation, behaves like a Hookean spring. Without linker histones, which are at the position where wrapped DNA enters and exits from the nucleosome, the Force-Extension traces show a plateau caused by the structural changes that increase the extension of the fiber. The stiffness of the chromatin fibers is independent of the presence of linker histones. Moreover, the difference of the stiffness between fibers with nucleosome repeat lengths of 167 bp and 197 bp reflects the difference between solenoid and zigzag structures. Mg^{2+} is a key player in the (re)folding of chromatin fibers. Without Mg^{2+} , the unfolded chromatin fibers cannot recover to the original structure. The stiffness of the chromatin higher-order folding shows that the chromatin fibers easily extend 30% of the rest length by thermal fluctuations at room temperature. This observation suggests that thermal fluctuations can make the DNA embedded in chromatin fibers accessible for enzymatic reactions.

In *Chapter 3* we quantified the mechanical properties of heterogeneous chromatin fibers using a two-state model for describing the Force-Extension traces of these fibers. At 3 to 4 pN the plateau shown in the Force-Extension trace indicates the exposure of linker DNA and first turn wrapped DNA. The free energy difference is quantified as $17 k_B T$ and decreases with the increase of monovalent cations. Some nucleosomes display H2A-H2B dimer dissociation in repeated Force-Extension cycles. For the transition between the fully folded chromatin fiber and the chromatin fiber containing nucleosomes with only one turn wrapped DNA, we proposed two possible mechanisms: coupled or decoupled nucleosome unstacking and DNA unwrapping. The two-state model not only provides insights in chromatin high order folding, it also allows for detail, quantitative assessment of the factors that influence chromatin structure, for example post-translational modifications.

In *Chapter 4* we investigated dynamics of nucleosomes within chromatin fibers. In the constant force measurements, the end-to-end distance of the stretched fiber shows reversible stepwise rupture events that correspond to discrete unstacking events. Obtaining the mechanical properties of chromatin fibers with a two-state model, we calculate the extension of those conformations. Using Hidden Markov analysis, we resolve the transitions in time, yielding the lifetimes of the closed and open states. The lifetime of the open state is extremely force sensitive and can be altered by six orders of magnitude when a force of a few pN is exerted. Compared to mononucleosomes, the single nucleosomes within chromatin fibers have a 1.5 fold higher free energy difference between the two states, and the lifetime of open state is three orders of magnitude less. These results show that nucleosomes in the closed state interact with adjacent nucleosomes only, and nucleosomes in the open state have no internucleosomal interactions

Summary

and have only one turn of wrapped DNA. Our results quantitatively describe the dynamics of nucleosomes within the chromatin higher-order folding.

Samenvatting

Om het fysisch mechanisme van de regulatie van genexpressie te achterhalen is het noodzakelijk om de structuur van chromatine te kennen. Deze is echter al 30 jaar het onderwerp van discussie. In voorliggende studie hebben we een magnetisch pincet gebruikt om een enkel DNA molecuul, opgevouwen in chromatine, voorzichtig te ontrafelen. Hiermee hebben we niet alleen de manier waarop het DNA opgevouwen zit kunnen achterhalen, maar ook de aard en sterkte van de interacties die hiervoor zorgen.

Histonen vormen het verpakkingsmateriaal van genen. De welbekende dubbele helix van DNA, die bij de mens bestaat uit 6 miljard baseparen (bp) en 2 meter lang is, is op een zeer gestructureerde manier georganiseerd. 147 bp aan DNA wikkelen zich in 1.7 windingen om een pakketje van 8 eiwitten, histonen genaamd, tot een nucleosoom. De structuur van het nucleosoom is opmerkelijk: de sterke elektrostatische interacties tussen het negatief geladen DNA en de positief geladen histonen maken het mogelijk om precies één persistentielengte aan DNA (50 nm) op te rollen tot een cilinder van 11 bij 6 nm. Door het DNA met behulp van nucleosomen op te vouwen wordt het fysiek mogelijk om al het DNA in een celkern van enkele micrometers te passen. De histonen vormen echter ook een obstakel voor andere eiwitten die een interactie met het DNA willen aangaan: waar de histonen binden kan bijvoorbeeld geen RNA polymerase, het enzym dat verantwoordelijk is voor transcriptie, binden. Deze sterische hindering is mede verantwoordelijk voor de regulatie van genexpressie.

De structuur van de 30 nm vezel. Nucleosomen staan nooit alleen. In een eukaryote cel is er gemiddeld één nucleosoom per 167 tot 207 bp DNA. Dit betekent dat 75% van al het DNA opgerold zit in nucleosomen die op hun beurt worden verbonden door 20 tot 50 bp aan DNA, dat linker DNA genoemd wordt. Deze kralenketting van DNA en nucleosomen heet chromatine. Het chromatine vormt een dynamische structuur. Nucleosomen kunnen spontaan bewegen over DNA, waarmee ze specifieke DNA sequenties kunnen vrijmaken die herkend wor-

den door transcriptiefactoren. Dit proces kan versneld worden door chromatin-remodellers, motoreiwitten die over het DNA bewegen en daarmee de nucleosomen verschuiven of verwijderen. Dus ondanks dat het meeste DNA in nucleosomen zit opgerold, hoeft dit, door verplaatsing van nucleosomen en het tijdelijk ontwikkelen van DNA, geen onoverkomelijke barrière te vormen voor andere eiwit-DNA interacties. De nucleosomen hechten echter ook nog aan elkaar waardoor zij het DNA verder afschermen. Onder fysiologische condities, dat wil zeggen ~ 150 mM zout en ~ 2 mM Mg^{2+} , stapelen de nucleosomen op elkaar om zo een hechte vezel te vormen van zo'n 30 nm dik. Hoewel deze structuur al 30 jaar uitvoerig onderzocht is met onder andere electronenmicroscopie (EM), X-ray scattering, sedimentatiesnelheidsmetingen, atomaire krachtmicroscopie en kristallografie, is de structuur van deze vezel tot nu niet opgehelderd. De literatuur is verdeeld tussen twee structurele modellen. In de spiraalstructuur stapelen naburige nucleosomen op elkaar en vouwt deze stapel zich in een enkelvoudige spiraal. In de zig-zag structuur daarentegen stapelen de even en de oneven nucleosomen op elkaar en vormen deze een dubbele spiraal. Omdat in het enkelvoudige spiraalmodel het linker DNA zeer sterk gebogen moet zijn, wat aanzienlijk veel meer energie kost dan de geschatte vrije energie winst voor nucleosoom-nucleosoom interacties, geniet de zig-zag structuur vaak de voorkeur. Recente electronen microscopie metingen laten echter zien dat de diameter van de 30 nm vezel onafhankelijk is van de lengte van het linker DNA, wat niet verenigbaar is met de zig-zag structuur. Hoewel de mate van DNA condensatie grofweg gelijk is in beide structuren maakt het op moleculaire schaal natuurlijk een groot verschil hoe het DNA is gevouwen.

Krachtspectroscopie met een magnetische pincet. De verbinding tussen nucleosomen in de 30 nm vezel is de sleutel tot het ophelderen van haar structuur. Met behulp van krachtspectroscopie aan een enkel molecuul is het tegenwoordig mogelijk een molecuul op te pakken, uit elkaar te trekken en daarmee de structuur letterlijk te ontrafelen. Zo wordt in magnetic tweezers (MT, of een magnetische pincet) één DNA molecuul in een waterige oplossing opgespannen tussen de bodem van een vloeistofcel en een micrometer groot paramagnetisch bolletje. Door een paar permanente magneten boven het bolletje te plaatsen wordt het bolletje in de richting van de hoogste magneetveldgradiënt getrokken en zal het DNA molecuul uitrekken. De afstand tussen de uiteinden van het DNA molecuul wordt bepaald met behulp van videomicroscopie en beeldanalyse. Door het diffractiepatroon van het bolletje te vergelijken met een van tevoren bepaalde referentiedataset van het bolletje op verschillende hoogten kan niet alleen het middelpunt maar ook de hoogte van het bolletje met enkele nm precisie bepaald

worden. Voor de calibratie van de magnetische kracht wordt gebruik gemaakt van de equipartitie theorie. Het DNA-bolletje systeem kan gezien worden als een nanoslinger waarvoor geldt dat in elke richting de potentiële energie gelijk is aan de thermische energie. De kracht is dan evenredig met de hoogte van het bolletje, en omgekeerd evenredig met de amplitude van de thermische fluctuaties evenwijdig aan het oppervlak. Door enige tijd de positie van het bolletje te volgen kan dus direct de kracht voor een bepaalde magneetpositie berekend worden. In onze opstelling neemt de kracht exponentieel af met de afstand tussen het bolletje en de magneten totdat de ‘excluded volume’ kracht, een entropische kracht als gevolg van de beperkte bewegingsvrijheid van het molecuul en het bolletje dichtbij een oppervlak, domineert. Door de magneten te bewegen kan met de magnetische pincet een rekcurve van een enkel DNA molecuul in slechts 10 s worden gemeten. In hoofdstuk 1 wordt een samenvatting gegeven van eerdere studies waarin individuele chromatine vezels met krachtspectroscopie zijn gemeten. Deze richten zich voornamelijk op het hoge krachtsregime, boven 15 pN, waarin het chromatine reeds grotendeels ontrafeld is. In dit proefschrift richten we ons niet op de vrijwel geheel ontrafelde chromatine vezel, maar op de meer fragiele volledig opgevouwen 30 nm vezel.

Van 30 nm vezel tot kralenketting. In hoofdstuk 2 worden experimenten beschreven waarin voor het eerst op gecontroleerde wijze chromatinevezels worden ontrafeld. Hiertoe hebben we een modelvezel gemaakt waarvan de lengte van het DNA, de plaats en het aantal nucleosomen exact bekend is. Hoewel histonen binden aan elk DNA zijn er bepaalde sequenties die een aanzienlijk hogere affiniteit voor histonen hebben. Het blijkt dat DNA, afhankelijk van de sequentie, al een beetje voorgebogen kan zijn. Met behulp van deze sequenties kan door middel van zoutdialyse zeer gecontroleerd een histon octameer op het DNA worden gezet. In deze DNA sequenties zit het nucleosoom vast en kan het niet meer spontaan over het DNA bewegen. Voor krachten onder 4 pN is de uitrekking van deze vezel maximaal 200 nm. Rond 4 pN vindt er een overgang plaats waarin de lengte, bij gelijkblijvende kracht, toeneemt tot meer dan 600 nm, om vervolgens te convergeren naar ongeveer 700 nm. Deze lengte wordt echter niet bereikt; rond 7 pN is de kracht zo groot dat het DNA ontwindt van de nucleosomen, waardoor de lengte aanzienlijk groter wordt dan die van een kralenketting van volledig opgewonden nucleosomen. De rekcurve tot 4 pN is goed te beschrijven met een model bestaande uit twee veren in serie: een die overeenkomt met de uitrekking van het DNA aan de flanken van de chromatinevezel en een Hooke veer die de uitrekking van de chromatinevezel zelf beschrijft. De rustlengte van de vezel komt goed overeen met elektronen microscopie metingen aan dit mate-

riaal. De veerconstante van chromatine blijkt kleiner te zijn dan die van DNA voor krachten boven 1 pN; in dit regime is het dus vooral de vezel die uitrekt en niet het kale DNA.

Sterke nucleosoom-nucleosoom interacties. De rekurve van de kralenketting van nucleosomen kan apart gemeten worden in een buffer zonder Mg^{2+} , waarin geen stapeling van nucleosomen kan plaatsvinden. Onder deze omstandigheden is de vezel veel langer en kan de curve goed gemodelleerd worden door twee zogenaamde Worm Like Chain (WLC) veren in serie. Dit gaat goed voor krachten boven 2 pN, waarbij de nucleosomen elkaar niet in de weg zitten. Het WLC model dat de kralenketting van chromatine beschrijft, heeft een persistentielengte van slechts 10 nm. De gefitte contourlengte per nucleosoom bedraagt ongeveer 40 nm, wat duidt op het gedeeltelijk ontwinden van DNA in nucleosomen. Nu de rekurven van zowel de gestructureerde 30 nm vezel als de ongestructureerde kralenketting bekend zijn, is het ook mogelijk om het verbreken van de interacties die de nucleosomen bij elkaar houden te kwantificeren. Het evenwicht tussen een gestapeld nucleosoompaar en twee losse nucleosomen is sterk krachtsafhankelijk en kan gemodelleerd worden door een arbeidsterm toe te voegen aan de thermodynamische beschrijving van het evenwicht. Met behulp van deze krachtsafhankelijke evenwichtsconstante kunnen we de veer die het chromatine beschrijft vervangen door een lineaire combinatie van een 30 nm vezel en een kralenketting. Dit model beschrijft de gehele meting in het bereik van 30 fN tot 6 pN en laat zien dat het plateau in de curve inderdaad toe te wijzen is aan het verbreken van de interacties tussen de nucleosomen. De interactie energie tussen de nucleosomen blijkt wel $17 k_B T$ te zijn, 5 maal sterker dan tot nu toe werd aangenomen.

Het linker DNA bepaalt de vouwing van de 30 nm vezel. Nu we weten dat de 30 nm vezel van 25 nucleosomen als een Hookse veer kan oprekken tot maximaal 150 nm, zonder de nucleosoom-nucleosoom interacties te verbreken, kunnen we ook meer zeggen over de structuur van de vezel zelf. Deze maximale uitrekking komt namelijk precies overeen met de hoogte van een stapel van 25 nucleosomen van elk 6 nm hoog. Dit betekent dat de vezel niet twee parallelle stapels nucleosomen bevat maar een enkele, die als een enkelvoudige spiraal is opgerold. De sterke interactie tussen de nucleosomen is blijkbaar voldoende om de kromming van het linker DNA te compenseren. Vezels met dezelfde samenstelling maar met linker DNA van slechts 20 bp, in plaats van 50 bp, vouwen tot een langere maar stijvere vezel, consistent met een zig-zag structuur van twee stapels nucleosomen. De controverse over de structuur van de 30 nm vezel kan dus worden

verklaard doordat beide vormen mogelijk zijn. Met behulp van de gevonden veerconstante kunnen we, gegeven de dimensies van de vezel, ook een schatting maken van de Young's modulus van de chromatine vezel. Deze blijkt duizend maal kleiner te zijn dan die van de meeste gestructureerde eiwitten en DNA, maar van dezelfde orde grootte als die van niet-gestructureerde eiwitten, waarin entropische krachten vervorming tegenwerken. Het was al bekend dat de niet-gestructureerde histonstaarten een belangrijke rol spelen in de vorming van de 30 nm vezel, maar hier hebben we een duidelijke aanwijzing dat deze staarten de verbinding vormen tussen de gestapelde nucleosomen.

Heterogene chromatinevezels. In hoofdstuk 3 hebben we de mechanische eigenschappen van heterogene chromatinevezels gekwantificeerd met behulp van een twee-toestanden-model dat de rekcurven van deze vezels beschrijft. Het plateau in de rekcurve tussen 3 en 4 pN geeft aan dat zowel het linker DNA als de eerste wikkeling van het nucleosomale DNA in één stap worden blootgelegd. Het verschil in vrije energie is $17 k_B T$ en neemt af bij hogere zoutconcentraties. Sommige van de nucleosomen vallen gedeeltelijk uit elkaar na herhaalde rekcycli. Voor de overgang tussen een compleet gevouwen chromatinevezel en een chromatinevezel die bestaat uit nucleosomen met slechts een enkele wikkeling van DNA, stellen we twee mogelijke mechanismen voor: het verbreken van nucleosoom-nucleosoom interacties wordt binnen de tijdsresolutie van het experiment gevolgd door het loslaten van de eerste wikkeling van het nucleosomale DNA, of het nucleosomale DNA is reeds gedeeltelijk ontwonden in de gevouwen chromatinevezel. Het twee-toestanden-model geeft niet alleen inzicht in de hogere-orde vouwing van chromatine, maar kan de factoren die de structuur van chromatine beïnvloeden, zoals post-translationele modificaties, kwantificeren.

Tijdopgeloste waarnemingen van chromatine dissociatie. In hoofdstuk 4 hebben we de dynamica van de wisselwerking tussen nucleosomen in een chromatinevezel bekeken. Bij metingen met een constante kracht laat de afstand tussen de extremen van de uitgerekte vezel omkeerbare, stapsgewijze lengteveranderingen zien die overeenkomen met discrete veranderingen van het aantal gepaarde nucleosomen. Doordat we de mechanische eigenschappen van chromatinevezels met behulp van het twee-toestanden-model hebben bepaald, kunnen we de levensduur van deze tussentoestanden achterhalen met behulp van een "Hidden Markovanalyse. De levensduur van de open toestand is zeer krachtsgevoelig en varieert 6 orden van grootte wanneer de uitgeoefende kracht enkele pN wordt vergroot. Vergeleken met geïsoleerde nucleosomen, die geen interactie hebben met hun burens, hebben nucleosomen in chromatinevezels een factor

1.5 groter verschil in vrije energie tussen de twee toestanden en is de levensduur van de open toestand 3 orden van grootte korter. Deze resultaten laten zien dat nucleosomen in de gesloten toestand alleen met naburige nucleosomen een interactie aan kunnen gaan, en dat in geopende nucleosomen een DNA wikkeling van de histoneiwitten loslaat. Onze resultaten beschrijven voor het eerst de dynamica van nucleosomen in de hogere-orde structuur van chromatinevezels op een kwantitatieve manier.

Relevantie voor chromatine-organisatie in de celkern. Het trekken aan een chromatinevezel lijkt ver te staan van de natuurlijke omstandigheden waaraan deze vezels worden blootgesteld. Maar dit is zeker niet het geval. In de cel zijn tal van moleculaire motoren, zoals RNA polymerase, chromatine remodellers en vele andere, die continue krachten uitoefenen op DNA. Deze motoren kunnen meer dan 10 pN aan kracht genereren. Alle kracht-geïnduceerde veranderingen aan chromatine zoals die hier beschreven zijn, vallen dus binnen het regime dat heerst in de kern van de cel.

List of Publications

1. W.H. Hsu, F.T. Chien, C.L. Hsu, T.C. Wang, H.S. Yuan, and W.C. Wang, *Expression, crystallization, and preliminary X-ray diffraction studies of N-carbamoyl-D-amino- acid amidohydrolase from Agrobacterium radiobacter.*, Acta Crystallographica Section D Biological Crystallography **55**: 694-695 (1999)
2. W.C. Wang, W.H. Hsu, F.T. Chien, and C.Y. Chen, *Crystal structure and site-directed mutagenesis studies of N-carbamoyl-D-amino-acid amidohydrolase from Agrobacterium radiobacter reveals a homotetramer and insight into a catalytic cleft.*, Journal of Molecular Biology **306**: 251-261 (2001)
3. F.T. Chien, S.G. Lin, P.Y. Lai, and C.K. Chen, *Observation of two forms of conformations in the reentrant condensation of DNA.*, Physical Review E **75**: 041922 (2007)
4. M. Kruithof, F.T. Chien, M. de Jager, and J. van Noort, *Subpiconewton dynamic force spectroscopy using magnetic tweezers.*, Biophysical Journal **94**: 2343-2348 (2008)
5. M. Kruithof, F.T. Chien, A. Routh, C. Logie, D. Rhodes, and J. van Noort, *Single molecule force spectroscopy reveals a highly compliant helical folding for the 30 nm chromatin fiber.*, Nature Structural & Molecular Biology **16**: 534-540 (2009)
6. F.T. Chien and J. van Noort, *10 years of tension on chromatin: results from single molecule force spectroscopy.*, Current pharmaceutical biotechnology **10**: 474-485 (2009)
7. F.T. Chien, A. Routh, T. van der Heijden, D. Rhodes, and J. van Noort, *Rigorous quantification of force induced structural changes in heterogeneous 30 nm chromatin fibers.*, in preparation

8. F.T. Chien, T. van der Heijden, A. Routh, N. Radja, D. Rhodes, and J. van Noort, *Quantification of force-dependent dynamics of single nucleosomes in chromatin fibers.*, in preparation

Curriculum Vitae

Fan-Tso Chien was born in Changhua in Taiwan on December 09, 1976. He started his undergraduate studies in Life Science at National Tsing Hua University in 1996. In 1999 he became a Bachelor of Science and joined Prof. Dr. Wen-Ching Wang's group at the National Tsing Hua University. In his research project he helped to solve the crystal structure of amidohydrolases. For this project he received the Research Creativity Award from the National Science Council for the outstanding achievement in crystallography. After receiving his Master of Science degree in 2001, he went for military service and was promoted to sub-lieutenant. From 2003 to 2006, he worked in Prof. Dr. Chi-Keung Chan's group as a research assistant in the Institute of Physics at the Academia Sinica where he investigated DNA condensation. In August 2006 he joined the Physics of Life Processes group at Leiden University as a PhD student. Supervised by Dr. Ir. John van Noort he studied the dynamics of chromatin using magnetic tweezers. During this period he was responsible for organizing the biweekly Biomolecular physics seminars. Further he assisted in the Physics for Biologists course and was teaching assistant on Optical Tweezers for a second year bachelors course. Fan-Tso will continue as a postdoctoral fellow in Dr. Jason Chin's group at Medical Research Council in Cambridge, UK.

